HIGH-CONTRAST AND THREE-COLOR ELECTROCHROMIC POLYMERS

By

DEAN M. WELSH

A DISSERTATION PRESENTED TO THE GRADUATE SCHOOL
OF THE UNIVERSITY OF FLORIDA IN PARTIAL FULFILLMENT
OF THE REQUIREMENTS FOR THE DEGREE OF
DOCTOR OF PHILOSOPHY

UNIVERSITY OF FLORIDA

2001

To Annie, Stanley, and Mary Ellen

ACKNOWLEDGMENTS

First, I would like to thank my advisor, Professor John Reynolds. Without his seemingly infinite patience and encouragement, this body of work would never have been possible. I would also like to thank him for giving me the opportunity to work on very interesting projects in an excellent research group. The guidance of the other faculty at the University of Florida is also very much appreciated; especially that of the members of my committee, whom I would like to thank for their time and support. This includes Professor Kenneth Wagener, Professor Kirk Schanze, Professor Daniel Talham, and Dr. Anthony Brennan.

I would also like to thank the staff of the graduate coordinator's office for their fantastic efforts in making life as a graduate student in chemistry a little easier. This includes Dr. James Deyrup, Donna Balkcom, and Lori Clark. Also, the support staff in the polymer office has been outstanding, and I would like to thank Lorraine Williams, Carol Lowe, Sara Klossner, Valerie Pierce, and the many student assistants who have helped me over the years.

I would like to thank the members of the Reynolds Group and the George and Josephine Butler Polymer Laboratories for friendship, stimulating conversations, and advice. The friendship and assistance of Dr. Anil Kumar is greatly appreciated, and he was instrumental in the success of the work in Chapter 2 of this dissertation. Dr. Jerry Reddinger initiated some aspects of the work in Chapter 4, and his early assistance in this

work was crucial. I would like to thank Dr. Greg Sotzing who was my hoodmate for my first two years at Florida and provided good advice about chemistry and life. Dr. Leroy Kloeppner started work on some aspects of Chapter 3, and his contributions were helpful and numerous. Barry Thompson provided the colorimetry results. I give special thanks to Carl Gaupp for his partnership in the measurement of coloration efficiency. Luis Madrigal graciously provided some of the MALDI-TOF results for this paper. I would like to thank Mike Ramey and Dr. Joanne Bedlak for helping with photoluminescence studies. Dr. Mauricio Pinto graciously provided quantum efficiency results. Irina Schwendeman took the polymers and applied them to electrochromic devices, and her efforts in this area are greatly appreciated. Other members of the Reynolds group past and present who deserve acknowledgment are Drs. David and Jennifer Irvin, Dr. Peter Balanda, Don Cameron, Dr. Hiep Ly, Dr. Barbara Tsuie, Chris Thomas, C. J. DuBois, Dr. Mark Morvant, Fabienne Piroux, Dr. Anthony Pullen, Roberta Hickman, Dr. Philippe Schottland, Dr. Kyukwan Zong, Ben Reeves, Jeff Bryant, Adam Reboul, Avni Argun, Dr. Youngkwan Lee, and Dr. Mohamed Bouguettaya. The list could be longer, and I would like to thank anyone whom I have mistakenly omitted. I thank the members of the polymer floor, including Dr. James Pawlow, Cameron Church, Jason Smith, Debby Tindall, and all others who have provided friendship and advice.

Dr. David Powell's expertise in mass spectrometry is greatly appreciated. I would also like to thank Dr. Khalil Abboud for solving the X-Ray crystal structures presented here, and for preparing the data tables and figures for publication. I extend special thanks to all of the research support staff at the University of Florida.

I would like to thank my family who were always interested in my endeavors and supported me in my decisions. Finally, my greatest gratitude goes to my wife, Annie. Her unwavering love, support, encouragement, and patience provide me with the will to persevere, and without her none of this would have been possible.

TABLE OF CONTENTS

page

Abstract of Dissertation Presented to the Graduate School
of the University of Florida in Partial Fulfillment of the
Requirements for the Degree of Doctor of Philosophy

HIGH-CONTRAST AND THREE-COLOR ELECTROCHROMIC POLYMERS

By

Dean M. Welsh

August 2001

Chairman: Professor John R. Reynolds
Major Department: Chemistry

We synthesized several new electrochromic polymers that can be used in electrochromic device applications. A series of cathodically coloring polymers, based on the 3,4-alkylenedioxythiophene structure, were synthesized electrochemically, with all of them exhibiting low polymer oxidation potentials (-0.2 to 0.0 V vs. Ag/Ag^{+}). The optical contrast and response times were enhanced in more highly substituted polymers when compared to the parent polymer poly(3,4-ethylenedioxythiophene) (PEDOT). In fact, the optical contrast in the dimethyl substituted 3,4-propylenedioxythiophene polymer (PProDOT-Me_2) is the highest for known conjugated polymers, and this polymer is a very good candidate for use as a cathodically coloring polymer for dual-polymer electrochromic devices. The superiority of PProDOT-Me_2 was verified by measurement of coloration efficiency and relative luminance values for these polymers.

Through the use of the Grignard metathesis reaction, soluble electroactive polymers with the PProDOT-Bu_2 structure were synthesized. The MALDI-TOF mass

spectrometry results indicate that polymers have X_n values of ca. 20, and the nature of the end groups have been identified. These polymers exhibit photoluminescence in solution, and can be doped in solution to a highly transparent conducting form. Solution cast films of these polymers show oxidation potentials and optical properties that are very similar to those of the electropolymerized polymers.

New extended conjugation carbazole and diphenylamine monomers with terminal EDOT moieties were synthesized with the amine group unsubstituted to allow easy synthesis of many derivatives. These two monomers electropolymerize at low potentials (0.44 and 0.32 V) to yield electroactive polymers that exhibit three distinct color states (yellow, green, and blue). The effect of substituting the terminal heterocycle with thiophene was studied for the carbazole polymer, and electropolymerization occurs at a slightly higher (0.67 V) monomer oxidation potential yielding a three color (yellow, green, and blue) electroactive polymer. All of these materials are good candidates as anodically coloring polymers in dual-polymer electrochromic devices.

CHAPTER 1
INTRODUCTION

1.1 Brief History of Conducting Polymers

The 2000 Nobel Prize in chemistry was awarded to Shirakawa, MacDiarmid, and Heeger for their discovery of high conductivity in doped polyacetylene.[1] This seminal discovery started a field that has exploded over the last three decades into thousands of publications, materials now commercially available, and consumer products on the market including polymers as antistatic coatings in photographic film, electrode materials in capacitors, and material for through-hole plating of printed circuit boards.[2,3] Although polyacetylene exhibits a very high conductivity in the doped form, the material is not stable to oxygen or humidity and is intractable. For these reasons, much work has been devoted to synthesizing soluble and stable polyacetylenes.[4,5] Unfortunately, these substituted derivatives exhibit electrical conductivities that are much lower than the parent polymer. The discovery of polyacetylene led to the search for new structures that could lead to new and improved polymer properties.

New conducting polymer structures (Figure 1.1) have been developed over the past two decades with the hope of obtaining better properties than polyacetylene. New classes of conducting polymers include polythiophene[6, 7] (PT), polyfuran[7] (PF), polypyrrole[8] (PPy), poly(p-phenylene)[9] (PPP), poly(p-phenylene vinylene)[10] (PPV), polyfluorene,[11] and polyaniline.[12] Although none have exhibited higher conductivity than

polyacetyelene, these polymers have been useful in designing new structures that are soluble and stable. Electron-rich heterocycle based polymers such as polythiophene and polypyrrole are very stable in the p-doped form and this has made these systems two of the most studied conducting polymers. Their stability is due to their lower polymer oxidation potentials which follow the order of polyactelyene>PT>PPy. Also, these structures are more easily modified than polyacetylene, allowing for more diversity of structures.

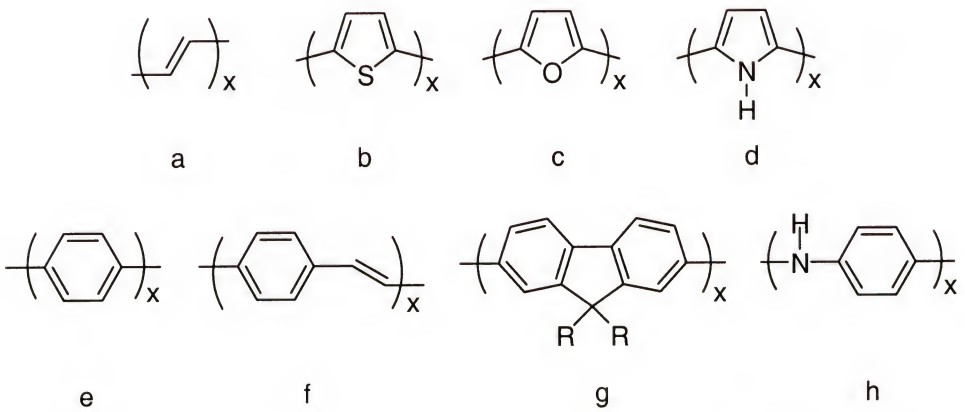

Figure 1.1 Conducting polymer structures: a) polyacetylene, b) polythiophene, c) polyfuran, d) polypyrrole, e) poly(p-phenylene), f) poly(phenylene vinylene), g) polyfluorene, h) polyaniline

1.2 Electropolymerization Mechanism

Electropolymerization is one of the most important tools in the synthesis of conducting polymers. It is an efficient method for synthesizing smooth polymer films on conductive substrates, and it allows for easy probing of electrical and optical properties. Oxidative polymerization is the most common type of electropolymerization, and it involves removal of an electron from a monomer unit to form radical cations, which then

couple to form polymer. More electron-rich monomers such as thiophene and pyrrole form more stable radical cations than electron-poor systems such as benzene, therefore they have lower oxidation potentials leading to more stable materials.

The mechanism for the electropolymerization of thiophene is shown in Figure 1.2, which can be extrapolated to other heterocycles. It is thought that the first step is the one-electron oxidation of monomer to form a radical cation. As shown in Figure 1.2, this radical cation is stabilized by resonance. Two different pathways can be followed. In one pathway, a radical cation couples with monomer to yield a radical cation dimer which then loses another electron before losing two protons to yield a neutral dimer.[13,14] The second pathway involves the coupling of two radical cations to form a dimer that loses two protons to form the neutral dimer.[15,16,17] This neutral dimer can then undergo further oxidation and coupling with other monomer and oligomer species until polymer is formed on the electrode surface.

Although forming polymer by electropolymerization is a valuable synthetic method, this method has disadvantages. The greatest disadvantage is that the materials are obtained as insoluble films making primary structure verification difficult. The typical spectroscopic, chromatographic, and mechanical techniques used to characterize synthetic polymers cannot be used on an electrode bound material. Also, processing on substrates that are not conducting is not easily accomplished. Because of these disadvantages, chemical polymerization is also important for the synthesis of conducting polymers.

1.3 Oxidative Chemical Polymerization

Oxidative chemical polymerization is the least expensive, most simple, and most widely used chemical synthesis of conducting polymers.[18,19] In oxidative chemical polymerization, a stoichiometric amount of oxidant is used to form polymer that is in its doped or conducting form, and the mechanism is believed to be similar to the electropolymerization mechanism discussed earlier. Figure 1.3 shows the oxidative

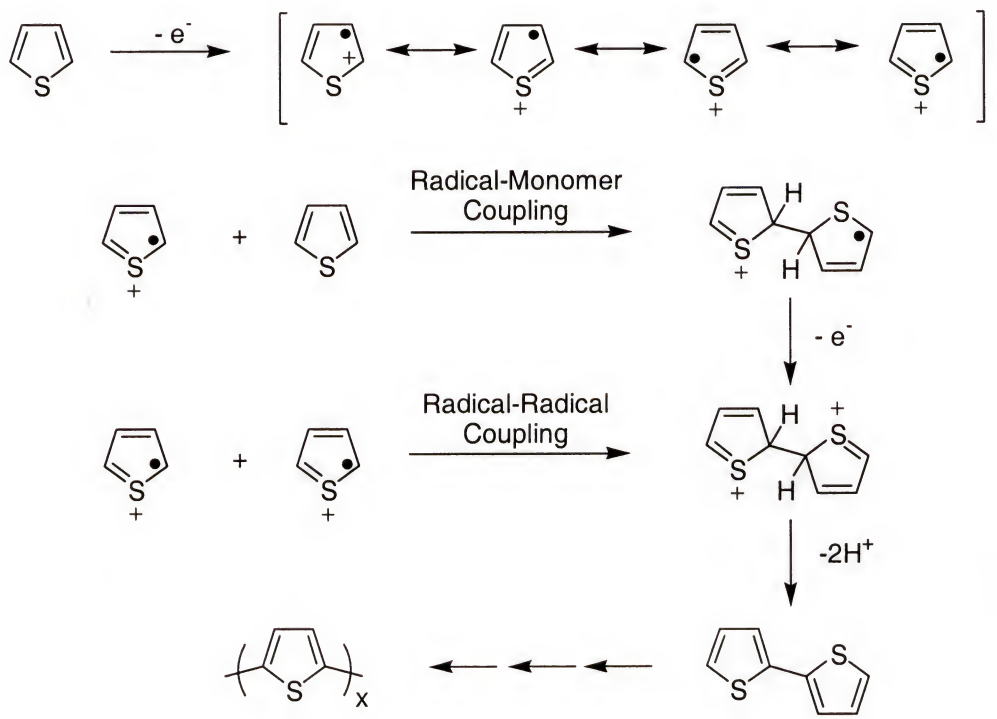

Figure 1.2 Proposed mechanism of the electropolymerization of thiophene.

polymerization of thiophene and benzene. Polyheterocycles are usually polymerized with $FeCl_3$ as the oxidant, [19, 20, 21, 22] although other oxidants also can be used.[19] Reduction to the neutral state is accomplished by addition of a strong base such as ammonium

hydroxide or hydrazine. Benzene can also undergo oxidative polymerization with $AlCl_3$ / $CuCl_2$ to yield poly(p-phenylene).[23]

There are many problems that are inherent to chemical oxidative polymerizations, which can cause the quality of the polymers formed to be unsatisfactory. Because the polymer is formed in its oxidized form, which is believed to be more rigid than the neutral form[24], the oxidized polymer chains can precipitate from the polymerization medium limiting degree of polymerization. Overoxidation and decomposition can also occur in these polymerizations as a result of the strong oxidizing agents used. This is a

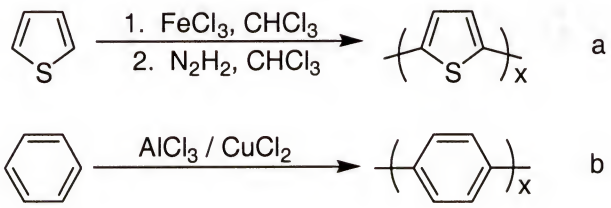

Figure 1.3 Oxidative polymerization: a) of thiophene, b) of benzene.

disadvantage that can be overcome by electrochemical oxidative polymerization, because the potential can be finely controlled. There is also an abundance of side reactions that can occur during both chemical and electrochemical oxidative polymerization of unsubstituted heterocycles like thiophene, including formation of "coupling defects" along the backbone (Figure 1.4).[25,26] Polymerization usually occurs through positions 2 and 5 of the thiophene, otherwise known as the α-positions, and the most conducting polythiophene backbone consists entirely of these linkages. Coupling can occur through the 3 and 4 positions, known as the β positions, yielding irregular backbones with poorer polymer electronic properties. Many of the problems of oxidative polymerization can be

solved by the use of substituents and non-oxidative polymerization chemistry (see below).

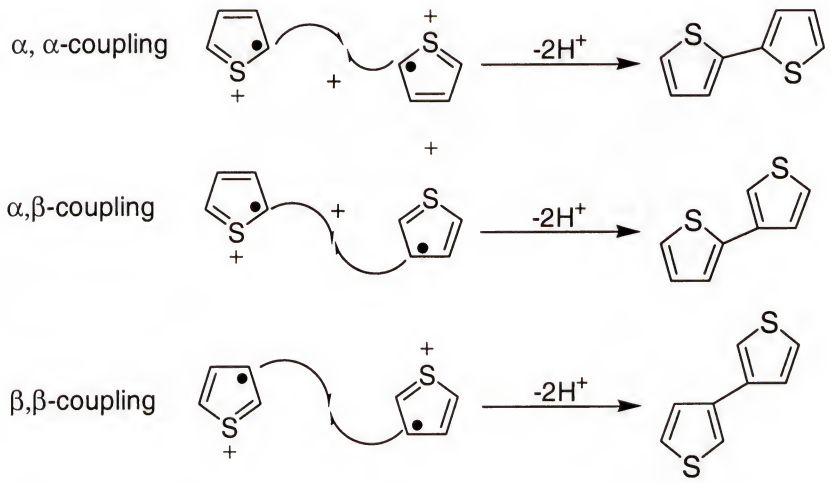

Figure 1.4 Available coupling pathways during the oxidative polymerization of thiophene.

1.4 Non-Oxidative Polymerizations

Because of the problems of solubility, overoxidation, and coupling defects involved in oxidative polymerizations, much research has been aimed at developing milder, non-oxidative polymerization reactions. In this case, conjugated polymers are synthesized in the neutral form, leading to fewer polymer precipitation problems. The conditions are usually milder, and as long as these reactions can proceed to high conversion, polymers with high molecular weight can be obtained.

One non-oxidative route that has been used effectively to synthesize conjugated polymers is the precursor route (Figure 1.5). In these routes, a soluble precursor polymer that can be fully characterized and purified is formed before further reaction; usually thermal or chemical elimination leads to the final conjugated polymer. The main

advantage of the precursor technique is that the polymer can be formed through chain polymerization, which allows high molecular weights to be obtained. Many precursor routes have been used to synthesize polyacetylene (Figure 1.5a) including routes using a ring-opening metathesis polymerization (ROMP) followed by thermolysis.[4,27,28,29,30] An advantage of this method is that the prepolymer can be stretch-oriented during thermal elimination, leading to better quality films with higher conductivities. Poly(p-phenylene)s can also be synthesized using a precursor method (Figure 1.5b) using

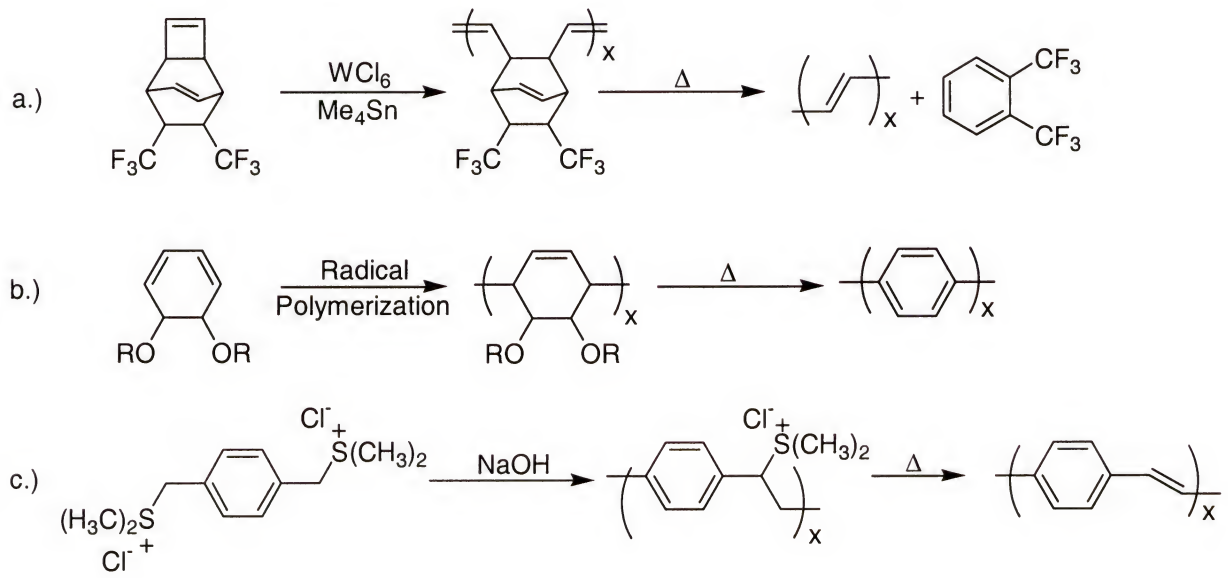

Figure 1.5 Conducting polymers synthesized through a soluble precursor route: a.) polyacetylene b.) poly(p-phenylene) c.) poly(p-phenylene vinylene)

radical chain polymerization followed by pyrolysis to yield high molecular weight PPP.[31,32,33,34,35] The original precursor methods to PPP yielded polymer with both 1,2- and 1,4-linkages, but this problem was later overcome with the use of a transition metal catalyst which yielded the desired 1,4-linkages exclusively.[34] Poly(p-phenylene

vinylene)s have been synthesized successfully with precursor routes (Figure 1.5c) which have been investigated extensively.[36,37,38,39] In this route, a base catalyzed polymerization of a disulfonium salt yields a soluble precursor polymer that can be converted to PPV when heated. Similar to the precursor method used to synthesize polyacetylene, the sulfonium salt precursor polymer can be processed into highly oriented, free-standing films or fibers during conversion to PPV.

In addition to the soluble precursor routes, conjugated polymers have been synthesized by non-oxidative coupling techniques. Although poly(thienylene vinylene) can be synthesized by precursor routes,[40] viable precursor routes to directly ring-linked polyheterocycles have not been found, and coupling polymerizations have been used extensively to prepare these polymers. Coupling polymerizations yield neutral soluble polymers in step growth polymerizations. Therefore according to the Carothers equation (1-1) high extent or fraction of conversion (p) along with good stoichiometric balance (r) is necessary to obtain high number-average degree of polymerization (X_n or DP).[41] In a typical polymerization of bifunctional monomers A-A and B-B (i.e., a dibromide and a

$$X_n = (1 + r) / (1 + r - 2rp) \qquad (1\text{-}1)$$

diorganometallic compound), obtaining stoichiometric balance is accomplished through careful measurement of monomer amounts. A so-called A-B type polymerization (i.e., a bromide and an organometallic on the same compound) takes place with internally supplied stoichiometry. In either case, the extent of conversion (p) must be close to unity

to prepare polymers with high DP values. Coupling polymerizations will be discussed in more detail in Section 3.1.2.

1.5 Band Theory and Conduction in Conjugated Polymers

Band theory has been used to describe the properties of insulators, metals, and semiconductors. Metals are materials that possess partially filled bands, where movement of charge carriers can occur freely leading to conduction. In a semiconductor, there is a filled valence band and an empty conduction band separated by a band gap (E_g) where no energy levels are present. The conduction band can be populated at the expense of the valence band by exciting electrons across the band gap either thermally or photochemically. Semiconductors can be doped which increases the conductivity of the material, and depending on the type of dopant used either holes (p-type) or electrons (n-type) are the charge carriers. Insulators have a band structure similar to semiconductors except they have very large band gaps that are inaccessible under normal environmental conditions.

Neutral conjugated polymers are usually treated as semiconductors and band theory can be used to describe their electronic energy levels. Figure 1.6 shows the formation of a band structure as conjugation increases from ethylene to polyacetylene. The energy difference between the highest occupied molecular orbital (HOMO) and the lowest unoccupied molecular orbital (LUMO) decreases as the conjugation length increases along with an increase in the number of energy levels. In polyacetylene, the energies of the molecular orbitals are so close that they are indistinguishable, leading to the formation of bands of allowed energies. When referring to discrete π-conjugated

molecules, the energy between the HOMO and the LUMO is a π to π* transition. The band gap of a polymer can be approximated from the onset of absorption of the π to π* transition in the UV-Vis spectrum. Conjugated polymers can also be doped to form materials with high conductivity. Although the term doping is borrowed from semiconductors, doping in conjugated polymers is much different. In semiconductors doping is a process that involves very low (<1%) doping levels as compared to conjugated polymers (20 to 60%). Also, doping in conjugated polymers is really a redox

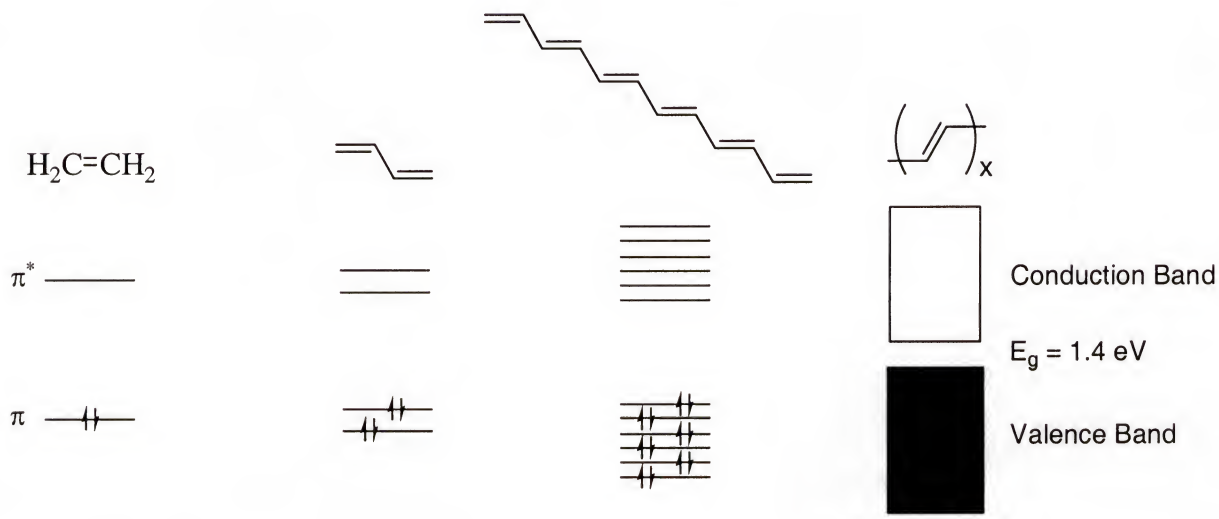

Figure 1.6 Evolution of energy levels in conjugated polyenes with increasing conjugation length.

reaction where polymer oxidation and reduction is referred to as "p-doping" and "n-doping" respectively.

Polyacetylene must be considered first when considering the doped forms of conducting polymers, because the two neutral resonance structures are degenerate, meaning that the ground states are thermodynamically equivalent (Figure 1.7). Upon

oxidation, radical cations form that can combine to form nonassociated positive charges called solitons. Most other organic conducting polymers, including the polythiophenes discussed in this dissertation, possess two nondegenerate ground states because of unequal resonance forms. For example, poly(p-phenylene) exhibits both benzenoid and quinoid configurations (Figure 1.7) of which the quinoid is the higher energy configuration. The mechanism of charge carrier generation in these systems has been studied extensively, and the most widely accepted mechanism is shown in Figure 1.8.[42]

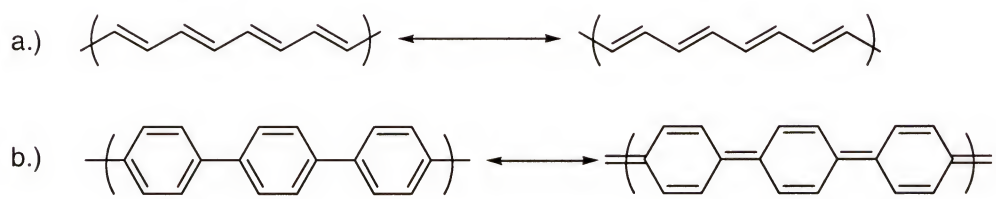

Figure 1.7 a) The degenerate ground state resonance structure for polyacetylene, b) The nondegenerate ground state resonance structures of poly(p-phenylene).

Upon oxidation in these systems, the energy level from which the electron is removed is raised in energy and now lies in the region of the band gap. During initial oxidation, radical cations known as polarons are the main charge carriers. Further oxidation causes more and more polarons to form and eventually the unpaired electron of the polaron is removed, or two close polarons can be combined to form dications or bipolarons. Unlike the solitons in polyacetylene, the two positive charges of the bipolarons stay associated and act as one charge carrier dispersed over many rings. The length of the bipolaron unit is thought to be 5 to 8 rings, although this is an arbitrary number that can be different depending on the specific polymer system. Experimental results from electron paramagnetic resonance spectroscopy (EPR) support this mechanism showing that

neutral and heavily doped polymers have no unpaired electrons, but moderately doped polymers do exhibit an EPR signal and are paramagnetic.[43,44] Although this representation for charge carrier generation has gained wide acceptance in the field, there are alternatives. In one example, the formation of diamagnetic π-dimers resulting from two polarons on separate chains interacting with one another is proposed as an alternative to bipolaron formation.[45,46,47] All of the evidence supporting π-dimer formation stems from experiments on small conjugated molecules, with very little evidence that they exist in polymers.

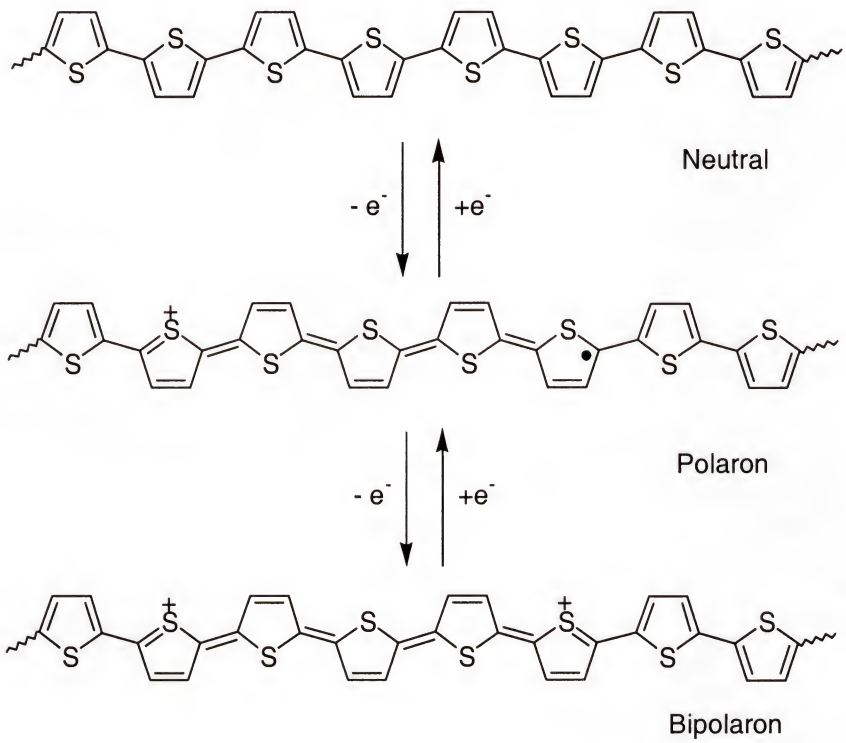

Figure 1.8 The charged states formed upon oxidation of polythiophene.

1.6 Monomer Structure and Substituent Effects in Electropolymerization

The structure and reactivity of the monomer will greatly affect the properties of the resulting polymer. Because of their availability and relative ease of polymerization, electron-rich heterocycles such as polythiophene and polypyrrole are the two most common monomers for electropolymerization. Because electropolymerization occurs at a potential that is higher than the redox processes of the polymer, side reactions such as cross-linking and overoxidation can occur. This behavior is best displayed by the electropolymerization of thiophene. The oxidation of thiophene occurs at a potential of 2.06 V vs. SSCE, which is much higher than the polymer redox processes at 0.96 V.[25] (Please note that the potentials reported for conducting polymers in the literature vary greatly and depend on experimental parameters such as solvent and concentration.) At 2.06 V, the polymer undergoes degradative side reactions known as overoxidation which can destroy its electroactivity, but because polymerization occurs at a faster rate than the side reactions, polymer is formed on the electrode, but exhibits poor electroactivity and a high polymer oxidation potential. This effect is known as the polythiophene paradox,[48] and although polymer is formed, these conditions are not ideal. Conversely, pyrrole polymerizes at a much lower potential of 1.2 V vs. SSCE[49], and the polymer peak oxidation occurs at –0.15 V.[25] The lower monomer and polymer oxidation potentials allow for fewer side reactions, and a polymer that is more stable in its conducting form. Both pyrrole and thiophene suffer from the effects of β coupling (see Section 1.3) which causes reduced conjugation lengths and poorer polymer properties.

One way to overcome the problems with high oxidation potentials and β coupling is to substitute the β positions. Electronic effects from electron-withdrawing and

electron- donating substituents drastically affect the electron density of the thiophene ring, and there is a linear correlation between the oxidation potential of substituted thiophenes and the Hammett substituent constant. Thiophenes substituted with electron-withdrawing groups such as cyano, carboxylic acid, aldehydes, and nitro groups have oxidation potentials that are ca. 0.5 to 0.7 V higher than thiophene, and they do not electropolymerize.[25,49] In the case of electron-donating groups, the oxidation potential decreases due to the stabilization of the radical cation formed upon oxidation. This is shown most simply by substitution of the 3 position by a methyl group. Polymers synthesized from 3-methylthiophene have increased mean conjugation lengths and higher conductivities when compared to polythiophene.[50] The methyl group serves to block one of the β positions and its inductively electron-donating effect lowers the oxidation potential of the monomer. The electron-donating ability of alkoxy substituents also has been used to lower monomer oxidation potentials.[51]

Because substitution in the 3 position has a positive effect on polymer properties, it might be suspected that substitution in both the 3 and 4 positions would further enhance polymer properties. However, disubstituted thiophenes suffer from a severe steric interaction between substituents on adjacent monomer units, and the mean conjugation length is greatly reduced. Poly(3,4-dialkylthiophenes) have higher oxidation potentials, band gaps, and lower conductivities than monosubstituted polymers[52] and the same results are observed for dialkoxy substituted thiophenes.[53] Poly(cyclopenta[c]thiophene) was synthesized in the hope that the cyclic alkyl substituent would decrease the steric problems with disubstitution, and this polymer did show oxidation potentials that were lower than poly(3,4-dimethylthiophene), but still higher than poly(3-methylthiophene).[54]

Substituents affect the oxidation potential of the monomers and polymers. They also affect the optical absorption and/or band gap of these systems. Electron-donating groups lower the band gap by raising the valence band or HOMO level. This is illustrated by the lowering of the band gap from polythiophene (2.0 eV)[55] to poly(3,4-ethylenedioxythiophene) (PEDOT) (1.6 eV). The band gap is affected by electronic effects, and by steric effects that can cause the rings to twist out of plane lowering the band gap. Likewise, the λ_{max} of poly(3,4-dimethylthiophene) exhibits a 170 nm blue shift when compared to poly(3-methylthiophene).[54]

1.7 Soluble Polymers and Poly(3-alkylthiophene)s

One of the main problems with electrochemically or chemically polymerized unsubstituted polythiophene is that it is unprocessable and insoluble. The use of long alkyl groups has become a common practice to solubilize conjugated polymers. The first soluble chemically polymerized poly(3-alkylthiophene)s were synthesized by Elsenbaumer in 1985, and polymers with alkyl groups longer than butyl can be processed from solution or the melt into films.[56,57,58] These original polymers were synthesized by a Kumada cross-coupling reaction starting with 2,5-diiodo-3-alkylthiophene, which is treated with Mg in THF, generating a mixture of Grignard species that are then polymerized by adding a $Ni(dppp)Cl_2$ catalyst. Many different routes to soluble poly(3-alkylthiophene)s have been developed since this initial discovery.[59,60]

Because 3-alkylthiophenes are not symmetric molecules, there are three ways that two molecules can couple (Figure 1.9). The first is 2,5' or head-to-tail (HT), the second is 2,2' or head-to-head (HH), and the third is 5,5' or tail-to-tail (TT). Both chemical and

electrochemical oxidative polymerization, and the original Kumada coupling methods discussed above yield polymers with a mixture of all three couplings. This leads to polymers containing the four triad regioisomers as displayed in Figure 1.9, and polymers that contain all of these different types of couplings are referred to as regioirregular. It has been shown that polymers with exclusively HT couplings result in a planar structure,

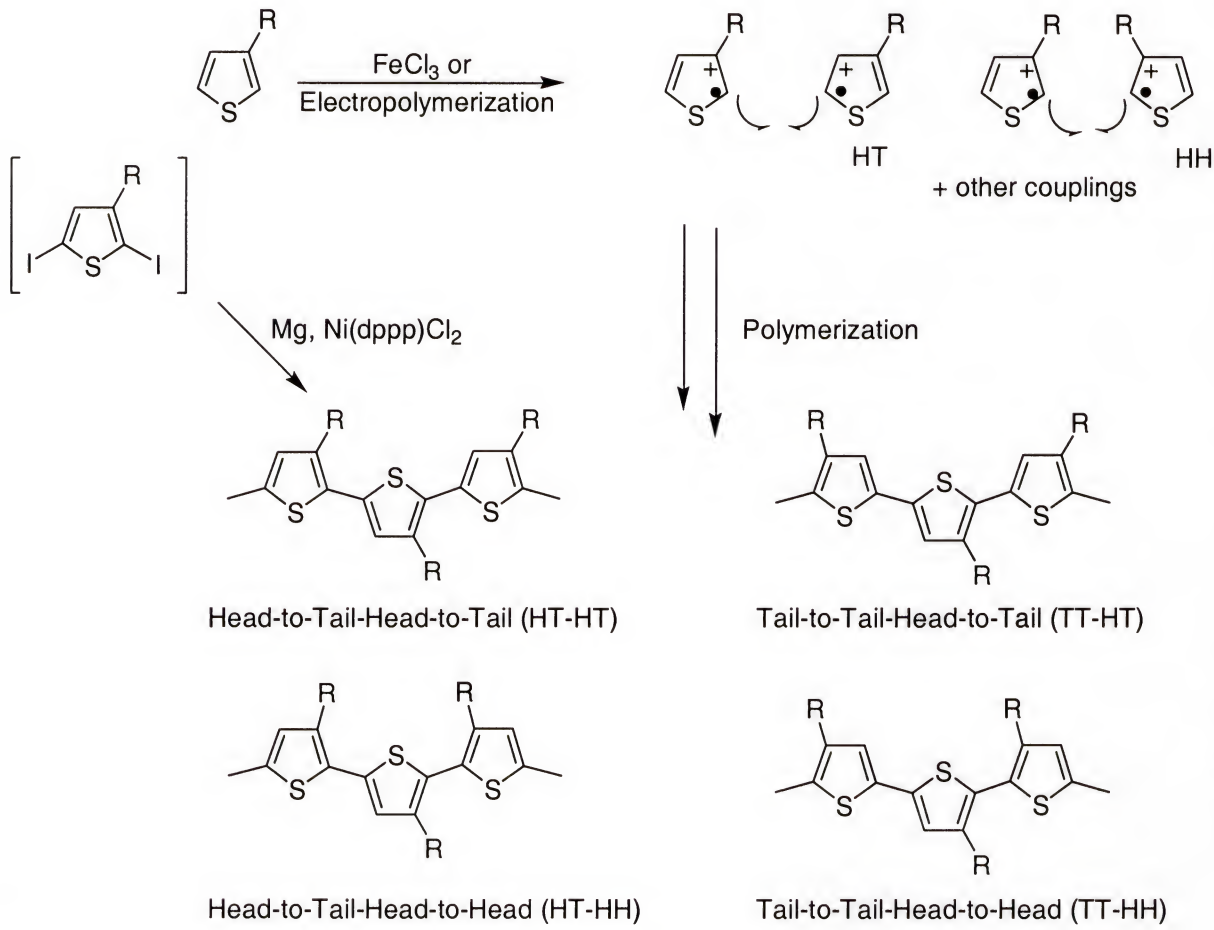

Figure 1.9 Possible regiochemical couplings in poly(3-alkylthiophene)s.[59]

where HH and TT structures cause a sterically driven twisting of the thiophene rings out of plane leading to a diminished mean conjugation length. However, synthetic methods

were devised to synthesize structurally homogenous, regioregular, HT poly(3-alkyl-thiophene)s first by McCullough and co-workers,[61,62] and then by Rieke and co-workers.[63,64] Both of these methods involve transition metal catalyzed coupling reactions, where an A-B monomer (2-bromo-5-Mg(or Zn)Br-thiophene) is generated in-situ which after treatment with Ni(dppp)Cl_2 leads to predominantly HT coupling. The regioregular polymers generated have lower band gaps, higher conductivities, lower polymer oxidation potentials, and longer mean conjugation lengths. McCullough improved on his method by using a Grignard metathesis polymerization (GRIM) that requires shorter reaction times, requires less expensive reagents, and can produce larger amounts of polymer.[65] This method also was used by other research groups.[66,67,68]

1.8 Polymers Based on 3,4-Ethylenedioxythiophene (EDOT)

A monomer that overcomes all of the electronic and steric difficulties discussed above is 3,4-ethylenedioxythiophene or EDOT (Figure 1.10). EDOT incorporates a cyclic ethylenedioxy substituent in the 3 and 4 positions, which incorporates the electron-donating ability of an alkoxy group that is "tied back" to eliminate the steric problems typically found with 3,4 disubstitution. EDOT was originally polymerized to poly(3,4-ethylenedioxythiophene) or PEDOT by Jonas et al.,[69,70] and the polymer and its derivatives were recently reviewed.[71] Although originally synthesized in hopes that the polymer would be soluble, it is not. However, it has many favorable properties. PEDOT exhibits low monomer (ca. 1.1 V vs. Ag/Ag^+) and polymer (ca. –0.2 V) oxidation potentials when compared to polythiophene, leading to films that are very stable in the doped or conducting form.[69,70,72] The band gap is also lowered by ca. 0.4 eV to 1.6 eV

when compared to polythiophene, leading to a polymer that is very absorptive in its reduced or neutral form and very transmissive in its oxidized or doped form. The solubility issue also has been solved by the synthesis of PEDOT as an aqueous dispersion with poly(styrene sulfonic acid) (PSS) as a polymeric dopant. This dispersion known as PEDOT/PSS can be easily cast into films with high conductivity, high transparency, and good stability.[73] Because of these favorable properties, much research effort has been exerted on PEDOT and its derivatives.

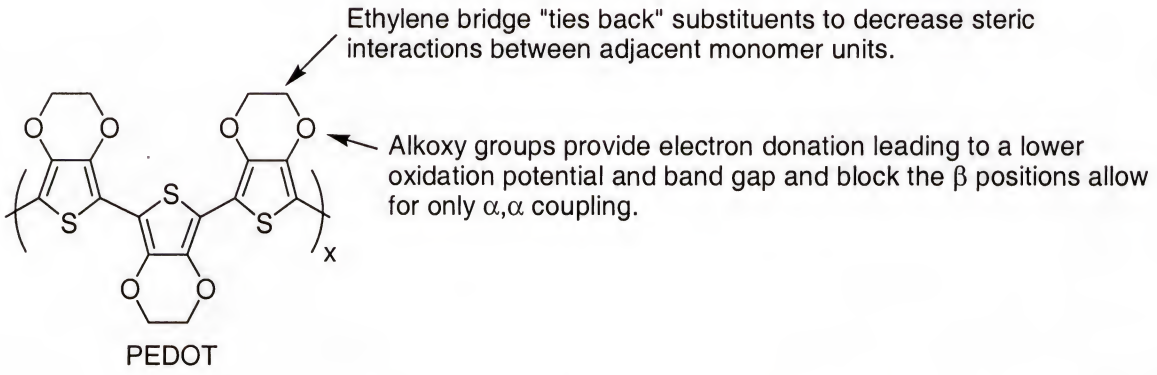

Figure 1.10 The structure of poly(3,4-ethylenedioxythiophene) (PEDOT) with description of favorable substituent effects.

1.9 Extended Conjugation Monomers

Another way to lower monomer oxidation potentials and limit degradative side reactions is to prepare and polymerize multi-ring or extended conjugation monomers. Increasing the conjugation length of the monomer raises the energy level of the HOMO and stabilizes the radical cations formed upon oxidation resulting in a decrease in oxidation potential. In addition, extended conjugation monomers with varying units can be prepared in order to synthesize polymers with differing properties.

The simplest example of this method is shown in the synthesis of polythiophene from thiophene and bithiophene. The polymer $E_{1/2}$ is lowered by 0.4 V vs. Ag/Ag^+ when comparing polythiophene to polybithiophene, thus indicating a higher mean conjugation length in polybithiophene.[25] The same results are seen for other heterocycles as in the polymerization of terfuran[74] and oligopyrroles.[75] Polymers based on EDOT also have been synthesized from extended conjugation monomers. While EDOT polymerizes at 1.1 V vs. Ag/Ag^+, the dimer 2,2'-bis(EDOT) polymerizes at 0.51 V,[76,77] and the trimer ter-EDOT polymerizes at 0.20 V.[78] It should be noted that, although extending the conjugation is favorable in lowering the oxidation potential, electron rich monomers such as ter-EDOT are difficult to handle because of spontaneous polymerization by environmental oxidation.

Extended conjugation monomers that use a combination of heterocycles, substituted phenylenes and vinylenes have been synthesized to produce polymers with a wide variety of optical and electrical properties. In this approach, symmetrical oligomers (trimers, tetramers, etc.) are prepared with the electron-rich heterocycles as the termini, and polymerization occurs through the α position of the heterocycle. This approach has an advantage over copolymerization, where statistical placement of comonomers occurs, and properties can vary from sample to sample.

Polymers that incorporate thiophene and phenylene show low oxidation potentials and disubstitution of the phenylene unit can be used to tailor polymer properties.[79,80,81,82,83] For example, 1,4-bis(2-thienyl)benzene polymerizes at a potential of 0.91 V vs. Ag/Ag^+, which is much lower than thiophene or benzene. Also, 1,4-bis(2-thienyl)-2,5-dimethoxybenzene polymerizes at an even lower potential of 0.71 V presumably due

to the electron-donating nature of the methoxy groups. Similarly, furan and phenylene polymers have been synthesized and studied.[82,84]

Analogous to the thiophene derivatives, the Reynolds group has synthesized a large number of bis-EDOT-arylene multi-ring monomers to produce polymers with varying optical, electrical, and electrochromic properties.[78,85,86,87] The benefits of EDOT over thiophene discussed earlier are transferred to these polymers with the polymers exhibiting low oxidation potentials and stable conducting forms. For example, 1,4-bis(EDOT)benzene polymerizes at a potential of 0.61 V vs. Ag/Ag^+ which is 0.3 V lower than the analogous thiophene derivative discussed earlier. Poly[1,4-bis(EDOT)benzene] exhibits a band gap of 1.8 eV, which is intermediate between the band gap of PEDOT (1.6 eV) and PPP(3.0 eV). The incorporation of a vinylene group into the polymer backbone causes a lowering of the band gap to 1.4 eV,[88,89]and further substitution of the vinyl group with a cyano group leads to an especially low gap polymer (1.1 eV).[90]

1.10 Applications

Numerous applications of conjugated polymers have been realized.[91] These numerous applications can be split into three main classes. The first use conjugated polymers in their neutral form, and take advantage of their semi-conducting and luminescent properties. Examples of applications that use neutral polymers are conjugated polymers as semiconducting materials for field effect transistors[92] and as the active material in an electroluminescent device.[93] The second category of applications involves using the polymer in its doped or conducting form, and some representative applications in this category are electrostatic charge dissipation and EMI shielding,[94,95]

and as electrode materials for capacitors.[70] The third category uses the ability of the polymer to reversibly switch between its conducting and reduced forms. Upon switching between these two states, the polymer undergoes color, conductivity, and volume changes. Applications that use these properties include battery electrodes,[96] mechanical actuators,[97] sensors,[98] drug delivery,[99] and electrochromics[100].

Of these applications, electrochromic devices are the most pertinent to the work in this dissertation. Electrochromics are materials that show a change in their optical absorption spectrum when switched between two electrochemical states. There are many different types of materials that are electrochromic including metal oxides, organic dyes, and conducting polymers. As mentioned previously, conducting polymers can be reversibly switched between their reduced and oxidized form, and the two states show very different optical spectra in the visible region and therefore the switching is accompanied by a color change.

Recently, dual polymer electrochromic devices have been developed by the Reynolds group, which exhibit high contrast, rapid response times, good stability, and high coloration efficiencies.[101,102] These devices utilize reversibly switching conducting polymers that are sandwiched together by a gel electrolyte. To make these types of devices work, two separate types of conjugated polymers are needed, cathodically coloring and anodically coloring. Figure 1.11 demonstrates the concept of complementary conjugated polymers for use in a device. A cathodically coloring polymer is one that is low gap (ca. < 1.6 eV), and is very absorptive in its reduced form

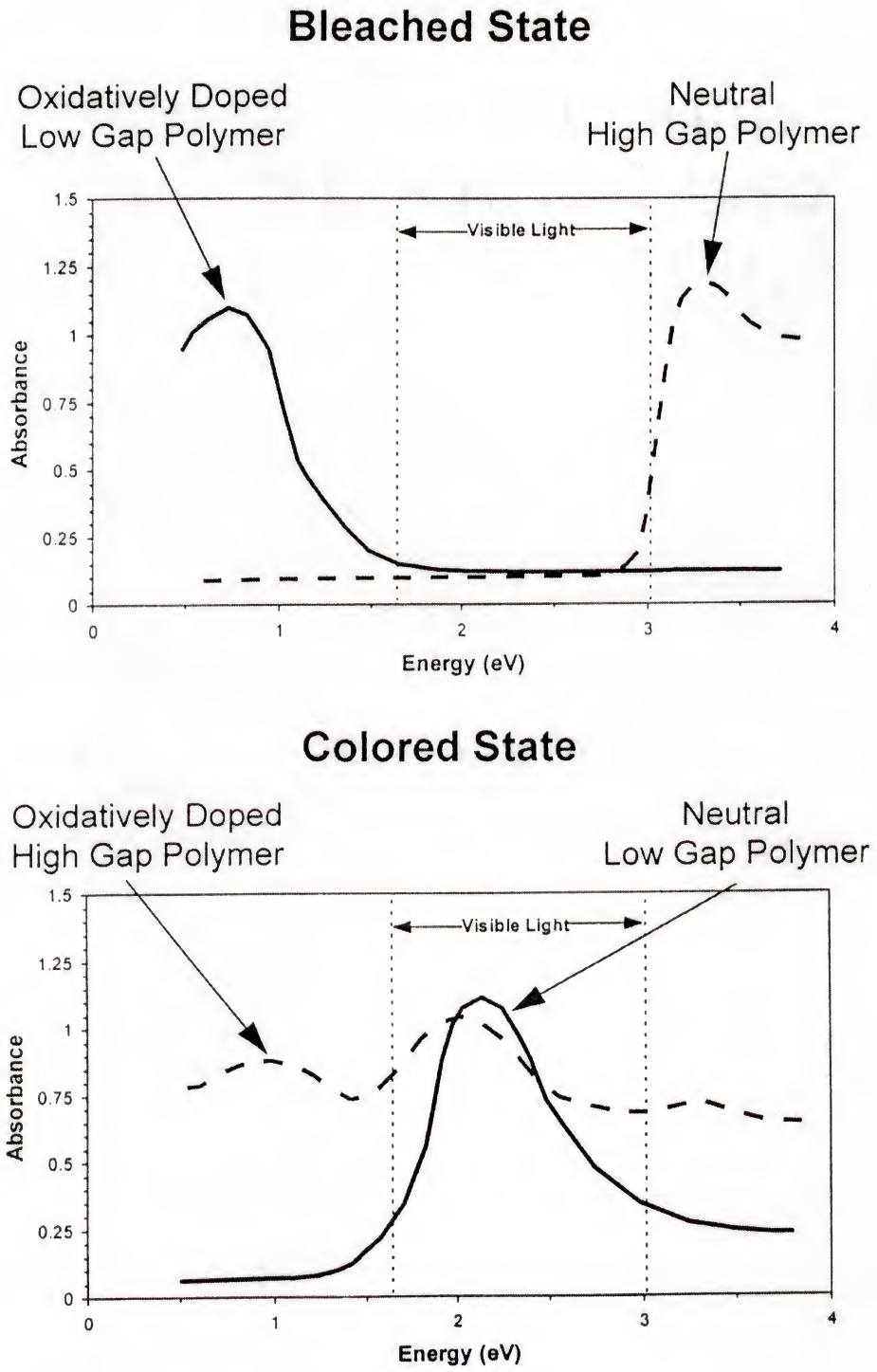

Figure 1.11 Schematic representation of the visible spectra for both an anodically and cathodically coloring polymer demonstrating the concept of dual polymer ECDs for absorptive/transmissive windows.[102]

(see solid line in the bottom portion of Figure 1.11). When oxidized, its main absorbance moves to the near-IR and it becomes very transmissive and lightly colored (see solid line in the top portion of Figure 1.11). For these devices PEDOT and derivatives of PEDOT were used, as it satisfies these criteria. In an ideal anodically coloring polymer, the band gap is high (ca. > 3.0 eV) with the π to π^* absorption found in the ultraviolet region and very little absorption in the visible region (see dashed line in the top portion of Figure 1.11), leading to a transmissive, lightly colored neutral form. Upon oxidation, charge carrier absorptions are present in the visible region and the material becomes more deeply colored (see dashed line in the bottom portion of Figure 1.11). Polymers composed of EDOT and carbazole units were chosen as the anodically coloring polymers, as they exhibit a band gap of 2.5 eV and switch from a highly transmissve yellow when reduced to a dark blue when oxidized. When the devices are constructed, one polymer is doped and one is in its neutral form. Reversal of the potential oxidizes the neutral polymer and neutralizes the doped polymer inducing either color formation or bleaching. Of course, choice of polymers for these devices is important. In addition to the color requirement discussed above, the polymers must have high contrast ratios, rapid response times, and good stability.

1.11 Thesis of this Work

This work focuses on the synthesis of new electrochromic polymers as high contrast and multi-color electrochromic materials. More specifically, this work tries to answer the question, how does the chemical structure of the polymer backbone modify the electrochromic properties of conducting polymers? The synthesis of many new

alkylenedioxythiophene monomers was accomplished, where the alkylenedioxy ring size and pendant group substitution was changed. These monomers were electropolymerized to form novel cathodically coloring polymers which exhibit high contrast ratios, rapid response times, and high coloration efficiencies. Through Grignard metathesis polymerization, soluble alkylenedioxthiophene polymers were synthesized and characterized fully by NMR, GPC, MALDI, TGA, and electrochemical and solution doping. These polymers exhibit electrochemical and spectroelectrochemical results that are very similar to those of the electropolymerized derivatives of comparable structure. Finally, extended conjugation monomers containing EDOT and thiophene heterocycles and carbazole or diphenyamine derivatives were synthesized which yield novel low oxidation potential, three color polymers upon electropolymerization. The unsubstituted carbazole and diphenyamine containing polymers open up the possibility of easy nitrogen substitution that could be used to synthesize many derivatives from one molecule or polymer.

CHAPTER 2
ELECTROPOLYMERIZED POLY(3,4-ALKYLENEDIOXYTHIOPHENE)S

2.1 Introduction

Building on the previously discussed benefits of 3,4-ethylenedioxythiophene (EDOT) as a monomer for electropolymerization, a series of 3,4-alkylenedioxythiophene derivatives (XDOTs) were synthesized to study the effect of pendant groups and alkylenedioxy ring size on the electronic, optical, and conductive properties of the resulting polymers. This chapter will outline the synthesis, electropolymerization, spectroelectrochemistry, and electrochromic properties of these materials.

2.2 Monomer Synthesis

2.2.1 Synthesis of XDOTs (**4a-h**) via Williamson Etherification

The first method used to synthesize XDOTs involved a double Williamson etherification reaction. This method was used to synthesize the original eight XDOT derivatives as outlined in Figure 2.1. The etherification step from **1** to **2** is the key step in the process. When primary bromides are used, this reaction occurs in good yields (50 to 84%), but when a secondary bromide is used, yields decrease significantly (21 to 40%). The ring-closed product then undergoes saponification to compound **3** in good yields (74

to 95%). The final step is decarboxylation using copper chromite to yield the final monomer **4** in moderate yields (45 to 64%).

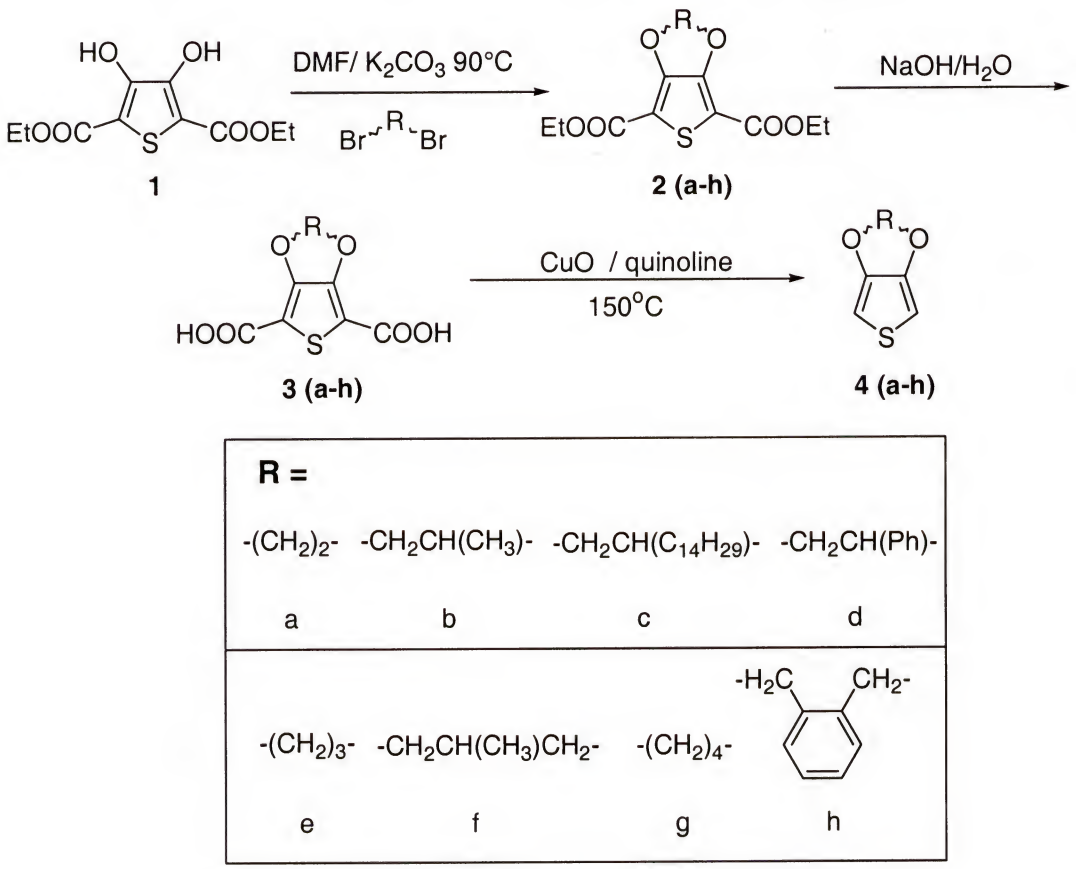

Figure 2.1 Synthesis of 3,4-alkylenedioxythiophenes via Williamson etherification.

2.2.2 Synthesis of ProDOTs (**10a-d**) via Transetherification

Of the derivatives synthesized, 3,4-propylenedioxythiophene (ProDOT) has an interesting structure, because it can be symmetrically substituted on the central carbon of the propylene bridge. Originally, the Williamson etherification between compound **1** and neopentylglycol was attempted to make dimethyl substituted ProDOT. Unfortunately,

this reaction only afforded starting material. This is not surprising, as the Williamson etherfication is an S_N2 process and does not proceed well with branched or neopentyl type substrates. Because of this failed reaction, a new type of reaction was needed.

Fortunately, disubstituted ProDOTs can be synthesized using a transetherification reaction as shown in Figure 2.2.[103, 104] Initially, thiophene is exhaustively brominated to yield **6**, which is then debrominated using zinc metal to yield compound **7**. Substitution of bromides with methoxy groups yield compound **8**, which is then used in the transetherification reaction to yield the disubstituted ProDOT derivatives **10(a-d)**. This

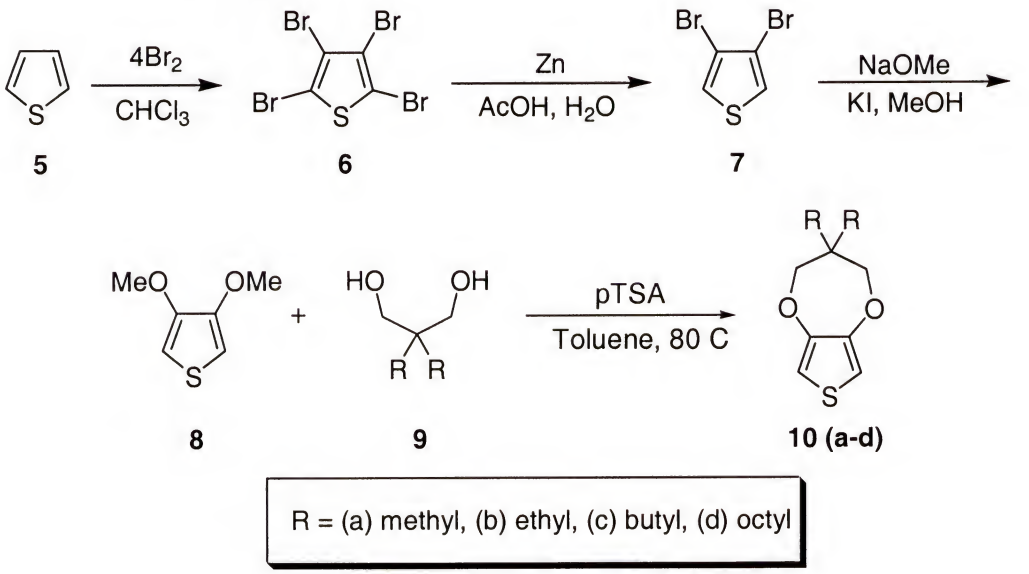

Figure 2.2 Synthesis of disubstituted ProDOTs via transetherification

reaction occurs in good yield (68 – 84 %) and was driven to completion by removal of the condensate, methanol, from the system. This was accomplished by use of a soxhlet extractor filled with type 4A molecular sieves.

2.3 Monomer Structure and Properties

The XDOTs have varying physical properties depending on the type of substitution. EDOT (**4a**), EDOT-Me (**4b**), BuDOT (**4g**), ProDOT-Bu_2 (**10c**), and ProDOT-Oct_2 (**10d**) are all liquids at room temperature, while EDOT-$C_{14}H_{29}$ (**4c**), EDOT-Ph (**4d**), ProDOT (**4e**), BuDOT-Xyl (**4h**), ProDOT-Me_2 (**10a**), and ProDOT-Et_2 (**10b**) are solids. As expected, when the molecular weight is increased significantly relative to EDOT, the monomers are solids. This changes in the longer chain ProDOT-R_2 derivatives, because the long alkyl chains introduce more degrees of freedom that prevent crystallization. Interestingly, when the ring size is increased from two to three carbons, from EDOT to ProDOT, a nicely crystalline solid is obtained, but when the ring size is further increased to four carbons, as in BuDOT, a liquid is obtained again. A crystal structure was obtained for ProDOT to try and explain this phenomenon, and it is shown in Figure 2.3. The crystallization of ProDOT can be attributed to strong intermolecular interactions between oxygen (O1 and O1A) and the adjacent thienyl hydrogen (H1 and H1A) as depicted in the dimer unit formed within the crystal structure. It is speculated that this interaction occurs only in ProDOT, because the seven membered ring orients the lone pairs on the oxygen in such a way to make this intermolecular interaction favorable. The crystal structure for the monomer unit of EDOT-Ph is shown in Figure 2.4. In this instance there are no intermolecular interactions. Of interest here is the fact that the phenyl ring is nearly (73.8°) orthogonal to the thiophene ring, suggesting that the phenyl group will serve to separate polymer chains in the solid state.

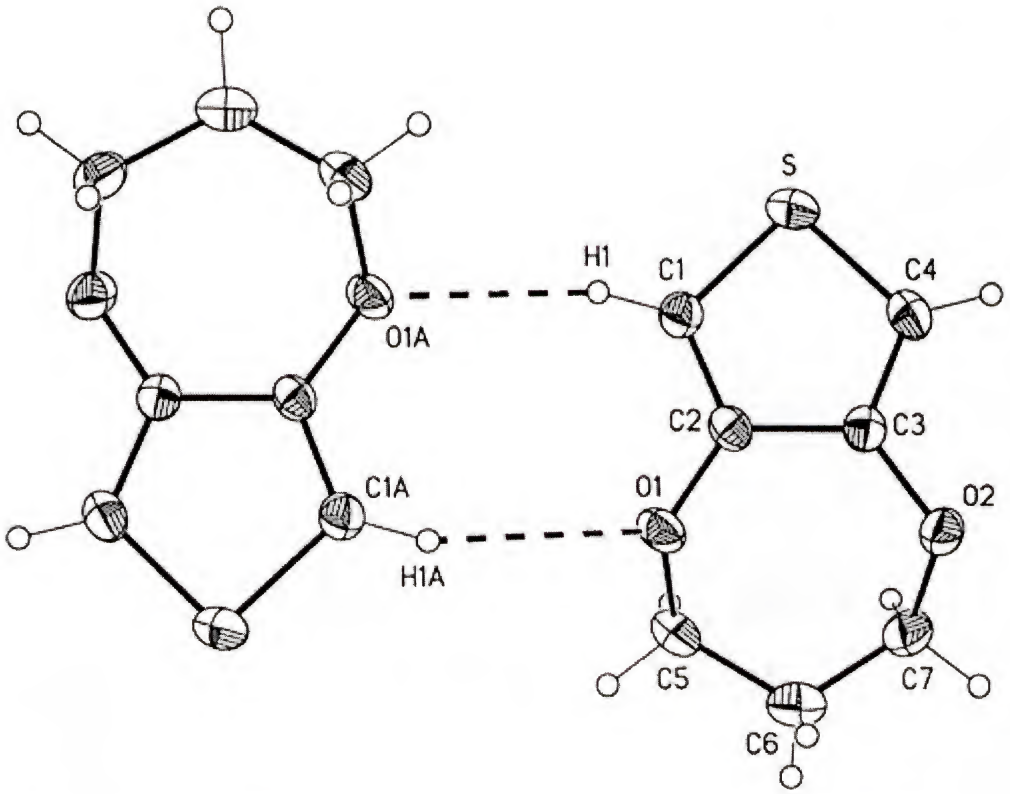

Figure 2.3 View of two adjacent molecules and atom labeling of the crystal structure of ProDOT.

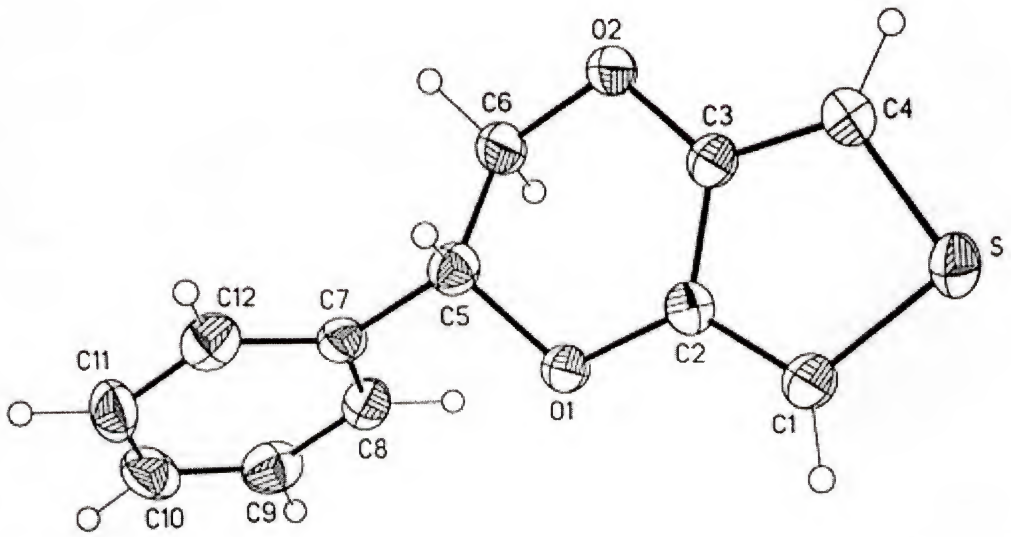

Figure 2.4 Perspective view and atom labeling of the crystal structure of EDOT-Ph.

2.4 Electropolymerization

2.4.1 Repeated Scan Electropolymerization Background and Techniques

As noted in Chapter 1, heterocyclic monomers such as thiophene can be polymerized electrochemically to form electroactive polymers on conducting substrates. In this process, when a potential is applied, the monomer approaches the working electrode surface, where it is oxidized. Oxidized monomers then couple to form oligomers, which deposit onto the electrode surface when they become insoluble in the polymerization medium.

Electropolymerization can be accomplished using cyclic voltammetry[105] with a standard three-electrode setup. Because it usually takes more than one scan to synthesize a conducting polymer film on the electrode surface, this technique is called repeated scan electropolymerization. A dilute solution of monomer is used in a solvent that is suitable for electrochemistry. Typically, solvents with high dielectric constants, such as acetonitrile, are ideal for electrochemistry. Solvents must also be electrochemically inert and non-nucleophilic. In addition to solvent, a supporting electrolyte must be used. The electrolyte serves to help current pass through the solution, and also to compensate charges that form on the polymer during oxidation and reduction (i.e., in this work the perchlorate ion serves as a dopant ion). In a typical experiment, the potential starts at a reducing value, and is scanned anodically until monomer oxidation and polymerization occurs. Subsequently, the potential is scanned cathodically back to the original value, where reduction of the polymer which has deposited on the electrode occurs. Repeated scanning causes more polymerization to occur, and more polymer to form on the electrode surface.

2.4.2 Electropolymerization of XDOTs (**4a-h**) and ProDOTs (**10a-d**)

A schematic diagram representing the repeated scan electropolymerization of the XDOT and ProDOT monomers and the subsequent polymer redox switching is shown in Figure 2.5. (The acronyms listed in Figure 2.5 will be used in place of compound numbers for the rest of the document.) Figure 2.6 shows the electropolymerization of a 0.01 M solution of BuDOT in 0.1 M tetrabutylammoniumperchlorate (TBAP) / acetonitrile (ACN), which is representative of all of the monomers. Starting at –1.0 V, the potential is scanned anodically until monomer oxidation occurs. The onset of monomer oxidation at the bare electrode is 0.9 V and peaks ($E_{p,\,m}$) at 1.1 V. These values stay relatively constant for all of the monomers. The value of the monomer oxidation potential is very important, where lower oxidation potentials mean less side reactions which leads to better-defined and stable polymers. The high oxidation potential (~2.0 V) of thiophene results in many degradative side reactions. However, the electron-donating oxygen substituents on the XDOTs and ProDOTs clearly reduce the oxidation potential by more than one volt, leading to milder polymerization conditions and less side reactions. On repeated scanning, a thin insoluble polymer film forms on the electrode surface. On the reverse scan, reduction of the polymer occurs around –0.1 V, and this peak increases in intensity with repeated scanning. The polymer oxidation is observed at –0.1 V, and this peak also increases with repeated scans. The current response for the monomer oxidation also increases with repeated scanning. This indicates that the polymer forming on the electrode is porous and conductive, and the current increase is due to greater electrode surface area.

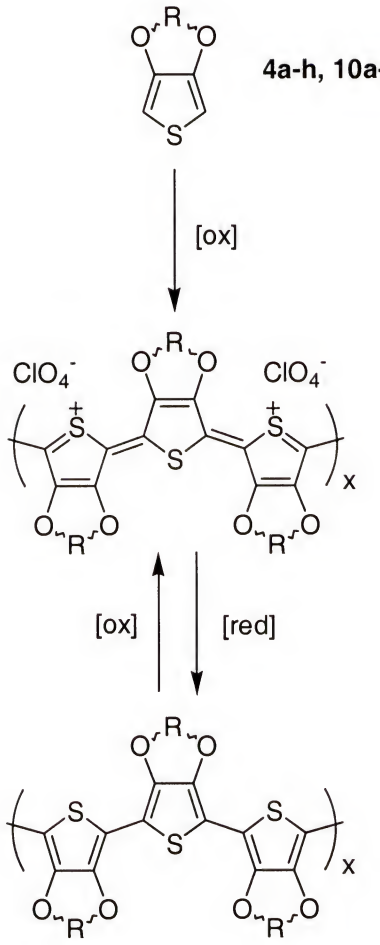

R = -$(CH_2)_2$-	**4a**: EDOT	**P4a**: PEDOT
R = -$CH_2CH(CH_3)$-	**4b**: EDOT-Me	**P4b**: PEDOT-Me
R = -$CH_2CH(C_{14}H_{29})$-	**4c**: EDOT-$C_{14}H_{29}$	**P4c**: PEDOT-$C_{14}H_{29}$
R = -$CH_2CH(Ph)$-	**4d**: EDOT-Ph	**P4d**: PEDOT-Ph
R = -$(CH_2)_3$-	**4e**: ProDOT	**P4e**: PProDOT
R = -$CH_2CH(CH_3)CH_2$-	**4f**: ProDOT-Me	**P4f**: PProDOT-Me
R = -$(CH_2)_4$-	**4g**: BuDOT	**P4g**: PBuDOT
R = 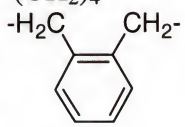	**4h**: BuDOT-Xyl	**P4h**: PBuDOT-Xyl
R = -$CH_2C(CH_3)_2CH_2$-	**10a**: ProDOT-Me_2	**P10a**: PProDOT-Me_2
R = -$CH_2C(CH_2CH_3)_2CH_2$-	**10b**: ProDOT-Et_2	**P10b**: PProDOT-Et_2
R = -$CH_2C((CH_2)_3CH_3)_2CH_2$-	**10c**: ProDOT-Bu_2	**P10c**: PProDOT-Bu_2
R = -$CH_2C((CH_2)_7CH_3)_2CH_2$-	**10d**: ProDOT-Oct_2	**P10d**: PProDOT-Oct_2

Figure 2.5 Representation of the repeated scan electropolymerization of XDOTs(**4a-h**) and ProDOTs(**10a-d**) including redox switching of the polymers.

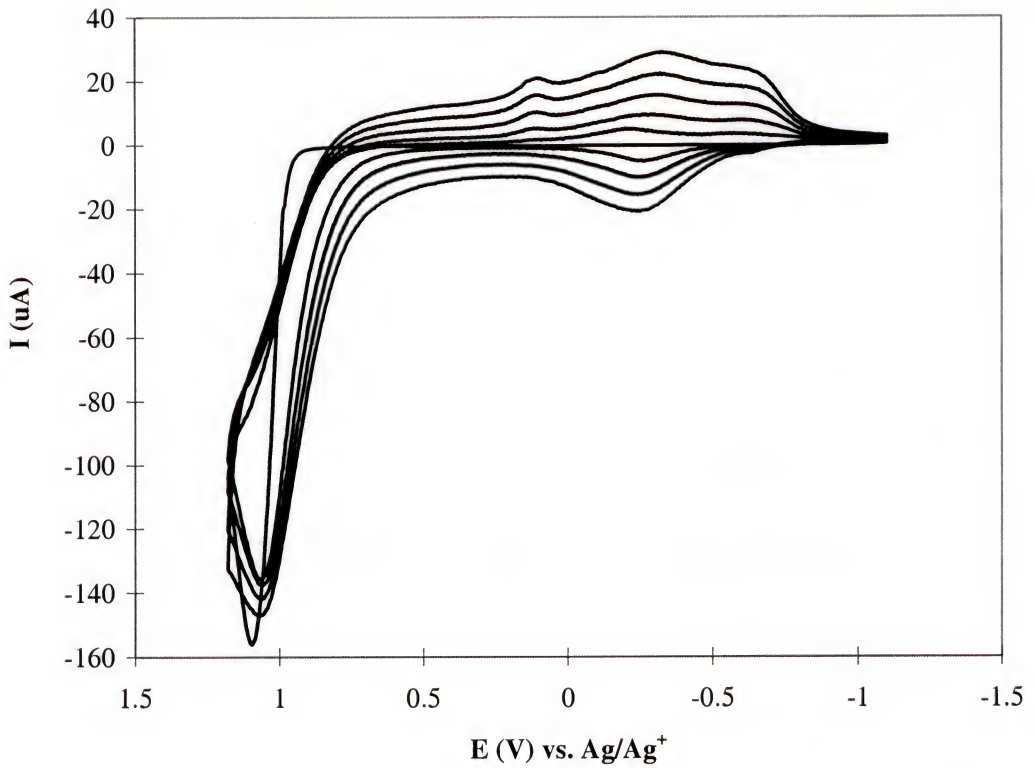

Figure 2.6 Repeated scan electropolymerization from a 0.01 M solution of BuDOT (**4g**) in 0.1 M TBAP/ACN at a scan rate of 100 mV/s on a platinum button.

2.5 Polymer Electrochemistry

2.5.1 Cyclic Voltammetry Background

In cyclic voltammetry (CV), the potential is increased linearly from an initial potential to a peak potential and back to the initial potential again, while the current response is measured. For freely diffusing species, as the potential is increased, easily oxidized species near the electrode surface react, and a current response is measured. When the direction of the scan is reversed, the oxidized species near the electrode surface

are reduced, and again a current response is measured. The Randles-Sevick equation[106] states that the peak current is given by:

$$i_p = (2.69 \times 10^5)n^{3/2}AD^{1/2}C^b\nu^{1/2} \quad (2\text{-}1)$$

where n is the number of electrons, A is the surface area of the electrode (cm^2), D is the diffusion constant (cm^2 / s), C^b is the bulk concentration of electroactive species (mol / cm^3), and ν is the scan rate (V / s). Therefore, for a diffusion-controlled system, the peak current is proportional to the square root of the scan rate.

Of course the rules change in electroactive polymer electrochemistry, because the polymer is adhered to the electrode surface. Therefore, the process is not diffusion controlled, and cannot be described by the Randles-Sevick equation discussed above. Instead, the peak current for a surface bound species is given by the following equation[107,108]:

$$i_p = n^2F^2\Gamma\nu / 4RT \quad (2\text{-}2)$$

where Γ is the concentration of surface bound electroactive centers (mol / cm^2) and F is Faradays constant (96, 485 C / mol). Thus, if a species is surface bound, both the anodic and cathodic peak current will scale linearly with scan rate. In a scan rate dependence experiment, the electroactive polymer is washed and placed in monomer-free electrolyte solution, and the polymer is then cycled between its oxidized and reduced forms at various scan rates while the i_p of both oxidation ($i_{p,a}$) and reduction ($i_{p,a}$) is monitored. If

the i_p scales linearly with scan rate, then the process is said to be non-diffusion controlled, and the electroactive centers of the polymer are adhered to the electrode surface.

2.5.2 Polymer Electrochemistry of PXDOTs (**P4a-h**) and PProDOTs (**P10a-d**)

The scan rate dependence of the polymer redox was studied in monomer-free 0.1 M TBAP/ACN solutions for each polymer. In all cases, a linear relationship was found between the peak current and scan rate, thus indicating that the electroactive centers of the polymers are adhered to the electrode surface. All of the polymers exhibit low oxidation potentials when compared to other polythiophenes. This low oxidation potential is beneficial in that it allows the polymers to be cycled at lower potentials, which leads to less degradative side reactions. In most polymers, the polymer redox occurs with an $E_{1/2}$ at –0.2 V, which is the same as the parent polymer PEDOT. In the PProDOT derivatives, this value increases slightly to –0.1 V, which can be attributed to the change in orientation of the oxygen lone pairs as discussed previously in reference to the ProDOT crystal structure. If the lone pairs are more available for intermolecular interactions, then the orbital overlap with the thiophene is weakened, leading to a slightly higher oxidation potential. As an example, Figure 2.7 shows the polymer electrochemistry for PProDOT-Me_2 (**10a**), this behavior is representative of the other polymers as well.

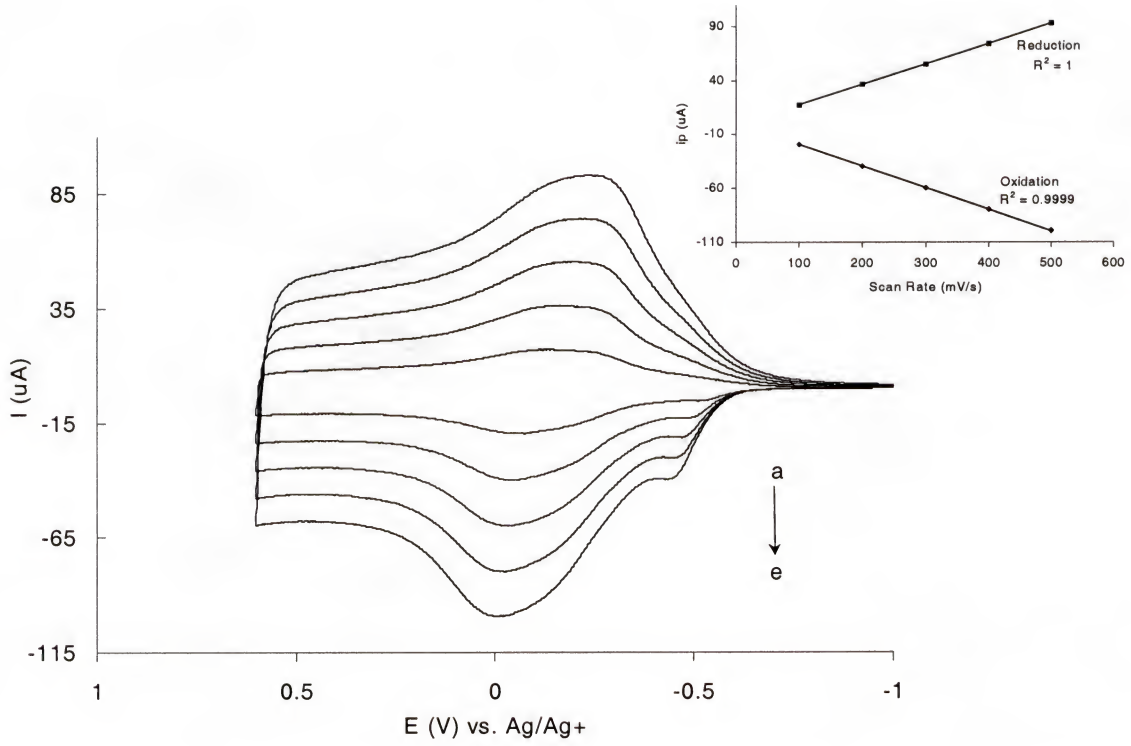

Figure 2.7 Scan rate dependence of PProDOT-Me_2 (**10a**) in 0.1 M TBAP/ACN at the following scan rates: (a) 100 (b) 200 (c) 300 (d) 400 (e) 500 mV/s. Inset graph displays the peak current vs. scan rate for oxidation and reduction with R-squared values displayed.

2.6 Spectroelectrochemistry

2.6.1 Background and Techniques

The redox switching of conjugated polymers is accompanied by changes in electronic transitions. These absorption changes are what make conjugated polymers useful in electrochromic applications such as smart windows, mirrors, etc. The electronic transitions of conjugated polymers have been the subject of many articles, and these transitions are nicely illustrated by using band theory as introduced in Chapter 1.[109,110,111]

Figure 2.8 shows the expected transitions in a conjugated polymer as described by Fesser et al.. (FBC Theory).[112] In the neutral state the polymer exhibits one transition from the valence band to the conduction band (π to π^*). The energy difference between these two levels is the band gap (E_g), and it is measured as the onset of the π to π^* absorption in the neutral state of the polymer. Initial oxidation of the polymer results in the formation of a radical cation or a polaron, which is free to move along the polymer chain. This also removes one electron from the valence band, resulting in an energy state with an unpaired electron that appears higher in energy than the valence band. There is also a lowering of the corresponding antibonding level in the conduction band, and two intragap states are introduced. This should lead to four new transitions, but FBC theory indicates that the oscillator strength of transitions **a** and **b** (Figure 2.8) are much greater than transition **c** or **d**. Therefore, two low energy transitions are expected as the signature for a polaron. Further oxidation of the polymer can either create more polarons by the removal of electrons from the valence band, or the unpaired electron of the polaron can be removed to form a dication or bipolaron. Because the bipolaron levels are unoccupied, there can only be transitions from the valence band. FBC theory indicates that transition **e** is much stronger than transition **f**, so the signature of a bipolaron is one low energy transition.

These electronic transitions can be probed by the use of UV-Vis-Near Infrared (NIR) spectroscopy. Spectra are recorded while the polymer is oxidized by increasing the potential stepwise. This experiment is commonly referred to as spectroelectrochemistry, and can be easily accomplished by constructing a three-electrode cell inside a normal cuvette.

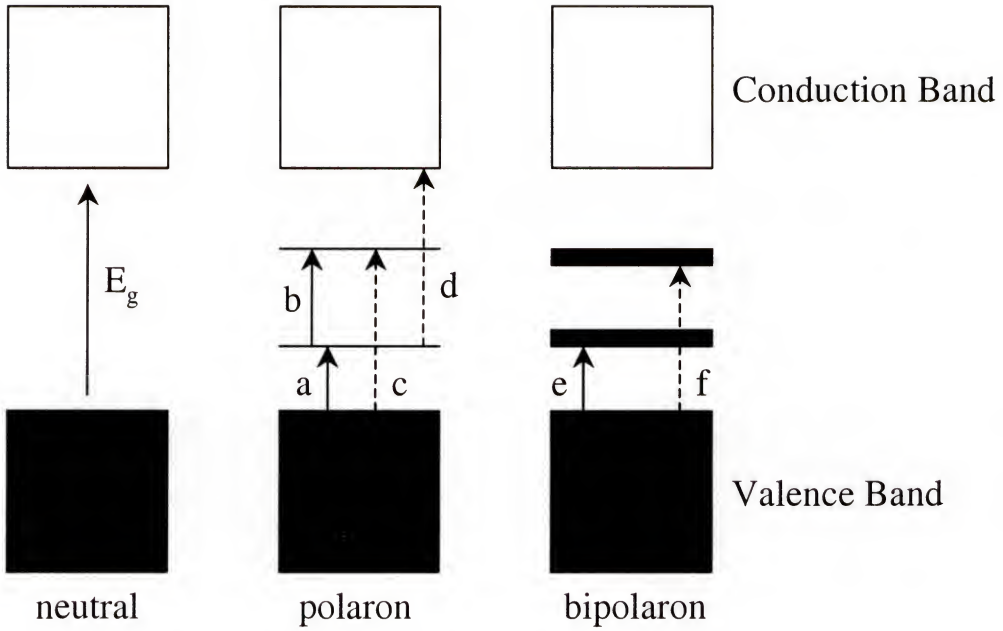

Figure 2.8 Electronic transitions in conjugated polymers in the neutral, polaron, and bipolaron state. Strongly allowed transitions are indicated with a solid arrow.

For these experiments, polymer films were synthesized on a glass slide coated with indium tin oxide (ITO) from a 0.01 M solution of monomer in 0.1 M TBAP/ACN. The polymers are synthesized by application of a constant potential, and during polymerization, the charge is monitored and is correlated to film thickness. After the desired charge is obtained, the polymerization is stopped; the polymer is reduced, washed with electrolyte solution, and placed in a cuvette that is equipped with a reference electrode (Ag / Ag^+) and a Pt wire counter electrode. The reference and counter electrodes must be carefully kept out of the path of the spectrophotometer beam. This cell is then connected to a potentiostat, and the polymer is oxidized stepwise (normally in 0.1 V steps) while obtaining a spectrum at each potential.

2.6.2 Spectroelectrochemistry of PXDOTs (**P4a-h**)

A spectroelectrochemical series for PEDOT in 0.1 M TBAP/ACN is shown in Figure 2.9. The neutral form of the polymer shows a distinct π to π* transition with a band gap of 1.6 eV, and a peak at 2.0 eV. Stepwise oxidation of the polymer shows reduction in absorbance throughout the visible region (1.7 to 3.1 eV) as the color changes from a dark blue, absorptive state to a highly transmissive, oxidized state. As the polymer is oxidized, the lower energy polaron peaks grow in at 1.25 eV and less than 0.75 eV. As the polymer is more fully oxidized, or at +0.3 V for PEDOT, the peak at

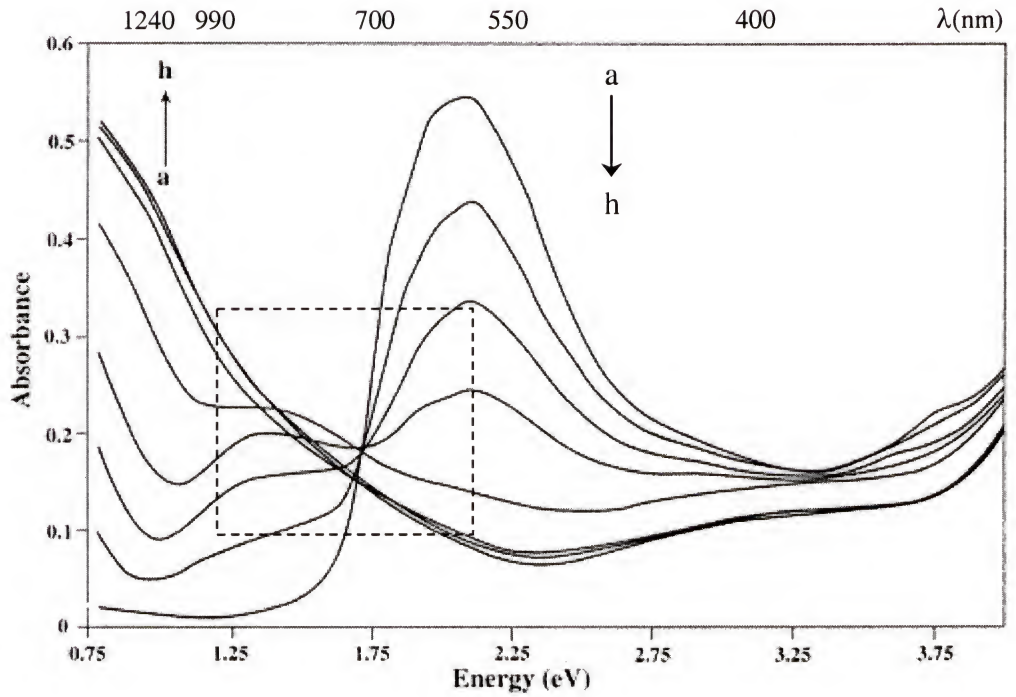

Figure 2.9 Spectroelectrochemistry of PEDOT in 0.1 M TBAP/ACN at applied potentials of: (a) –0.3 V, (b) –0.1, (c) 0, (d) +0.1, (e) +0.2, (f) +0.3, (g) +0.6, (h) +1.2 V vs. Ag/Ag^{+}.

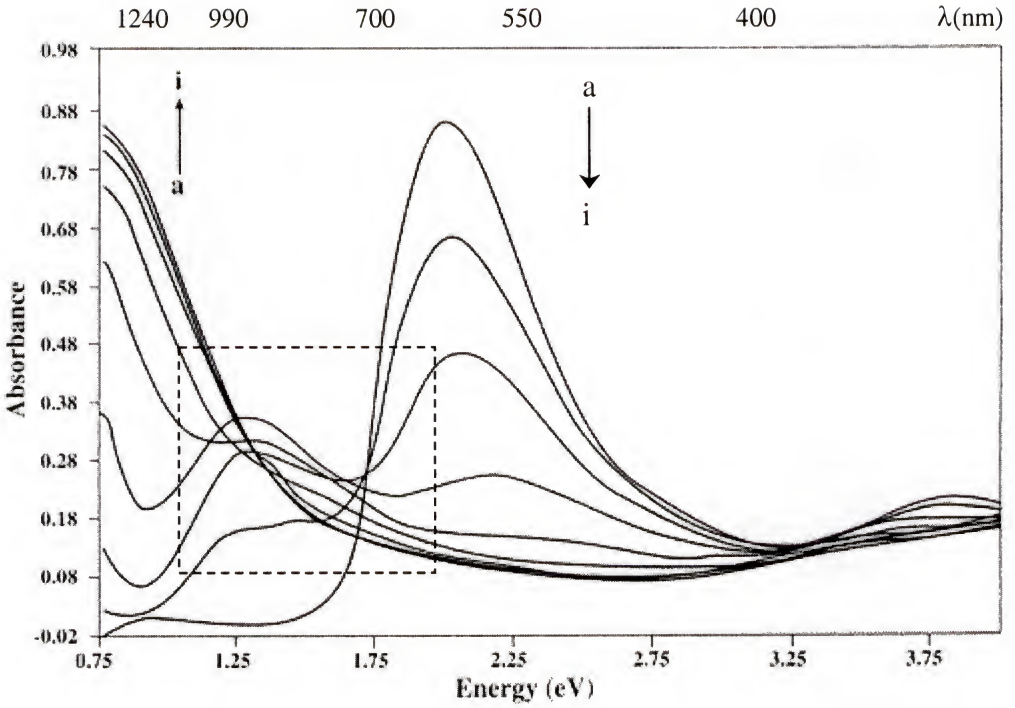

Figure 2.10 Spectroelectrochemisty of PEDOT-Ph in 0.1 M TBAP/ACN at applied potentials of: (a) –0.3 V, (b) –0.1, (c) +0.1, (d) +0.3, (e) +0.5, (f) +0.7, (g) +1.0, (h) +1.3, (i) 1.5 V vs. Ag/Ag^{+}.

1.25 starts to disappear, leaving only one low energy peak in the near IR. This suggests that in the more fully oxidized form, the charge carriers are predominantly bipolarons.

The spectroelectrochemistry of PEDOT-Ph is shown in Figure 2.10. Again, the neutral form of the polymer shows a distinct π to π^* transition with a band gap of 1.6 eV, and a peak at 2.0 eV. Upon oxidation the π to π^* transition decreases, and the polaron transitions increase in intensity until +0.3 V; again one peak in the NIR is formed due to bipolaric charge carriers. The difference between PEDOT-Ph and PEDOT is that the spectrum for the fully oxidized form for PEDOT-Ph does not "tail" as much through the visible region (see the region outlined by the dashed box in Figures 2.9 and 2.10), leading

to a more transparent oxidized form. This type of behavior is seen in all of the polymers (**P4c-g**) with larger ring sizes and pendant groups.

The PProDOT family of polymers shows the most interesting spectroelectrochemistry results of the polymers investigated. Figure 2.11 shows a spectroelectrochemical series for PProDOT. Notice that the band gap is slightly higher in these derivatives (1.75 eV) relative to the PEDOT case. This can be attributed to the decrease in overlap between the p-orbitals of the oxygen lone pairs and the thiophene ring, but the band gap does not increase dramatically, and the polymer is dark blue-purple in its reduced form. Unlike PEDOT, PProDOT exhibits a split interband transition with peaks

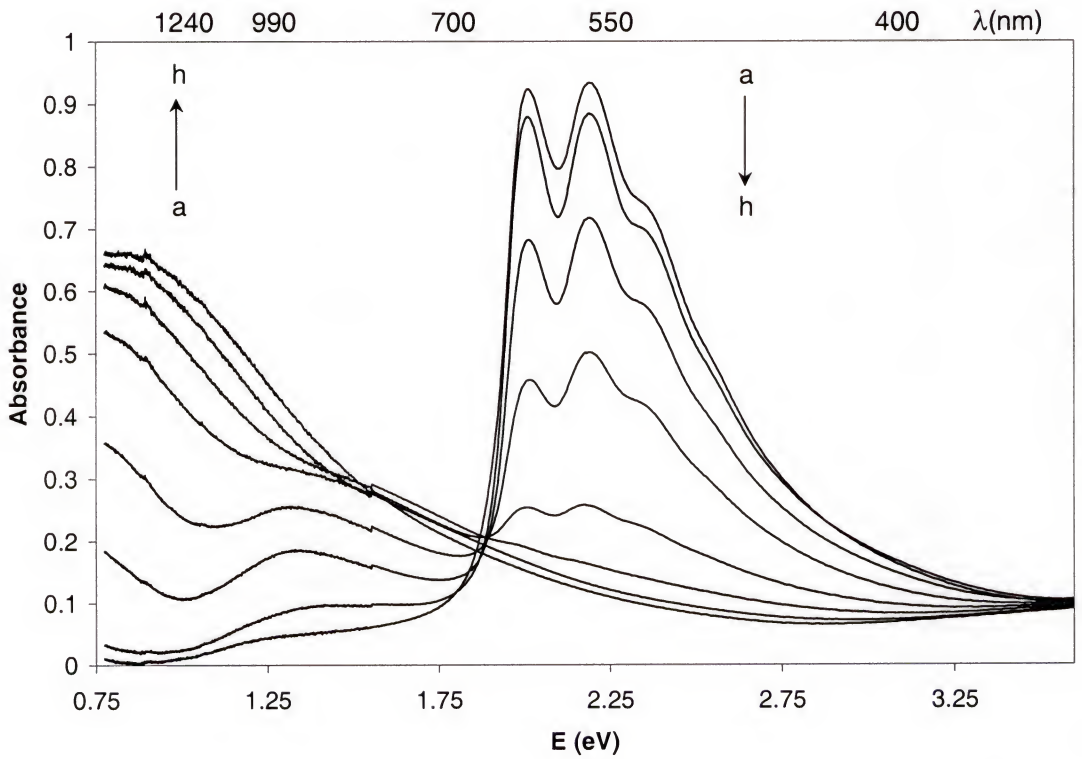

Figure 2.11 Spectroelectrochemistry of PProDOT in 0.1 M TBAP/ACN at applied potentials of: (a) –1.0 V, (b) –0.2, (c) 0, (d) +0.1, (e) +0.2, (f) +0.3, (g) +0.5, (h) +1.0 V vs. Ag/Ag^{+}.

at 2.0 and 2.2 eV. This splitting also occurs in PEDOT-$C_{14}H_{29}$[113] and in PEDOT-C_6H_{13}[114] and is attributed to vibronic coupling which suggests a high degree of regularity along the polymer backbone.[115] Similar to the other derivatives, the higher energy polaron peak in PProDOT decreases in the highly oxidized state as one bipolaron peak is formed at low energy.

The disubstituted PProDOT derivatives show the most promise as high contrast electrochromic polymers. The structure of this polymer combines a larger seven-membered ring with pendant groups. The spectroelectrochemistry of PProDOT-Me_2 is shown in Figure 2.12. The spectoelectrochemistry is very similar to that of PProDOT

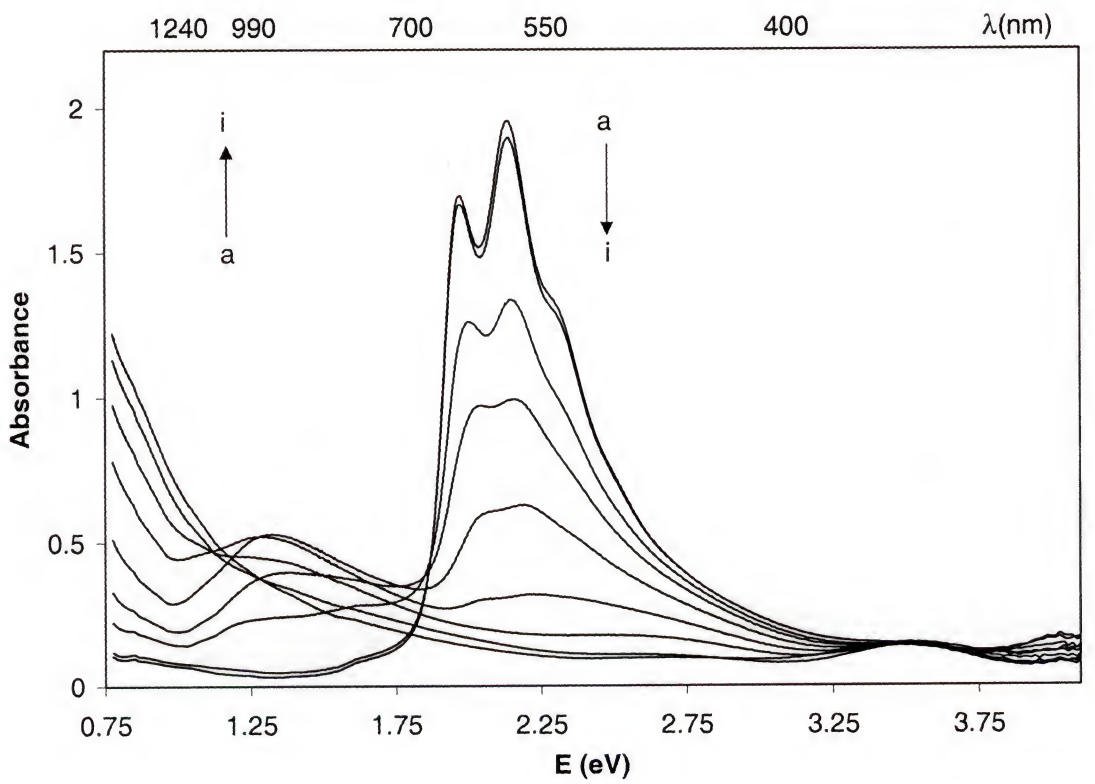

Figure 2.12: Spectroelectrochemistry of PProDOT-Me_2 in 0.1 M TBAP/ACN at applied potentials of: (a) –1.0 V, (b) –0.6, (c) –0.3, (d) –0.2, (e) –0.1, (f) 0, (g) +0.1, (h) +0.3 V, (i) +1.0 V vs. Ag/Ag^+

with a similar band gap and vibronic coupling. The main difference is in the fully oxidized form. Again, the polaron peak at 1.3 eV starts to disappear after a potential of 0 V is reached. At +1.0 V, there is only one peak in the NIR indicating that bipolarons are the prominent charge carriers. Reflectance spectroscopy performed by our group, which measures from the mid-IR to the UV (0.25 to 4 eV), also shows that PProDOT-Me_2 has only one peak in the NIR in the doped form. The peak is also sharper than in the case of PProDOT, leading to less absorption in the visible region and a more transmissive oxidized form. Because of these interesting spectroelectrochemical properties, the optical properties of these polymers were studied in detail with switching repeated switching studies and coloration efficiency analyses.

2.7 Electrochromic Switching

2.7.1 Background and Techniques

For electrochromic applications, the ability of a polymer to switch rapidly and to exhibit a striking color change is important. Also, there are many applications that require a transparent conductive material. Electrochromic switching studies can monitor these types of properties.

A square wave potential step method coupled with optical spectroscopy known as chronoabsorptometry is used to probe switching times and contrast in these polymers. In this double potential step experiment, the potential is set at an initial potential for a set period of time, and is stepped to a second potential for a set period of time, before being

switched back to the initial potential again. During the experiment, the % transmittance (%T) at λ_{max} of the polymer is measured using a UV-Vis-NIR spectrophotometer.

The set-up for chronoabsorptometry is the same as for spectroelectrochemistry as described in Section 2.6.1. The polymer film is synthesized on ITO-coated glass slides using constant potential polymerization until the desired film thickness or charge is obtained. The %T is then monitored at λ_{max} while the polymer is switched from –1.0 V to +1.0 V. The contrast is measured as the difference between %T in the reduced and oxidized forms and is noted as Δ%T. Response times are measured as explained for each experiment.

2.7.2 Electrochromic Switching of PXDOTs (**P4a-h**)

Before transetherification allowed the synthesis of disubstituted PProDOTs, five of the PXDOT derivatives (PEDOT, PProDOT, PBuDOT, PEDOT-$C_{14}H_{29}$, and PEDOT-Ph) were subjected to electrochromic switching studies. For each polymer, film thickness was determined to be linearly proportional to charge density. Changes in film thickness as a function of charge density values over the thickness range of 100 to 250 nm are listed in Table 2.1. All of the polymers except PEDOT-$C_{14}H_{29}$ have comparable film thickness for a given charge density, while PEDOT- $C_{14}H_{29}$ is about six times as thick for a given charge. It is likely that the long alkyl chains hold the conjugated backbones apart from one another, leading to a more expanded morphology.

For electrochromic switching studies, polymer films of constant thickness (ca. 300 nm) were switched by repeated potential steps between their reduced (-1.0 V) and oxidized (+1.0 V) states in 0.1 M TBAP/ACN. In these studies, the Δ%T of the polymer

films were monitored as a function of time at a constant wavelength near λ_{max} (590 nm). For this study, response times were measured as time to oxidize at full contrast. It should be noted that the techniques used to measure response times in the electrochromic literature are varied and often undefined.[100] In latter sections (see below), we attempt to define a sensible standard in measuring response times. To allow a comparison of the systems, the results of these switching studies for PEDOT and PBuDOT are shown in Figures 2.13 and 2.14. In the case of PEDOT and PProDOT, the response time to full contrast was found to be 2.2 s, whereas it was found to be 1.3 s for PBuDOT. In addition, PEDOT-$C_{14}H_{29}$ and PEDOT-Ph response times were found to be even faster at 0.8 s. Reviewing these results, it is evident that increasing ring size or size of the substituent on the alkylenedioxy bridge reduces the response time. This trend is not surprising, as more highly substituted polymers should polymerize to a morphology

Table 2.1 Electrochromic properties for PXDOTs derivatives

Polymer	dt/dQ[a]	Δ%T[b]	Switching Time (s)[b]
PEDOT	5.2	44	2.2
PProDOT	6.0	54	2.2
PBuDOT	5.5	63	1.3
PEDOT-$C_{14}H_{29}$	28.7	63	0.8
PEDOT-Ph	5.8	45	0.8

[a] Change of film thickness (nm) as a function of charge density (mC/cm^2).
[b] As determined by electrochromic switching studies (see text for details).

where the chains are spaced farther apart, therefore allowing faster ion movement, which is often the rate-limiting process, during redox switching.[116] For comparison, poly(3-methyl thiophene) (P3MT) films switch in 4 s with much lower contrasts.[117]

These results also show that the electrochromic contrast (Δ%T) increases with the size of the alkylenedioxy ring from 44% for PEDOT to 54% for PProDOT to 63% for

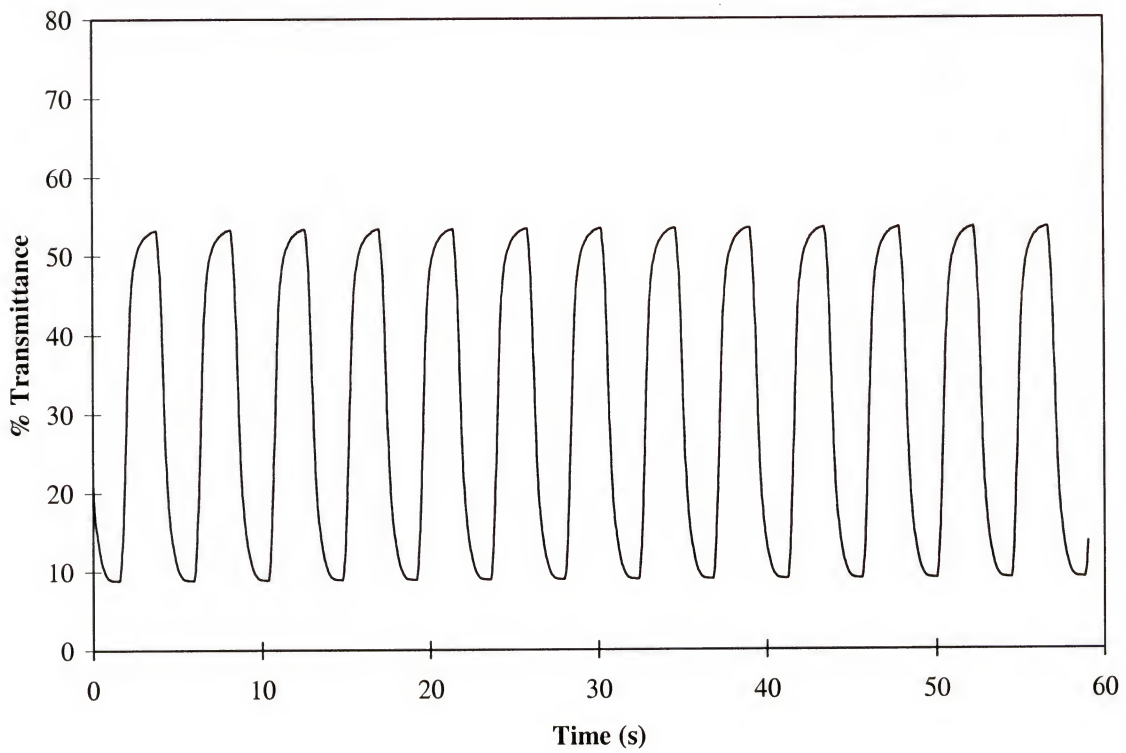

Figure 2.13 Electrochromic switching of PEDOT in 0.1 M TBAP/ACN for one minute of switching (step time 2.2 s) between –1.0 and +1.0 V vs. Ag/Ag^+ at 300 nm film thickness.

PBuDOT. The Δ%T for PEDOT-$C_{14}H_{29}$ and PEDOT-Ph was found to be 63% and 45% respectively. As with the response times discussed above, increasing the ring size or size of the substituent on the alkylenedioxy bridge enhances the electrochromic contrast. The enhanced contrast in all of these derivatives comes from higher %T values in the oxidized

form. This is explained by referring to the spectroelectrochemical results, and the fact that the higher contrast polymers have one bipolaron peak in the NIR, that causes less absorption in the visible region than in PEDOT or P3MT. Apperloo et al.[118] report that poly(3-octylthiophene) (P3OT) can exhibit a highly transmissive state in solution if highly doped with a strong electron acceptor such as thianthrenium perchlorate. Their

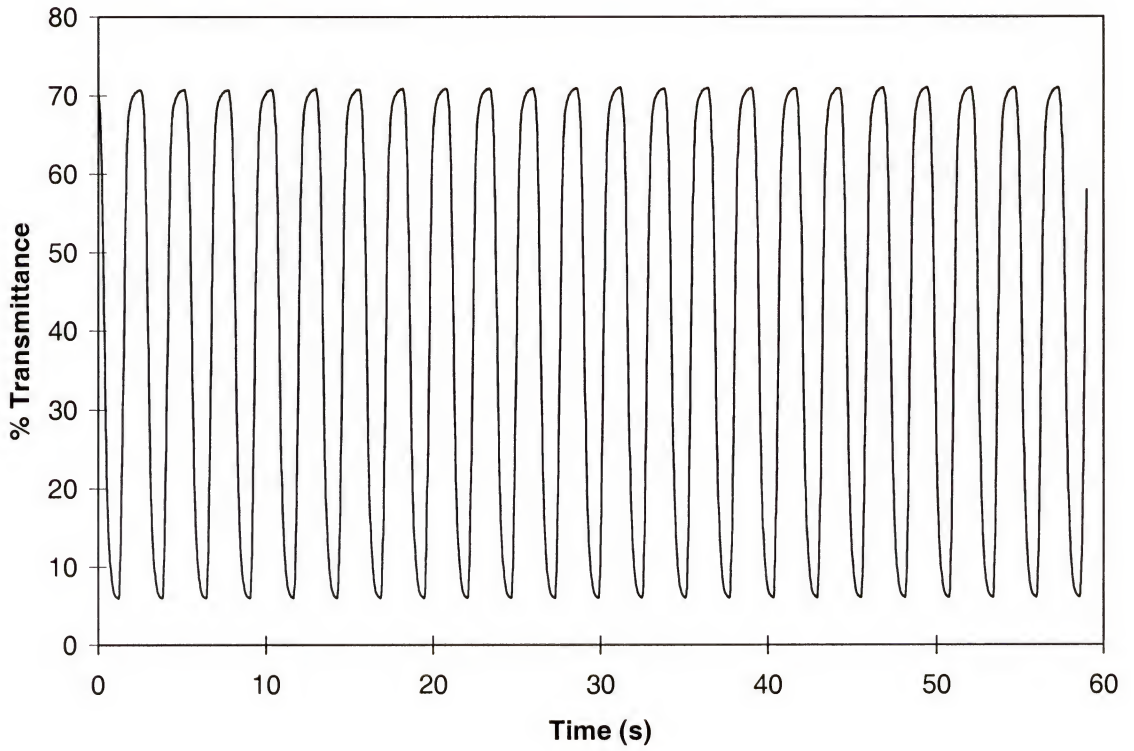

Figure 2.14 Electrochromic switching of PBuDOT in 0.1 M TBAP/ACN for one minute of switching (step time 1.3 s) between –1.0 and +1.0 V vs. Ag/Ag^+ at 300 nm film thickness.

results show that when high doping levels are obtained, polarons on the same chain combine to form bipolarons. At these high doping levels, the UV-Vis-NIR spectra exhibit a single strong electronic absorption in the near-IR region but almost no absorption in the visible region. This is very similar to our results in the solid state. It is

possible that the spaced chains in high contrast PXDOTs allows for a higher doping level than in a more closely packed system. If the polymers are more highly doped, bipolaron formation would be favored, and absorption in the visible region would be suppressed.

2.7.3 Electrochromic Switching of PProDOTs (**P10a-d**)

Once the transetherification reaction was discovered to be a useful tool to synthesize disubstituted PProDOTs, their electrochromic switching could be studied. For electrochromic switching studies, polymer films were synthesized with four different thicknesses from 100 to 250 nm, and each film was potential stepped between its reduced

Table 2.2 Electrochromic properties of PProDOT derivatives

Polymer	dft/dQ[a]	Film Thickness (nm)[b]	Δ%T	t_{ox} (s)[c]	t_{red} (s)[c]
PProDOT	6.0	100	62	0.20	0.29
		150	65	0.35	0.51
		200	42	0.47	0.62
		250	49	0.62	0.79
PProDOT-Me	5.9	100	77	0.27	0.49
		150	74	0.29	0.48
		200	67	0.36	0.58
		250	71	0.47	0.60
PProDOT-Me_2	8.4	100	68	0.18	0.28
		150	78	0.25	0.39
		200	60	0.35	0.79
		250	80	0.43	0.81

[a] Change of film thickness (nm) as a function of charge density (mC/cm^2)
[b] As measured by profilometry
[c] Measured at 95% of full contrast. Standard deviation is ± 0.1 s.

(-1.0 V) and oxidized (+1.0 V) state. During switching, the %T at 578 nm was monitored as a function of time. The results of these studies are summarized in Table 2.2. For each polymer, film thickness was determined to be linearly proportional to charge density. The data from Table 2.2 show that all of the polymers have comparable thickness at a given charge density, with PProDOT-Me_2 growing most rapidly.

As expected from the spectroelectrochemistry results discussed in Section 2.6.2, PProDOT-Me_2 shows a maximum Δ%T of up to 80%, which is significantly higher than the 65% of PProDOT, or the 45% of PEDOT. To the best of our knowledge, this value constitutes the highest contrast reported in the literature to date for an electrochromic polymer. Figure 2.15 shows the electrochromic switching for a 150 nm PProDOT-Me_2 film. PProDOT-Me also shows a high contrast of 77% at optimum film thickness. Response times are also important, and each of these polymers switches very rapidly. The response times shown in Table 2.2 were measured at 95% of full contrast. As discussed above, the proper method of measuring response time is not clear, as some groups measure response time at 60 to 100% of the full contrast. We have chosen to measure the response time at 95% of full contrast, as at this point most of the color change is finished and the human eye cannot notice the last 5 %. Of the three polymers, PProDOT-Me_2 switches the fastest, followed by PProDOT-Me, and PProDOT. This trend conforms to the idea that more highly substituted polymers polymerize with the chains spaced further apart, and therefore allow for faster ion movement in the film.

The switching of PProDOT-Et_2 and PProDOT-Bu_2 was studied to see if even longer alkyl substituents would further improve the response times and contrast

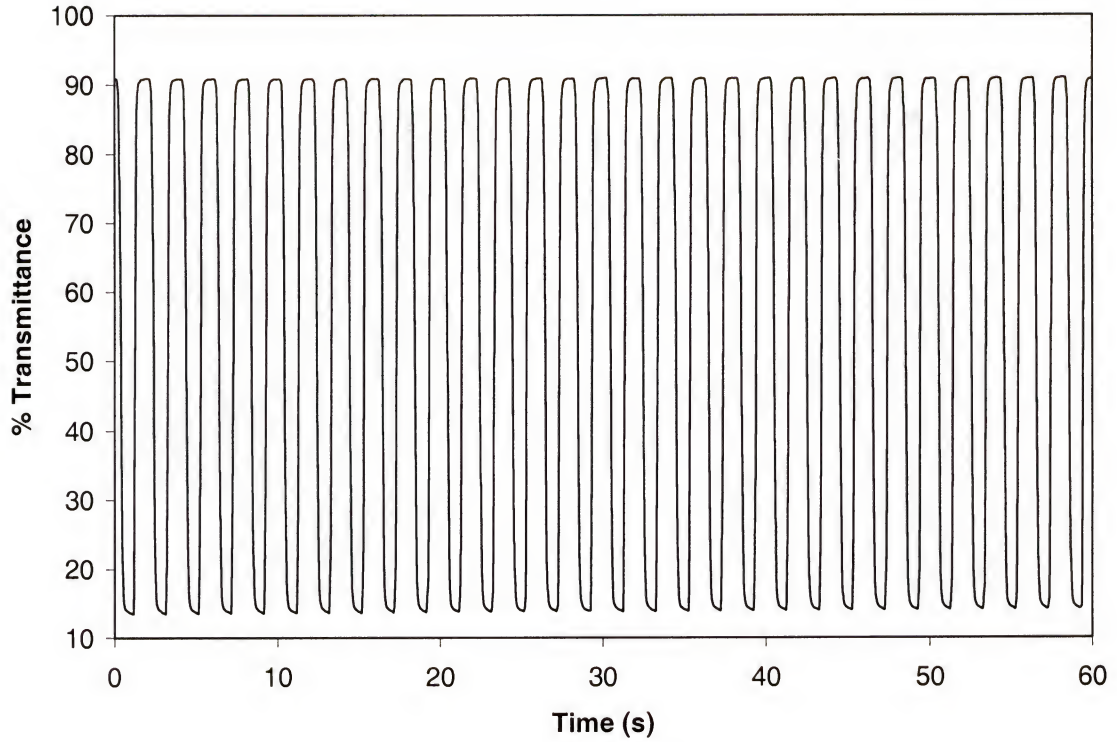

Figure 2.15 Electrochromic switching of PProDOT-Me_2 in 0.1 M TBAP/ACN for one minute of switching (step time 1.0 s) between –1.0 and +1.0 V vs. Ag/Ag^+ at 150 nm film thickness.

Table 2.3 Electrochromic properties of PProDOT-R_2 with longer alkyl groups

Polymer	Charge Density (mC / cm^2)	Δ%T	t_{ox} (s)[a]	t_{red} (s)[a]
PProDOT-Et_2	15	40	0.2	0.3
	29	71	0.36	0.53
	44	73	0.54	0.66
	57	63	0.60	0.78
PProDOT-Bu_2	14	67	0.19	0.30
	28	66	0.39	0.57
	43	61	0.50	0.71
	57	58	0.48	0.51

[a] Measured at 95% of full contrast.

ratios, and a study of contrast ratios and response times at different charge density values was accomplished. The results of these experiments are summarized in Table 2.3. The longer alkyl chain does not increase contrast, and the response times are very similar to PProDOT-Me_2 with no decrease observed.

To summarize, electrochromic switching studies show that more highly substituted polymers exhibit a higher electrochromic contrast and faster response times than the parent polymer PEDOT. PProDOT-Me_2 exhibits the highest contrasts and fastest response times, and it is the best polymer that we have synthesized for use as a cathodically coloring polymer in a dual-polymer electrochromic device. Increasing the length of the alkyl group of PProDOT-Me_2 from methyl to ethyl (PProDOT-Et_2) and butyl (PProDOT-Bu_2) does not enhance the electrochromic properties any further.

2.7.4 Coloration Efficiency

An important factor used in evaluating electrochromic materials is coloration efficiency (CE). The CE is obtained by determining the injected/ejected charge as a function of electrode area (Q_d) and the change in optical density $\Delta OD(\lambda)$when switching an EC device from one state to another, and is given by equation 2-3 (where T_b and T_c are the bleached and colored transmittance values respectively).[119] This quantity is

$$CE(\lambda) = \Delta OD(\lambda) / Q_d = \log[T_b(\lambda)/T_c(\lambda)] / Q_d \qquad (2\text{-}3)$$

important, because in addition to measuring the contrast between colored states, it takes into account the amount of charge needed to affect a certain color change. The ideal

material or device would exhibit a large transmittance change with a small amount of charge giving a large CE. Because this quantity has been used extensively in the inorganic electrochromic literature, measuring CE for organic polymers is important to compare them to other types of materials.

For comparison sake, CE values have been recorded for various inorganic and organic molecules, polymers, and devices. Tungsten trioxide prepared by thermal evaporation gives a CE of 115 cm^2 / C, and the same material prepared by sputtering gives a value of 42 cm^2 / C.[120] Another inorganic electrochromic material is IrO_2, which exhibits a CE of 15 to 18 cm^2 / C.[121] Conducting polymers exhibit higher CE values than inorganic materials, for example poly(bithiophene) and P3MT electropolymerized on ITO coated glass slides give CE values of 110 and 240 cm^2 / C, respectively.[117] CE values for complementary devices also have been recorded. A device consisting of poly(aniline) and tungsten trioxide with a gel electrolyte give a CE value of 170 cm^2 / C.[122] The Reynolds group has reported on dual polymer devices using PEDOT and PEDOT-$C_{14}H_{29}$ as cathodically coloring polymers, and EDOT / carbazole containing polymers as anodically coloring polymers.[101] These devices exhibited very high coloration efficiencies of up to 1400 cm^2 / C.

In order to obtain CE values, the charge must be measured while the polymer is switched between the reduced and oxidized states, and can be accomplished with chronocoulometry. Simultaneously, chronoabsorptometry is performed so that the proper response times and %T values can be recorded. Charge response times are correlated with the %T values to calculate CE. In Section 2.7.3, the response times were measured at 95% of full contrast. To determine an appropriate and comparative CE, the charge

values were measured at 80, 90, 92, 95, 98, and 100% of full contrast to better understand how the CE value changes depending on when the charge is recorded. In the future we would like to establish 95% as a standard value to report CE values in the literature.

CE values were measured for PEDOT, PProDOT, and PProDOT-Me_2. The film thickness was chosen as the thickness that yielded the maximum Δ%T for that polymer, which happened to be 150 nm for each polymer. Polymer films were synthesized by applying a constant potential of 1.2 V. The films were then switched ten times, and simultaneously subjected to chronoabsorptometry and chronocoulometry for one switch having a five second duration. Figure 2.16 shows the CE measured for the polymers measured as a function of percentage of full contrast, and the full CE results for the three

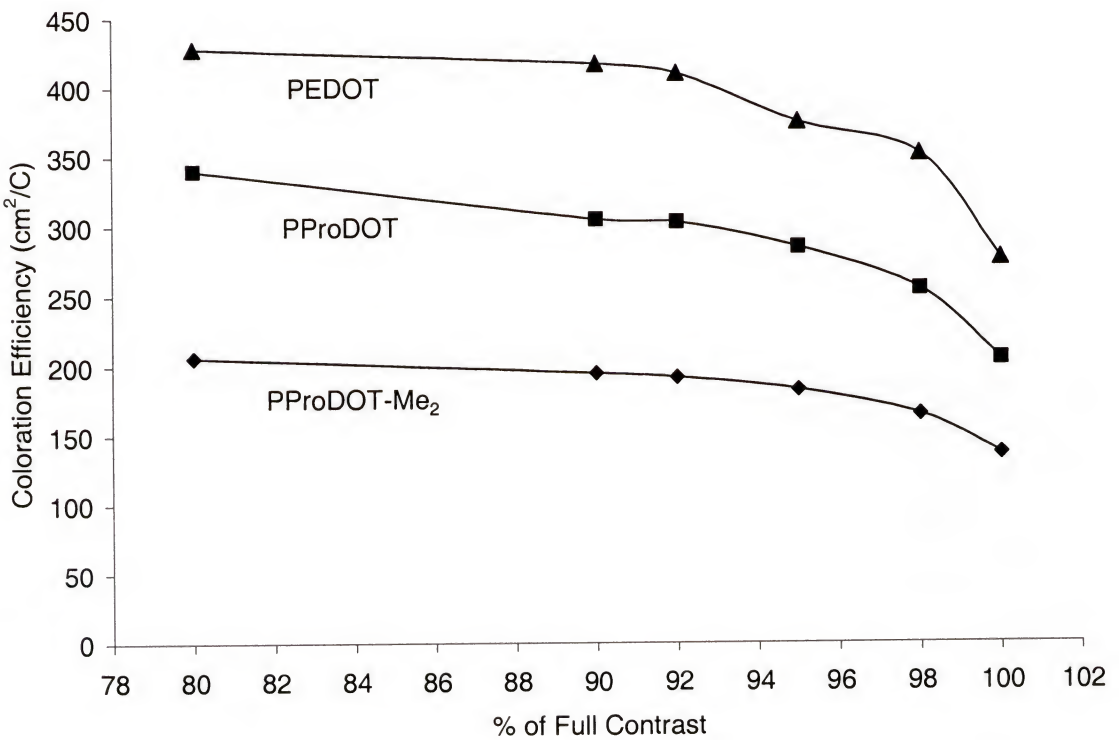

Figure 2.16 Relationship of the coloration efficiency values of PEDOT, PProDOT, and PProDOT-Me_2 to the percentage of full electrochromic contrast.

polymers are summarized in Table 2.4. The results show that CE values are highest for PProDOT-Me_2, then decrease for PProDOT, and are the lowest for PEDOT. This supports the trends that are seen in the electrochromic switching data. This data confirms that PProDOT-Me_2 is a much better cathodically coloring polymer than PEDOT. The CE values are also high compared to inorganic materials and other conducting polymers. The CE decreases as 100% of the full switch is approached, and this is due to the increase in charge passed being greater than the increase in ΔOD. Taking PEDOT as an example, the CE changes greatly (ca. 100 cm^2/C) depending on when the charge is recorded.

In order to further understand the charge reading, a chronocoulometric experiment for PProDOT is displayed in Figure 2.17. It should be noted that there was a background current present in the cell set-up, and it could be measured by cycling the potential through the same waveform used for the experiment with the cell assembled without polymer on the working electrode. The background charge was subtracted from the charge obtained for polymer switching, and as seen by the flatness of the initial data this method seems to work rather well. The horizontal lines show where the charge is measured for 80, 95, and 100 % of a full electrochromic switch are displayed on the charge curve to illustrate the importance of when the charge is measured. The 80% value is only half way up the curve, and the 95% value, which is where we have chosen to measure response times, is barely three quarters of the way up the curve. Where the chronoabsorptometry data is flat at the 100% value, the charge curve is still increasing. After 100%, the charge still increases with time, even though the transmittance is constant, and the background current has been subtracted. Therefore, it is very important

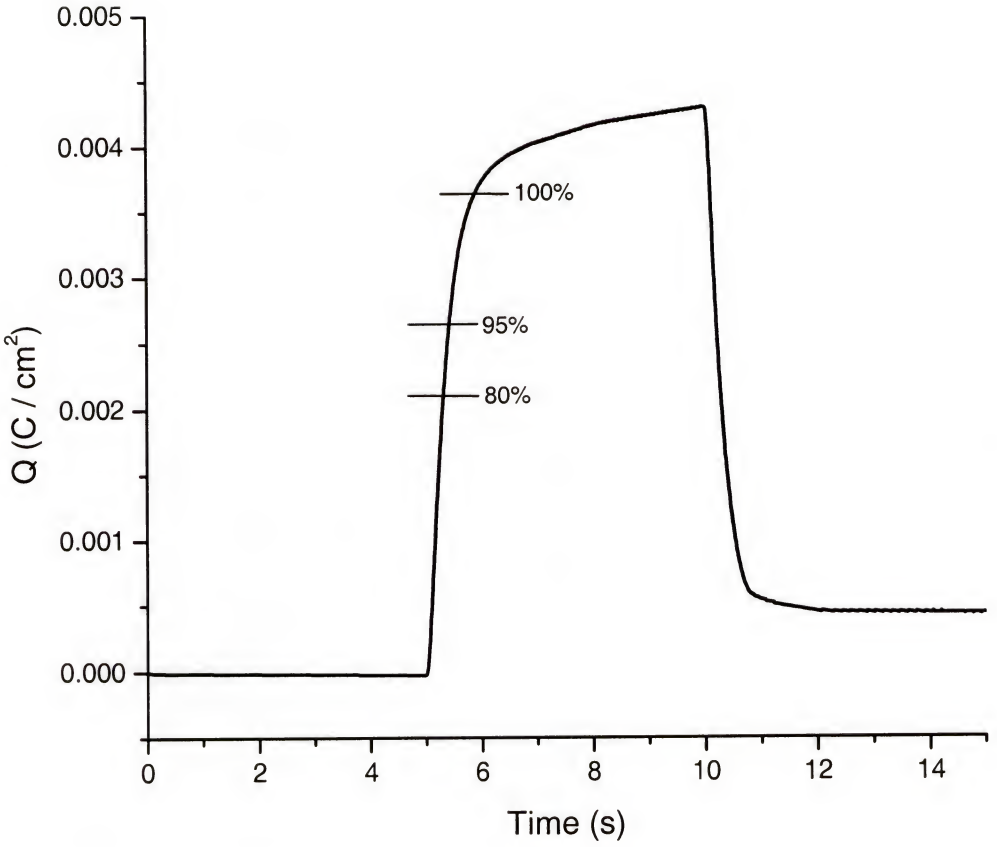

Figure 2.17 Chronocoulometry for PProDOT. Horizontal lines show 80%, 95%, and 100% of full contrast. The background current is subtracted from the data.

to measure the charge at a predefined response time, so that comparison between materials can be accurate.

Coloration efficiencies have been measured extensively in the literature, but a survey of the literature indicates that CE is measured in different ways by different researchers. For example, in work by Habib et al.[123] the coloration efficiency is defined as the change in absorbance per unit area charge injected per unit area of the active electrode, and they measure the change in absorbance of WO_3 and other inorganic

Table 2.4 Coloration efficiency values for PEDOT, PProDOT, and PProDOT-Me_2

Polymer[a]	% of Full Contrast	Δ%T[b]	ΔOD[b]	Q_d (mC / cm^2)[b]	CE (cm^2 / C)
PEDOT	80	43	0.44	2.13	206
	90	48	0.47	2.41	195
	92	49	0.48	2.49	192
	95	51	0.49	2.68	183
	98	53	0.50	3.04	165
	100	54	0.50	3.64	137
PProDOT	80	53	0.69	2.04	340
	90	59	0.73	2.39	305
	92	61	0.74	2.44	303
	95	63	0.75	2.63	285
	98	65	0.76	2.97	255
	100	66	0.77	3.75	205
PProDOT-Me_2	80	61	0.75	1.75	428
	90	68	0.79	1.89	417
	92	70	0.80	1.95	410
	95	72	0.82	2.19	375
	98	75	0.83	2.36	352
	100	76	0.83	3.00	277

[a] Film thickness = 150 nm for all polymers.
[b] Values are an average of two different films.

electrochromic materials as a function of time as they pulse the potential and measure the charge injected. Although this method is effective, they do not discuss where they actually measure the charge value as the graphs of variation of absorbance with time quickly level off. Recent work by Choy et al.[124] measures the CE for hybrid films of poly(acrylic acid)/WO_3 using the same equation given above by us, where they report CE as a function of charge passed through the material. In other work by Cummins et al.[125] the CE values of EC windows based on organic chromophores chemisorbed on a nanostructured TiO_2 film were measured. In this case, CE was measured by plotting absorbance vs. accumulated charge and measuring the slope, which would correspond to CE, of the original linear portion of the plot. Finally, there is work where the method in

determining CE is not described, and values are simply reported.[117,126] The validity of the methods described above is not in question; the problem is the ability to compare CE values between different types of materials is compromised when different methods are used. Therefore, we propose that response times and CE values should be measured at 95% of the full change in transmittance between the oxidized and reduced forms in order to establish a standard, so that CE values measured in different research groups can be compared more easily.

2.8 Colorimetry

Colorimetry is used to make the measurement of color an objective and quantitative practice, which can allow for matching of colors in electrochromic devices.[127] Color is made up of three attributes; hue, saturation, and luminance, and color systems such as the often-used CIE system[128] are used as a quantitative scale to define and compare colors. The CIE- defined color matching functions take into account the manner in which the human eye perceives color. Colorimetry has been used to study the properties of electrochromic and light-emitting polymers.[129,130,131,132,133,134,135,136] Recently, the Reynolds group has reported colorimetry results for a wide variety of electrochromic polymers.[137] In this work, colorimetry was not only used to define the color of the polymer, but the light transmission also was measured in detailed luminance studies. The luminance is usually written as a percentage relative to the background luminance (Y_0) or a standard light source as written in equation 2-4:

$$\% Y = Y / Y_0 \times 100 \qquad (2\text{-}4)$$

Luminance measurements offer an advantage over spectroelectrochemistry and electrochromic switching, because it allows for examination of spectral changes over the entire visible range in one plot, while in electrochromic switching, one wavelength from the visible region is selected to monitor the transmittance of a film.

In this study, the relative luminance of the film is measured as the polymer is switched stepwise between its oxidized and reduced forms, and the results for PProDOT-Me_2 are displayed in Figure 2.18. When the film is at reducing potentials, it is highly absorptive and not much light can pass through the sample. When the film is oxidized,

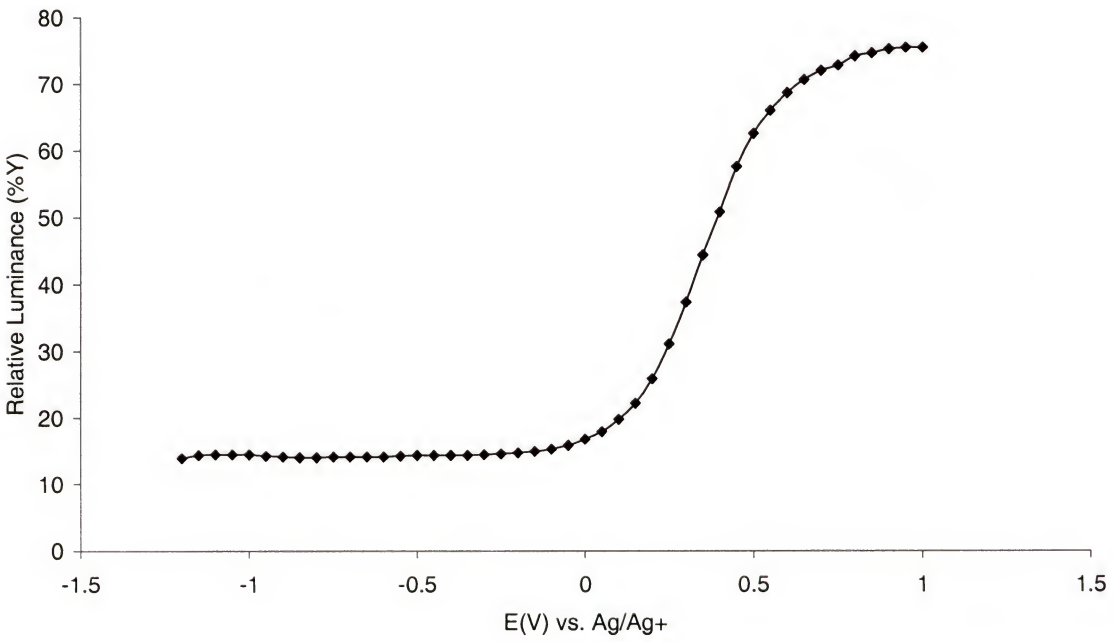

Figure 2.18 Relative luminance vs. applied potential for PProDOT-Me_2 in 0.1 M TBAP/ACN where the potential was increased by 50 mV steps from the fully neutral state to the fully doped state.[137]

the film is highly transmissive and much more light gets through. Now the contrast between the reduced and oxidized states can be given as Δ%Y. The luminance studies uphold the results of the electrochromic switching studies in that PProDOT-Me_2 exhibits a Δ%Y of 61% and PEDOT exhibits a value of 33%. This reaffirms the earlier conclusion that PProDOT-Me_2 has a much better electrochromic contrast than PEDOT. For comparison, P3MT exhibits a Δ%Y value of 14%, which is much lower than PEDOT or PProDOT-Me_2.

2.9 Discussion

Although we have clearly established that increasing the size of the alkylenedioxy ring and placing a pendant group off of the main chain increases the electrochromic contrast and response times, the relationship of these values to structure are still not clear. The response times can be rationalized by the argument that larger ring size and pendant groups serve to space the polymer main chains apart. During electrochromic switching dopant ions move in and out of the film. If there is more room for the ions to move, then they can diffuse more rapidly into and out of the film, thus leading to more rapid response times.

As discussed previously in Section 2.7.2, the high contrast of the highly substituted derivatives such as PProDOT-Me_2 can be attributed to the ability to dope the films to a greater extent. Again, if the main chains are spaced farther apart, then there is space available for more dopant ions per chain than if the chains were tightly packed. At these high doping levels, a polymer is formed where the main charge carrier present is a bipolaron, which gives only one strongly allowed transition in the near-IR. Measuring

doping levels in the films can prove this hypothesis, and should be the next step in this work.

2.10 Conclusions

A series of 3,4-alkylenedioxythiophene monomers have been synthesized, which have been electropolymerized at moderate (1.1 V vs. Ag/Ag^+) potentials to yield electroactive polymers with low $E_{1/2}$ values (-0.2 to 0.0 V). These polymers have band gaps of 1.6 to 1.75 eV, and exhibit an absorptive dark blue color in the reduced form, and a transmissive sky blue in the oxidized form. Electrochromic switching studies have shown that polymers with large pendant groups or larger alkylenedioxy ring size have larger optical contrast (Δ%T) than the parent polymer PEDOT. PProDOT-Me_2 has a particularly large contrast ratio of 78% compared to a value of 65% for PProDOT at the same film thickness. Response times measured at 95% of full optical contrast are very rapid for all of the polymers and range from 0.2 to 0.8 s, depending on film thickness. Coloration efficiency (CE) values were measured for PEDOT, PProDOT, and PProDOT-Me_2 and confirmed the results from electrochromic switching. The CE results fall in this order, PProDOT-Me_2 > PProDOT > PEDOT. In order to show that it is very important where the charge is read in measuring CE values, values were reported at various percentages of full optical contrast. A value of 95% of full optical contrast was chosen as the standard place to measure response times and charge values for reporting purposes. Colorimetry was used to measure the relative luminance of PProDOT-Me_2 as the polymer is oxidized stepwise. The change in luminance (Δ%Y) between the reduced and oxidized

form is 61% for PProDOT-Me_2 which is much higher than the 33% result for PEDOT. These cathodically coloring polymers, and especially PProDOT-Me_2,, are now being successfully by our group in the fabrication of dual-polymer electrochromic devices.[138]

2.11 Experimental

2.11.1 Materials

EDOT was provided by Bayer and was purified by vacuum distillation (65 °C at 0.2 mmHg) prior to use. 3,4-Dihydroxy-2,5-carboethoxythiophene (**1**) was synthesized from thiodiglycolic acid as described previously.[139] The monomer PEDOT-$C_{14}H_{29}$ was synthesized as previously reported.[113] Compound 2,2-dioctyl-1,3-propanediol was prepared as previously described.[140] TBAP was prepared by mixing a 1:1 mole ratio of tetrabutylammonium bromide (Aldrich) dissolved in water with perchloric acid. The precipitate was filtered, recrystallized from ethanol and dried in vacuo. Acetonitrile (Aldrich) was dried over calcium hydride and distilled under argon. Toluene (Fisher) was dried over sodium metal and distilled under argon. Methanol was dried over magnesium and distilled under argon. Anhydrous *N,N*-dimethylformamide (DMF), copper chromite, quinoline, zinc metal, sodium methoxide, p-toluenesulfonic acid, neopentyl glycol, 2,2-diethyl-1,3-propanediol, 2,2-dibutyl-1,3-propanediol, and thiophene were obtained from Aldrich and used as purchased. Potassium carbonate, sodium hydroxide, bromine, chloroform, acetic acid, and potassium iodide were obtained from Fisher and used as purchased. Prior to all experimentation, the glassware was flame dried under vacuum, and back-filled with argon. All reactions were performed under argon.

2.11.2 Characterization of Monomers and Polymers

NMR spectra were recorded on a Gemini 300 FT-NMR, VXR 300 FT-NMR, or a Varian XL-300 FT-NMR. Mass spectrometry was carried out a Finnigan MAT 95Q mass spectrometer. Elemental analyses were accomplished at Robertson Microlit Laboratories, Inc., Madison, NJ.

Electropolymerization and polymer electrochemistry was carried out on an EG&G Princeton Applied Research model 273A potentiostat/galvanostat employing a platinum button working electrode, a platinum plate counter electrode, and a Ag/Ag^+ reference electrode. The monomer concentration for polymerization is 10 mM in all cases, and the supporting medium is 0.1 M TBAP/ACN.

For spectroelectrochemistry, spectra were recorded using a Varian Cary 5E UV-Vis-NIR spectrophotometer. Polymers were prepared using a constant potential of 1.2 V vs. Ag/Ag^+. The working electrodes were ITO coated glass slides (7 x 50 x 0.6 mm, 20 Ω/□) from Delta Technologies. The reference electrode was Ag/Ag^+, and the counter electrode was a platinum wire. Polymer synthesis and electrochemistry were controlled by an EG&G Princeton Applied Research model 273A potentiostat / galvanostat.

For electrochromic switching, transmittance was monitored using a Varian Cary 5E UV-Vis-NIR spectrophotometer with a cell similar to that used in spectroelectrochemistry employed. Polymers were prepared using a constant potential of 1.2 V vs. Ag/Ag^+. Polymer synthesis, electrochemistry, and chronocoulometry were controlled by a EG&G Princeton Applied Research model 273A potentiostat / galvanostat. Film thicknesses were measured using a Sloan Dektak II profilometer. Colorimetry was performed as described previously.[137]

2.11.3 Synthesis

2,5-Dicarbethoxy-3,4-alkylenedioxythiophenes (2b,d-h). In a general synthesis, one equivalent of 2,5-dicarbethoxy-3,4-dihydroxythiophene was stirred at 90°C under argon for 48 hours in the presence of 1 equivalent of corresponding dibromoalkane and 3 equivalents of anhydrous K_2CO_3 in anhydrous DMF. The resultant mixture was cooled to room temperature, poured into an excess of water and extracted with diethyl ether. The organic layer was washed with water and dried over anhydrous magnesium sulfate before removing ether at reduced pressure to obtain the corresponding product. All compounds gave appropriate analyses by ^1H and ^{13}C NMR, and elemental analysis.

2-methyl-2,3-dihydro-thieno[3,4-*b*][1,4]dioxine-5,7-dicarboxylic acid diethyl ester (2b). Yield = 21%; mp = 144-145 °C; ^1H NMR ($CDCl_3$): δ 1.4(t, 6H), 1.55(d, 3H), 4.0-4.6 (m, 7H); ^{13}C NMR (CDCl3): δ 14.01, 16.33, 62.85, 68.31, 70.09, 116.12, 144.88, 145.34, 162.10; Elemental analysis: Calculated for $C_{13}H_{16}O_6S$: C, 51.99%; H, 5.37%. Found: C, 51.87%; H, 5.40%.

2-phenyl-2,3-dihydro-thieno[3,4-*b*][1,4]dioxine-5,7-dicarboxylic acid diethyl ester (2d). Yield = 30%; mp = 116-117 °C; ^1H NMR ($CDCl_3$): δ 1.3 (t, 6H), 4.15-4.5 (m, 6H), 5.3 (dd, 1H), 7.4 (m, 5H); ^{13}C NMR ($CDCl_3$): δ 15.13, 62.89, 70.12, 76.34,

112.65, 123.87, 126.21, 129.55, 136.90, 144.52, 145.37, 162.94; Elemental analysis: Calculated for $C_{18}H_{18}O_6S$: C, 59.66%; H, 5.01%. Found: C, 59.60%; H, 5.01%.

3,4-dihydro-2H-thieno[3,4-b][1,4]dioxepine-6,8-dicarboxylic acid diethyl ester (2e). Yield = 84%; mp = 85-87 °C; ^{1}H NMR ($CDCl_3$): δ 1.3 (t, 6H), 2.3 (p, 2H), 4.15-4.4 (m, 8H); ^{13}C NMR ($CDCl_3$): δ 15.31, 36.89, 62.13, 71.43, 117.99, 152.12, 162.55; Elemental analysis: Calculated for $C_{13}H_{16}O_6S$: C, 51.92%; H, 5.40%. Found: C, 51.99%; H, 5.37%.

3-methyl-3,4-dihydro-2H-thieno[3,4-b][1,4]dioxepine-6,8-dicarboxylic acid diethyl ester (2f). Yield = 50%; mp = 105-108 °C; ^{1}H NMR ($CDCl_3$): δ 1.0 (d, 3H), 1.25 (t, 6H), 2.48 (m, 1H), 3.95 (dd, 2H), 4.15(q, 4H), 4.31 (dd, 2H); ^{13}C NMR ($CDCl_3$): δ 13.31, 14.55, 36.87, 51.16, 61.99, 75.73, 115.31, 152.35, 161.88; Elemental analysis: Calculated for $C_{14}H_{18}O_6S$: C, 53.49%; H, 5.77%. Found: C, 53.83%; H, 6.07%.

2,3,4,5-tetrahydrothieno[3,4-*b*][1,4]dioxocine-2,3-dicarboxylic acid diethyl ester (2g). Yield = 60%; mp= 185-188 °C; ^{1}H NMR ($CDCl_3$): δ 1.45 (t, 6H), 2.1 (m, 4H), 4.4 (q, 4H), 4.6 (m, 4H); ^{13}C NMR ($CDCl_3$): δ 16.13, 27.44, 62.23, 72.87, 117.22, 152.52, 162.15; Elemental analysis: Calculated for $C_{14}H_{18}O_6S$: C, 53.10%; H, 6.37%. Found: C, 53.10%; H, 5.80%.

5,10-dihydrobenzo[*f*]thieno[3,4-*b*][1,4]dioxocine-2,3-dicarboxylic acid diethyl ester (2h). Yield = 40%; mp = 147-148 ^{o}C; ^{1}H NMR ($CDCl_3$): δ 1.3 (t, 6H), 4.4 (q, 4H), 5.6(s, 4H), 7.3(m, 4H); ^{13}C NMR ($CDCl_3$): δ 16.54, 62.22, 75.53, 108.21, 128.53, 130.88, 136.23, 152.66, 162.98; Elemental analysis: Calculated for $C_{18}H_{18}O_6S$: C, 59.66%; H, 5.01%. Found: C, 59.62%; H, 5.01%.

2,5-Dicarboxy-3,4-alkylenedioxythiophenes (3b,d-h). One equivalent of 2,5-dicarbethoxy-3,4-alkylenedioxythiophene was stirred at 90^{o}C under argon for 10 hours with 3 equivalents of NaOH in water. The resulting solution was cooled to room temperature and acidified with 1M HCl to precipitate a white solid product. The product was filtered, washed with water, and dried under vacuum. All compounds gave appropriate analyses by ^{1}H and ^{13}C NMR, and elemental analysis.

2-methyl-2,3-dihydro-thieno[3,4-*b*][1,4]dioxine-5,7-dicarboxylic acid (3b). Yield = 95%; ^{1}H NMR (DMSO-d6): δ 1.45 (d, 3H), 3.9-4.5 (m, 3H); ^{13}C NMR (DMSO): δ 16.51, 68.33, 70.12, 112.89, 142.22, 143.69, 162.88; Elemental analysis: Calculated for $C_9H_8O_6S$: C, 44.26%; H, 3.30%. Found: C, 44.20%; H, 3.20%.

2-phenyl-2,3-dihydro-thieno[3,4-*b*][1,4]dioxine-5,7-dicarboxylic acid (3d). Yield = 90%; ^{1}H NMR (DMSO-d6): δ 4.15-4.3 (m, 2H), 5.4 (dd, 1H), 7.4 (m, 5H); ^{13}C NMR (DMSO): δ 68.23, 75.89, 112.17, 123.34, 126.76, 129.35, 136.87, 144.52, 145.28,

162.42; Elemental analysis: Calculated for $C_{14}H_{10}O_6S$: C, 54.90%; H, 3.29%. Found: C, 53.00%; H, 3.14%.

3,4-dihydro-2H-thieno[3,4-b][1,4]dioxepine-6,8-dicarboxylic acid (3e). Yield = 90%; ^{1}H NMR (DMSO-d6): δ 2.2 (p, 2H), 4.2 (t, 4H); ^{13}C NMR (DMSO): δ 34.23, 72.28, 118.55, 152.97, 162.84; Elemental analysis: Calculated for $C_9H_8O_6S$: C, 44.26%; H, 3.30%. Found: C, 44.26%; H, 3.20%.

3-methyl-3,4-dihydro-2H-thieno[3,4-b][1,4]dioxepine-6,8-dicarboxylic acid (3f). Yield = 74%; ^{1}H NMR (DMSO-d6): δ 0.99 (d, 3H), 2.35 (m, 1H), 3.90 (dd, 2H), 4.30 (dd, 2H); ^{13}C NMR (DMSO): δ 14.12, 36.89, 75.33, 116.21, 153.67, 161.55; Elemental analysis: Calculated for $C_{10}H_{10}O_6S$: C, 46.51%; H, 3.90%. Found: C, 43.56%; H, 4.31%.

2,3,4,5-tetrahydrothieno[3,4-*b*][1,4]dioxocine-2,3-dicarboxylic acid (3g). Yield = 92%; ^{1}H NMR (DMSO-d6): δ 1.95 (m, 4H) 4.4 (m, 4H), 13.2 (s, br); ^{13}C NMR (DMSO):δ 26.23, 72.78, 118.45, 152.31, 162.89; Elemental analysis: Calculated for $C_{10}H_{10}O_6S$: C, 46.15%; H, 4.65%. Found: C, 46.11%; H, 4.00%.

5,10-dihydrobenzo[*f*]thieno[3,4-*b*][1,4]dioxocine-2,3-dicarboxylic acid (3h). Yield = 85%; ^{1}H NMR (DMSO-d6): δ 5.3 (s, 4H), 7.3 (m, 4H); ^{13}C NMR (DMSO): δ

75.23, 108.55, 128.98, 130.42, 136.63, 152.97, 162.32; Elemental analysis: Calculated for $C_{14}H_{10}O_6S$: C, 54.90%; H, 3.29%. Found: C, 54.70%; H, 3.29%.

3,4-alkylenedioxythiophenes (4b,d-h). One equivalent of 2,5-dicarboxy-3,4-alkylenedioxythiophene was heated at 150°C with 17 mol% of copper chromite in quinoline for 20 hours under argon. After cooling, the mixture was filtered through celite and poured into an excess of 1M HCl. The product was extracted with ether, washed with 1M HCl until the washings were acidic, and washed with water. Ether was removed under reduced pressure after drying the organic layer over anhydrous magnesium sulfate. The products obtained were purified by flash chromatography on silica gel with methylene chloride as eluent. All compounds gave appropriate analyses by ^1H and ^{13}C NMR, HRMS, and elemental analysis.

2-methyl-2,3-dihydro-thieno[3,4-*b*][1,4]dioxine (EDOT-Me) (4b). Yield = 64%; ^1H NMR ($CDCl_3$): δ 1.45 (d, 3H), 3.9-4.5 (m, 3H), 6.5 (s, 2H); ^{13}C NMR ($CDCl_3$): δ 16.54, 68.33, 70.77, 100.34, 142.88, 143.90; Elemental analysis: Calculated for $C_7H_8O_2S$: C, 53.83%; H, 5.16%. Found: C, 53.61%; H, 5.09%; HRMS Calculated for $C_7H_8O_2S$: 156.0245. Found: 156.0242.

2-phenyl-2,3-dihydro-thieno[3,4-*b*][1,4]dioxine (EDOT-Ph) (4d). Yield = 54%; mp = 86-88 °C; ^1H NMR ($CDCl_3$): δ 4.15-4.3 (m, 2H), 5.4 (dd, 1H), 6.5(dd, 2H), 7.4 (m, 5H); ^{13}C NMR ($CDCl_3$): δ 69.54, 76.33, 100.04, 123.99, 126.36, 129.14, 136.69,

140.23, 141.88; Elemental analysis: Calculated for $C_{12}H_{10}O_2S$: C, 66.04%; H, 4.62%. Found: C, 66.01%; H, 4.60%; HRMS Calculated for $C_{12}H_{10}O_2S$: 218.0417. Found: 218.0452.

3,4-dihydro-2H-thieno[3,4-b][1,4]dioxepine (ProDOT) (4e). Yield = 60%; mp = 82-84 ^oC; ^1H NMR ($CDCl_3$): δ 2.2 (p, 2H), 4.2 (t, 4H), 6.6 (s, 2H); ^{13}C NMR ($CDCl_3$): δ 34.33, 72.89, 116.12, 150.44; Elemental analysis: Calculated for $C_7H_8O_2S$: C, 53.83%; H, 5.16%. Found: C, 53.85%; H, 5.12%; HRMS Calculated for $C_7H_8O_2S$: 156.0245. Found: 156.0241.

3-methyl-3,4-dihydro-2H-thieno[3,4-b][1,4]dioxepine (ProDOT-Me) (4f). Yield = 50%; mp = 57-60 ^oC; ^1H NMR ($CDCl_3$): δ 0.99 (d, 3H), 2.35 (m, 1H), 3.65 (dd, 2H), 4.10 (dd, 2H), 6.45 (s, 2H); ^{13}C NMR ($CDCl_3$): δ 13.01, 37.70, 76.05, 106.15, 150.80; Elemental analysis: Calculated for $C_8H_{10}O_2S$: C, 56.45%; H, 5.92%. Found: C, 56.75%; H, 5.93%; HRMS Calculated for $C_8H_{10}O_2S$: 170.0402. Found: 170.0407.

2,3,4,5-tetrahydrothieno[3,4-*b*][1,4]dioxocine (BuDOT) (4g). Yield = 60%; ^1H NMR ($CDCl_3$): δ 1.95 (m, 4H), 4.4 (m, 4H), 6.6 (s, 2H); ^{13}C NMR ($CDCl_3$): δ 26.03, 72.55, 116.94, 148.62; Elemental analysis: Calculated for $C_8H_{10}O_2S$: C, 56.46%; H, 5.93%. Found: C, 56.47%; H, 6.00%; HRMS Calculated for $C_8H_{10}O_2S$: 170.0402. Found: 170.0406.

5,10-dihydrobenzo[*f*]thieno[3,4-*b*][1,4]dioxocine (BuDOT-Xyl) (4h). Yield = 45%; mp = 80-83 °C; ^{1}H NMR ($CDCl_3$): δ 5.3 (s, 4H), 6.6 (s, 2H), 7.3(m, 4H); ^{13}C NMR ($CDCl_3$) : δ 74.08, 107.50, 128.89, 130.03, 136.23, 148.10. Elemental analysis: Calculated for $C_{12}H_{10}O_2S$: C, 66.04%; H, 4.62%. Found: C, 66.00%; H, 4.73%; HRMS Calculated for $C_{12}H_{10}O_2S$: 218.0401. Found: 218.0417.

2,3,4,5-tetrabromothiophene (6). 25.3 g (0.3 mol) of thiophene and 100 mL of chloroform were combined in a 3-neck flask equipped with an addition funnel, reflux condenser, and sodium bicarbonate gas trap to trap HBr. The flask is cooled with an ice bath, and 66 mL of bromine was added slowly over a three hour period. The flask was warmed to room temperature and stirred for 16 hours. 50 mL of 2M ammonium hydroxide was added and the mixture was heated to 60 °C for 30 minutes. The mixture was transferred to a separatory funnel, and 1.1 L of chloroform was added. The chloroform layer was washed with 2M ammonium hydroxide and dried with magnesium sulfate. The chloroform was removed under vacuum to yield the crude product, which was recrystallized from chloroform to yield 93.8 g (78%) of **5**. mp = 118-120 °C. (lit.[141] 115-116 °C) ^{13}C NMR ($CDCl_3$) : δ 110, 117.

3,4-dibromothiophene (7). 53 g (0.8 mol) and 100 mL of water were combined in a 3 neck flask equipped with a simple distillation apparatus and reflux condenser. With vigorous stirring, 60 mL of acetic acid was added, and the mixture was heated to reflux. 65 g (0.16 mol) compound **6** was added slowly and the mixture was allowed to distill. Every hour, the aqueous layer of distillate was separated and added back to the

reaction flask, while the organic layers were collected, and after 4.5 hours the distillate only contained an aqueous layer indicating that the reaction is over. The combined organic layers were washed with water and satd. sodium bicarbonate solution, and dried with magnesium sulfate. The crude oil was fractionally distilled under vacuum (92-94 °C / 11 mmHg), (lit.[141] 96.5 – 99 °C / 11 mmHg) to yield 25 g (65%) of **7**. ^{1}H NMR ($CDCl_3$) : δ 7.3 (s, 2H).

3,4-dimethoxythiophene[142] (8). 6.6 g (0.083 mol) of CuO, 0.14 g (0.00083 mol) of KI, 20 g (0.083 mol) of compound **7**, 22.41 g (0.415 mol) of sodium methoxide, and 90 mL of methanol were combined in a 2-neck flask equipped with a reflux condenser. The black mixture was refluxed for 3 days. 0.14 g (0.00083) of KI was added and the mixture was refluxed for an additional 24 hours. The dark mixture was cooled, filtered, and diluted with 200 mL of water, and extracted 3 times with ether. The combined ether layers were washed with water and dried with magnesium sulfate. The ether was removed under vacuum, and the crude product was purified by vacuum distillation (61-64 °C / 0.5 mmHg), (lit.[141] 59-65 °C / 0.5 mm Hg) to yield 6.3 g (53 %) of **8**. ^{1}H NMR ($CDCl_3$) : δ 3.8 (s, 6H), 6.2 (s, 2H).

3,3-dimethyl-3,4-dihydro-2H-thieno[3,4-b][1,4]dioxepine (ProDOT-Me$_2$) (10a). 5.3 g (0.037 mol) of compound **8**, 7.7 g (0.736 mol) of neopentyl glycol, 0.7 g (0.0037 mol) of p-toluenesulfonic acid, and 200 mL and toluene were combined in a 2-neck flask equipped with a soxhlet extractor with type 4A molecular sieves in the

thimble. The solution was heated to reflux and allowed to reflux for 1 day. The reaction mixture was cooled and washed with water. The toluene was removed under vacuum, and the crude product was purified by column chromatography on silica gel with 3:2 hexanes / methylene chloride as the eluent to yield 5.2 g (77%) of compound **10a** as a white solid. mp 49-51 °C. ^{1}H NMR δ ($CDCl_3$) 1.02 (s, 6H), 3.73 (s, 4H), 6.48 (s, 2H); ^{13}C NMR ($CDCl_3$) δ 22.25, 39.44, 80.62, 105.09, 150.05. Elemental analysis: Calculated for $C_9H_{12}O_2S$: C, 58.67%; H, 6.56%; S, 17.40. Found: C, 58.81%; H, 6.76%; S, 16.98%; HRMS calculated for $C_9H_{12}O_2S$: 184.0558. Found: 184.0561.

3,3-diethyl-3,4-dihydro-2H-thieno[3,4-b][1,4]dioxepine (ProDOT-Et_2) (10b). Compound **10b** was synthesized using the same procedure as compound **10a** using 4 g (0.028 mol) of compound **8**, 3.85 g (0.029 mol) of 2,2-diethyl-1,3-propanediol, and 0.2 g of p-toluenesulfonic acid. Yield 3.9 g (68 %). ^{1}H NMR ($CDCl_3$) : δ 0.9 (t, 6H), 1.4 (q, 4H), 3.8 (s, 4H), 6.4 (s, 2H). ^{13}C NMR ($CDCl_3$) : δ 7.19, 23.41, 43.64, 76.82, 104.60, 149.66. Elemental Analysis: Calculated for $C_{11}H_{16}O_2S$: C, 62.23%; H 7.60%; S 15.10% Found: C, 61.99%; H, 7.49%; S 14.75%.

3,3-dibutyl-3,4-dihydro-2H-thieno[3,4-b][1,4]dioxepine (ProDOT-Bu_2) (10c). Compound **10c** was synthesized using the same procedure as compound **10a** using 5.0 g (0.035 mol) of compound **8**, 6.86 g (0.036 mol) of 2,2-dibutyl-1,3-propanediol, and 0.20 g of p-toluenesulfonic acid. Yield 6.5 g (69%). A clear oil. ^{1}H NMR ($CDCl_3$): δ 0.92 (t, 6H); 1.20-1.42 (m, 12H); 3.85 (s, 4H); 6.42 (s, 2H). ^{13}C NMR ($CDCl_3$): δ 14.05, 23.53, 25.00, 31.53, 43.62, 77.53, 104.64, 149.68. MS (CI) exact mass calcd. (m+1): 269.1575.

Found: 269.1572. Elemental Analysis: Calculated for $C_{15}H_{24}O_2S$: C, 67.12; H, 9.01; S, 11.94. Found: C, 66.83; H, 9.00; S, 11.54.

3,3-dioctyl-3,4-dihydro-2H-thieno[3,4-b][1,4]dioxepine (ProDOT-Oct$_2$) (10d). Compound **10d** was synthesized using the same procedure as compound **10a** using 1.7 g (0.0011 mol), 3.5 g (0.011 mol) of 2,2-dioctyl-1,3-propanediol, and 0.05 g of p-toluenesulfonic acid. Yield 3.7 g (84%). A clear oil. ^{1}H NMR ($CDCl_3$): δ 0.88 (t, 6H); 1.27 (bs, 24H); 1.35 (t, 4H); 3.84 (s, 4H); 6.42 (s, 2H). ^{13}C NMR ($CDCl_3$): δ 14.11, 22.66, 22.79, 29.29, 29.48, 30.46, 31.79, 31.86, 43.71, 77.53, 104.62, 149.70. MS (CI) exact mass calcd. (m+1): 381.2827. Found: 381.2824. Elemental Analysis: Calculated for $C_{23}H_{40}O_2S$: C, 72.58; H, 10.59; S, 8.42. Found: C, 73.87; H, 10.88; S, 8.45.

2.11.4 X-Ray Crystallography; Data Collection, Structure Solution, and Refinement

Both structures were solved by the Direct Methods in *SHELXTL5,* and refined using full-matrix least squares on F^2.[143] The non-H atoms were refined with anisotropic thermal parameters and all of the H atoms were located in Difference Fourier maps and refined without constraints. For ProDOT, 124 parameters were refined in the final cycle of refinement using 1468 reflections with I > 2s(I) to yield R_1 and wR_2 of 2.78 and 6.57, respectively. And for EDOT-Ph, 177 parameters were refined in the final cycle of refinement using 1871 reflections with I > 2s(I) to yield R_1 and wR_2 of 3.68 and 8.23, respectively. Data tables for the X-Ray structures are located in the appendix.

CHAPTER 3
SOLUBLE DISUBSTITUTED POLY(3,4-PROPYLENEDIOXYTHIOPHENE)S

3.1 Introduction

3.1.1 Motivation for Research

The polymers discussed in Chapter 2 were successfully synthesized by electrochemical polymerization, but if large amounts of processable polymer are needed, then chemical polymerization is necessary. Chemical polymerizations allow the synthesis of materials that can be characterized by traditional analytical techniques used for other soluble polymers. Solubility allows for processing from solution, which opens up the possibility of fabricating devices etc. This chapter outlines the synthesis and characterization of well-defined and soluble polymers by transition metal-mediated coupling reactions based on the PProDOT-R_2 structure, which was shown to exhibit favorable electrochromic properties in Chapter 2.

3.1.2 Coupling Polymerizations

Metal-mediated coupling reactions have been used extensively to synthesize both small molecules[144,145] and polymers[146,147]. Although many different types of substrates have been used in these reactions, one frequently used route is the coupling of an aryl

halide with an organometallic species. These reactions are catalogued by the type of metal and catalyst used, and are usually named after the scientist who performed groundbreaking work in the area. If the catalyst is palladium (0) and the organometallic species is an aryl trialkyltin compound, then the reaction is called the Stille coupling[148,149]. If the catalyst is palladium (0) and the organometallic species is an aryl zinc halide, then the reaction is called the Negishi coupling.[150,151] If the catalyst is palladium (0) and the organometallic species is an aryl boronic acid or ester, then the reaction is called the Suzuki coupling.[152] Finally, if the catalyst is nickel (0) and the organometallic species is an aryl magnesium bromide, then the reaction is called the Kumada or Yamamoto coupling.[153,154,155,156]

Regardless of the type of coupling used, they all exhibit the same commonly accepted, general reaction mechanism as illustrated in Figure 3.1. [144,145] A palladium(II) or nickel(II) catalyst is sometimes used instead of a palladium (0) catalyst, because they are generally more air stable. When a metal (II) catalyst is used, then it is believed that the catalyst is first reduced to the metal (0) species by two equivalents of the organometallic reagent. The resulting metal (0) reacts with the aryl halide to form the organometallic halide intermediate by oxidative addition. This intermediate then undergoes transmetalation, which yields a trialkylmetalhalide as the by-product. Finally, a reductive elimination affords the coupled product and the metal (0) species to complete the cycle.

Conjugated polymers have been successfully synthesized by all of these coupling reactions. The Suzuki reaction has been utilized very successfully in synthesizing poly(p-phenylene)s (PPPs).[146,151,157] The major advantage of the Suzuki reaction is that

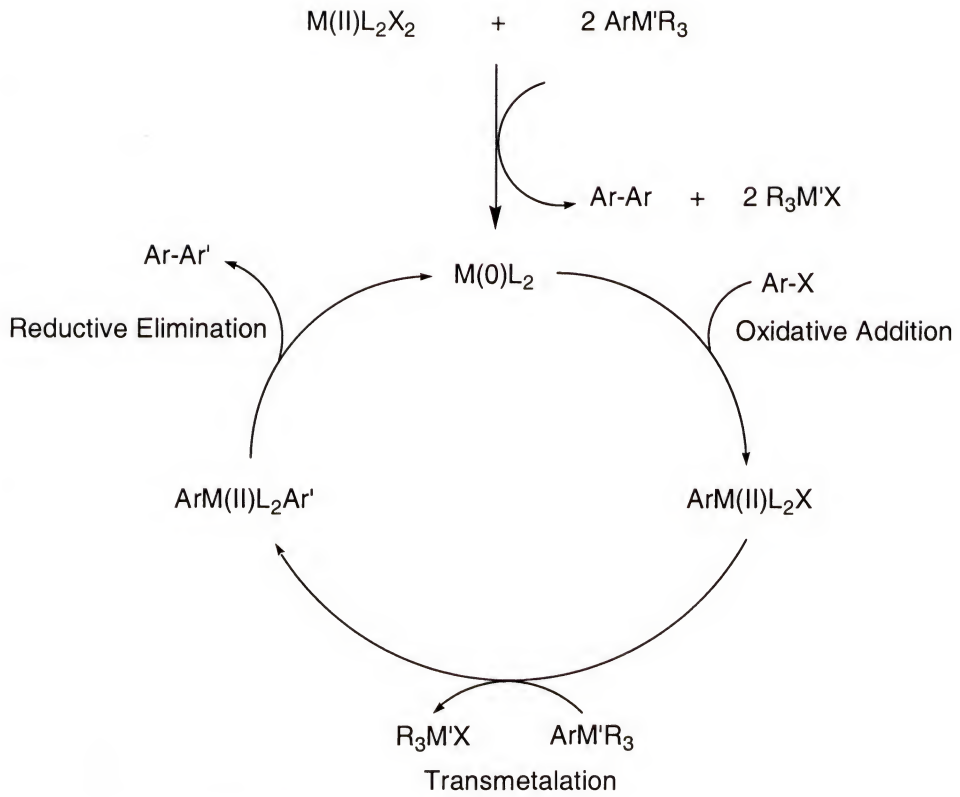

Figure 3.1 General mechanism for a transition-metal catalyzed coupling reaction between and aryl halide and an aryl organometallic compound.

the aryl boronates used are stable (as long as they are not overly electron rich) and non-toxic. Many different types of conjugated oligomers and polymers have been synthesized by the Stille reaction.[146,147,158,159,160] The Stille reaction is relatively rapid, and the organotin species can be isolated and purified. The major disadvantage of the Stille reaction is the toxicity of the organotin species used. Yamamoto coupling has been employed as a polymerization reaction.[161,162] While the Yamamoto coupling is relatively rapid, the aryl Grignard species cannot be isolated and must be generated in-situ, which can be a problem in trying to achieve the exact stoichiometric balance needed to produce high polymer.

The McCullough group has exploited the Kumada coupling to synthesize regioregular head-to-tail poly(3-alkylthiophene)s (HT-PATs) that exhibit relatively high molecular weights (20000 – 40000 g/mol), desirable optical properties, and high conductivity.[59] The advantages of regioregularity were discussed in Chapter 1. More recently, the McCullough group has updated their methodology to synthesize regioregular PATs using a modification of the Yamamoto coupling called Grignard metathesis or GRIM (Figure 3.2).[65] In this reaction, 2,5-dibromo-3-alkylthiophene (**11**) is treated with one equivalent of methylmagnesium bromide in refluxing tetrahydrofuran that affords intermediate **12**, which when treated with Ni(dppp)Cl_2 yields head-to-tail poly(3-dodecylthiophene) (HT-PDDT) (**13**). GRIM is able to yield regioregular polymer, because of the differing reactivities of the two bromides in compound **11**, where the Grignard prefers to be formed on the 5 position furthest away from the electron donating alkyl group. This idea of differential reactivity was exploited by the Reynolds group in the synthesis of linear and star branched poly(EDOT-didodecyloxybenzene) polymers,

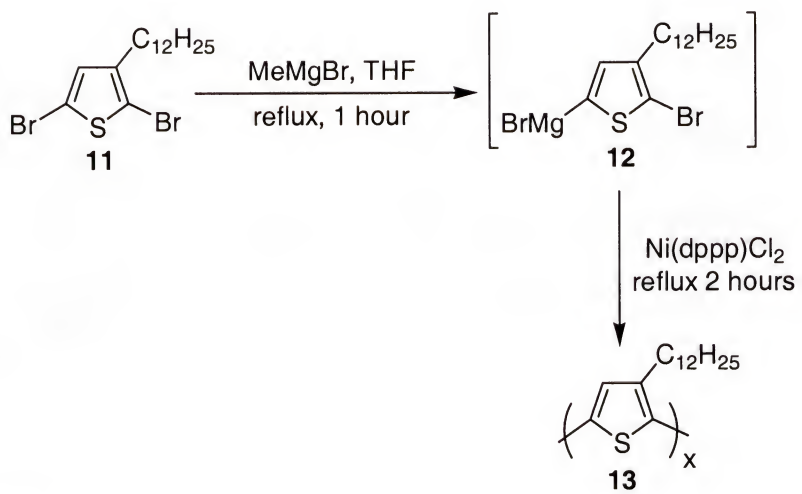

Figure 3.2 GRIM synthesis of head-to-tail coupled, regioregular poly(3-dodecylthiophene).

where they took advantage of the differing reactivities between a thienyl bromide and a bromobenzene to form linear and star polymers of high molecular weight (40000 and 65000 g/ mol).[68] The advantages of GRIM over previous methods are shorter reaction times, less rigorous conditions, and larger scale preparation. Also, GRIM proceeds through an A-B monomer, which eliminates the stoichiometric problems associated with A-A / B-B polymerizations. For these reasons, the GRIM reaction was chosen as the polymerization method for this work.

3.1.3 Molecular Weight Determination

There are many different methods used to obtain molecular weight information on polymers, such as NMR end group analysis, gel permeation chromatography (GPC), vapor pressure osmometry (VPO), membrane osmometry, viscometry, laser light scattering, and matrix assisted laser desorption/ionization time-of-flight mass spectrometry (MALDI-TOF-MS). All of these methods have their advantages and disadvantages, and they should be used together to achieve a more complete picture of the polymer molecular weight. In this chapter, GPC and MALDI-TOF-MS are used to probe molecular weight, therefore a more detailed discussion of these two methods has been included.

GPC or size exclusion chromatography (SEC) is a widely used method of determining molecular weights relative to standards of known molecular weight.[163] This method provides number average (M_n) and weight average (M_w) molecular weight as well as the molecular weight distribution (polydispersity, M_w/M_n) and can be used in

conjugation with other methods such as viscometry and light scattering to obtain quantitative molecular weights.

Because GPC separates by detecting difference in hydrodynamic volume, polymers with the same molecular weight can exhibit different retention times by GPC. Polystyrene is the most frequently used standard, because of its low cost and availability. Since many polymers behave differently in solution than polystyrene; the molecular weights obtained from most GPC analyses are approximate. This is especially true for polymers that are rigid rods in solution. For this reason, GPC tends to overestimate the molecular weights of these polymers. To help circumvent these problems, universal calibration has been developed for substituted PPPs in THF.[164]

MALDI-TOF mass spectrometry has recently created new opportunities in analyzing the molecular weight of synthetic polymers.[165,166,167] Because MALDI-TOF yields simple mass spectra that show mainly singly-charged ions with little fragmentation, it is ideally suited for polymer analysis. The molecular weight distribution and the type of end groups or functionality type distribution (FTD) can be obtained with MALDI-TOF, although low polydispersity samples are necessary to obtain accurate molecular weight distributions. An advantage of this technique is that a very small amount (ng-μg) of polymer is needed for analysis. Typical sample preparation involves the mixture of the polymer with a matrix, solvent, and cationization salt. The solution is dripped onto the sample plate, and the solvent is allowed to dry. Although the physical process of sample preparation is easy, the choice of solvent, matrix, and cationization salt is not. The goal of sample preparation is molecular entrapment of the polymer in a crystalline matrix. Because synthetic polymer samples exist as a

distribution of chain lengths, separation of single chains throughout the matrix is more difficult to achieve than in proteins. Trying many different combinations of components is sometimes necessary to obtain a mass spectrum. The process is based on trial-and-error with no exact formula to follow, but once successful sample preparation conditions are found, accurate molecular weight distributions can be calculated with MALDI-TOF if the polydispersity is lower than 1.2.[165,167] For wide distributions, there is some mass discrimination by the detector towards lower molecular weight ions, leading the results to be biased towards lower values. This type of problem can be solved by pre-fractionation, or by coupling chromatography with MALDI.[168]

3.2 Monomer Synthesis

For the GRIM polymerization, dibrominated thiophenes were needed. The synthesis of 2,5-dibromo-ProDOT-Bu_2 (**14**) and 2,5-dibromo-ProDOT-Oct_2 (**15**) is displayed in Figure 3.3. Bromination with excess *N*-bromosuccinimide affords **14** (97%) and **15** (35%) after column chromatography. It should be noted that the low yield obtained in synthesizing compound **15** occurred because it was isolated in an attempt to

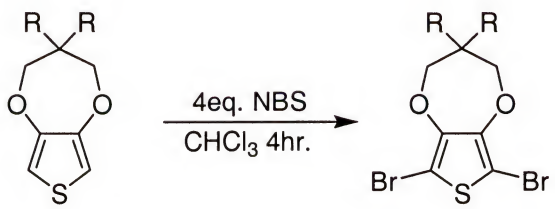

10c or **10d** R = butyl (**14**) and octyl (**15**)

Figure 3.3 Synthesis of monomers **14** and **15**

make the monobrominated material with one equivalent of NBS. Both compounds are viscous oils (they do not solidify even at –20 °C) that cannot be distilled by normal vacuum methods or Kugelrohr distillation, leaving column chromatography as the only purification method. The compounds were characterized by ^{1}H and ^{13}C-NMR, HRMS, and elemental analyses and show the expected results for the desired structures. While only one peak was detected by HPLC, the GC of the compound shows one main peak along with a very small impurity peak. This peak could not be identified by GC-MS, and could not be removed by column chromatography. For step-growth polymerization, it is very important to have highly pure monomers in order to obtain high molecular weights. Although monomers **14** and **15** yield useful polymers with interesting properties, the synthesis of solid monomers was attempted in order to make handling and purification easier.

Monomers with ether and phenyl functional groups were synthesized in the hope that they would be solids, as outlined in Figure 3.4. The additional ether group could increase the polarity of the compound, and the oxygen lone pairs could possibly interact with the thienyl hydrogen similar to the situation with ProDOT (see Section 2.3). With the phenyl substitution, it was hoped that π-stacking would occur to help crystallization. Transetherification of 3,4-dimethoxythiophene and compound **16** yields compound **17**, which can then undergo nucleophilic substitution to yield compounds **18** and **19**. It was thought that the added ether group in both monomers and the phenyl group in **19** would facilitate crystallization, but both compounds were obtained as clear oils and were not polymerized. It should be noted that bromination of compound **18** led to only mono-brominated product, and bromination of compound **19** was not attempted.

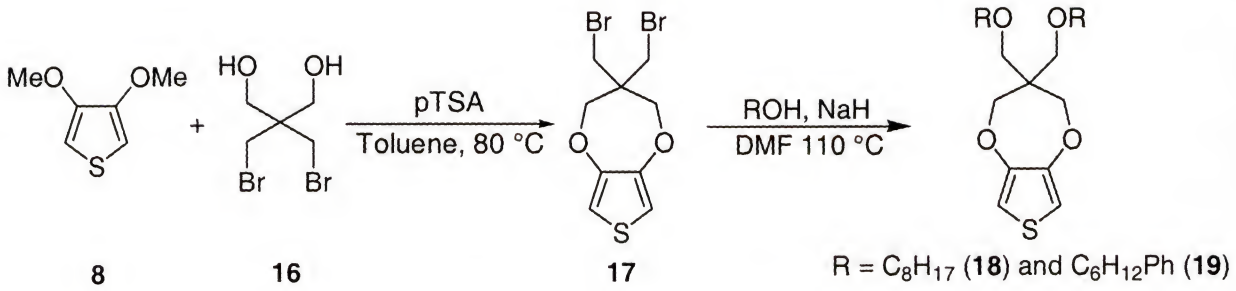

Figure 3.4 Synthesis of compounds **18** and **19**.

3.3 Polymer Synthesis

Figure 3.5 shows the synthesis of PProDOT-Bu_2 and PProDOT-Oct_2 using the GRIM method. The monomer was treated with one equivalent of MeMgBr and refluxed for one hour, followed by addition of 2 mol % of Ni(dppp)Cl_2. After precipitation into methanol followed by soxhlet extractions with methanol, hexanes, and chloroform, the reaction yields the polymer as a purple solid in 40 to 60% yield. **P15** was synthesized first, and was found to be soluble in chloroform, methylene chloride, toluene, and benzene. Because the molecular weights obtained were modest (see below) and monomer **15** was a hard to handle viscous oil, **P14** was also synthesized. **P14** exhibits similar properties to **P15**, but as reported in section 3.2, monomer **14** is also a viscous oil. **P14** is also a purple solid which is soluble in chloroform, methylene chloride, toluene, and benzene. Because **P14** was a soluble polymer, and the structure was simpler than **P15**, it was chosen as the polymer to study in full detail, and the characterization of this polymer is the subject of the rest of this chapter.

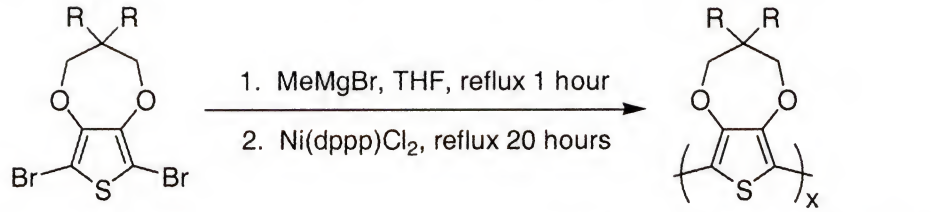

14 or **15**

R = butyl (**P14**) and octyl (**P15**)

Figure 3.5 Grignard metathesis polymerization of compounds **14** or **15**.3.4 Polymer Characterization

3.4.1 Structural Characterization

Figure 3.6 shows the ^{1}H and ^{13}C-NMR of **P14**. The proper peaks are present for the alkyl groups, and the methylenes adjacent to the oxygens. There are no end-group peaks evident for thienyl protons, which based on the ProDOT-Et_2 dimer NMR (see below) would occur around 6.3 ppm. It should be noted that these polymers oxidize quite rapidly in solution, and choice of NMR solvent made a difference. When deuterated chloroform was used, the polymer peaks were distorted, but when deuterated benzene was used the peak shapes were resolved. There were also problems with polymer oxidation in obtaining the ^{13}C-NMR. To obtain a ^{13}C-NMR of **P14**, the experiment had to be run overnight. Originally, the experiment was performed in $CDCl_3$ and when the spectrum was obtained only the peaks attributed to the alkyl groups were present. To remedy this problem, two drops of hydrazine were added to the solution to reduce the polymer. The spectrum obtained is displayed in Figure 3.6, and all of the proper shifts for the alkyl groups are present along with the methylene protons next to the oxygens. Two peaks would be expected for the thiophene carbons, but four peaks are present. The identity of peaks b and c is unknown at this time.

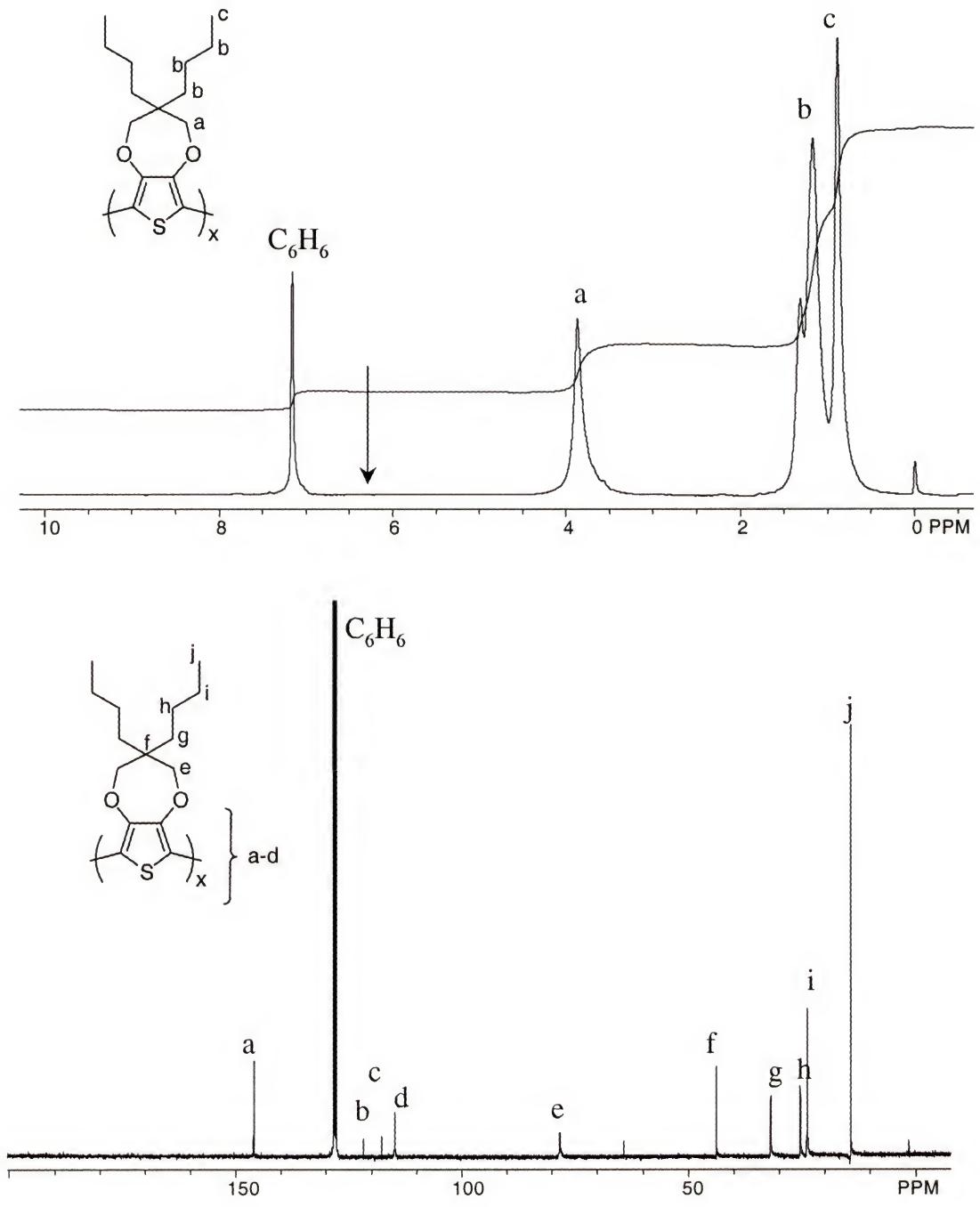

Figure 3.6 ^{1}H (top) and ^{13}C (bottom) NMR spectra of **P14** in C_6D_6 with the chemical shifts and structures labeled. The arrow shows where an end group shift would occur.

P14 was analyzed with infrared (IR) spectroscopy, and the results along with the IR spectra of ProDOT-Bu_2 and compound **14** (2,5-dibromoProDOT-Bu_2) are displayed in Figure 3.7. The IR spectrum of ProDOT-Bu_2 (**10c**) clearly exhibits a peak at 3113 cm^{-1}, which is assigned to the thienyl C-H stretch. When the compound is brominated and subsequently polymerized this stretch is no longer evident in the IR spectrum. The spectrum of **P14** exhibits three C-H stretch peaks between 2863 and 2957 cm^{-1} with no peaks above 3000 cm^{-1}. It is fairly difficult to determine the presence or absence of a halide in a compound using IR.[169] An aryl bromide usually exhibits a C-Br stretch between 1075 and 1030 cm^{-1}.[169] There is no peak in this range, but there is a peak at 933 cm^{-1} in compound **14**, that is not present in ProDOT-Bu_2 (**10c**). This peak also is not present in the spectrum of **P14**, leading to the conclusion that it could be the C-Br stretching vibration.

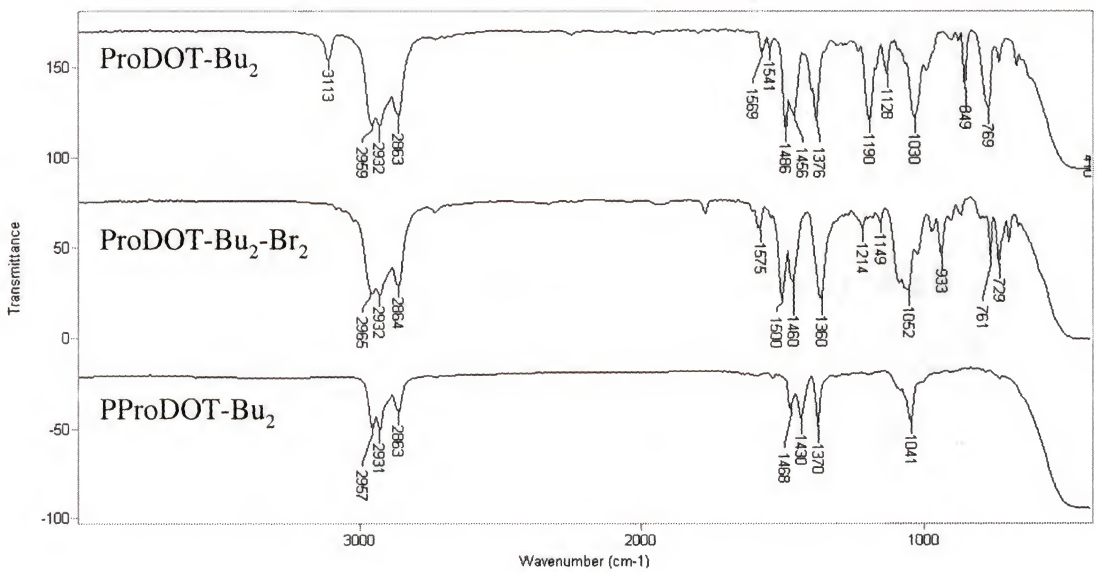

Figure 3.7 Stacked IR spectra of ProDOT-Bu_2 (**10c**), ProDOT-Bu_2Br_2 (**14**), and PProDOT-Bu_2 (**P14**) taken as thin films on NaCl salt plates.

3.4.2 Molecular Weight Analysis

Polymer molecular weight was analyzed by both GPC and MALDI-TOF-MS. GPC results obtained for these polymers were not very useful. Both **P14** and **P15** showed the same type of strange peak shape in GPC. There is severe tailing, indicating some sort of chemical interaction with the columns is occuring, which makes calculation of molecular weight distributions difficult. M_p values vs. polystyrene standards can be reported and they range from 4000 for **P15** to 6000 for **P14** which corresponds to a degree of polymerization (X_n) of 11 and 23 respectively. It should be noted that very high X_n is not needed to obtain the electrical and optical properties that are desired, although higher molecular weights may enhance polymer processing and film formation.

MALDI-TOF-MS was a useful tool in the molecular weight characterization of **P14**, and the results with terthiophene as the matrix are displayed in Figure 3.8. No cationization salt (typically a silver(I) salt) was used for these polymers, because they oxidized the polymer, and these polymers form stable radical cations without cationization salts. The correct repeat unit mass difference (266 amu) is observed between the peaks. Because this polymer has been fractionated by solvent extraction, accurate molecular weight distribution can be calculated from the MALDI spectrum. According to MALDI, **P14** has a M_n value of 5400, M_w of 5900, a polydispersity of 1.08, and an X_n value of 20, which is more than adequate for the desired optical properties. There are three different distributions stemming from chains with three different types of end groups. Figure 3.9 shows a close-up of the MALDI peaks, and shows how the functional group distribution was determined. The results are the same as seen by previous work by McCullough in the GRIM polymerization, where chains with three

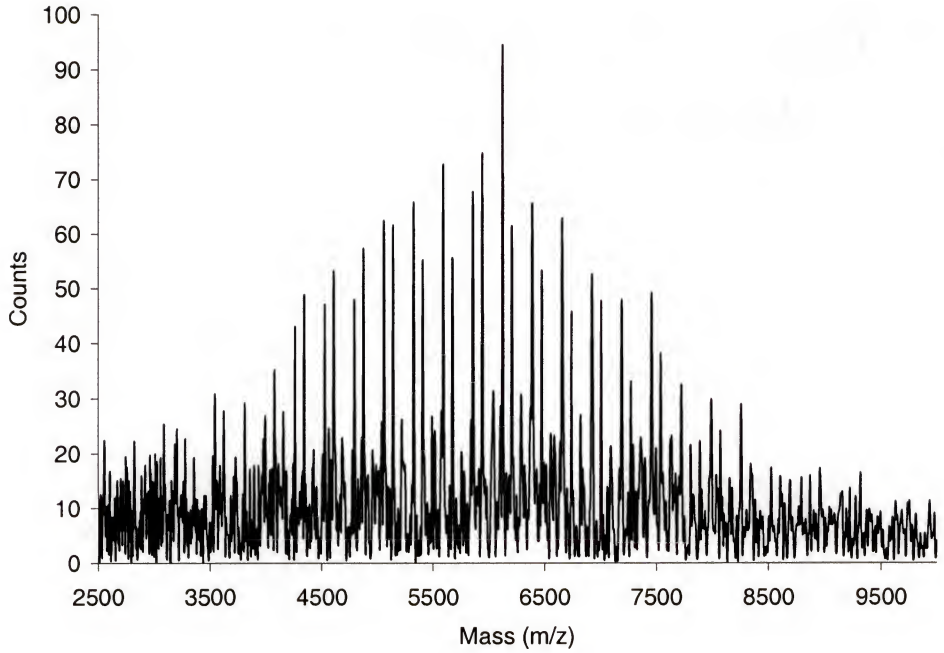

Figure 3.8 MALDI-TOF-MS of **P14** showing the full range of molecular weights.

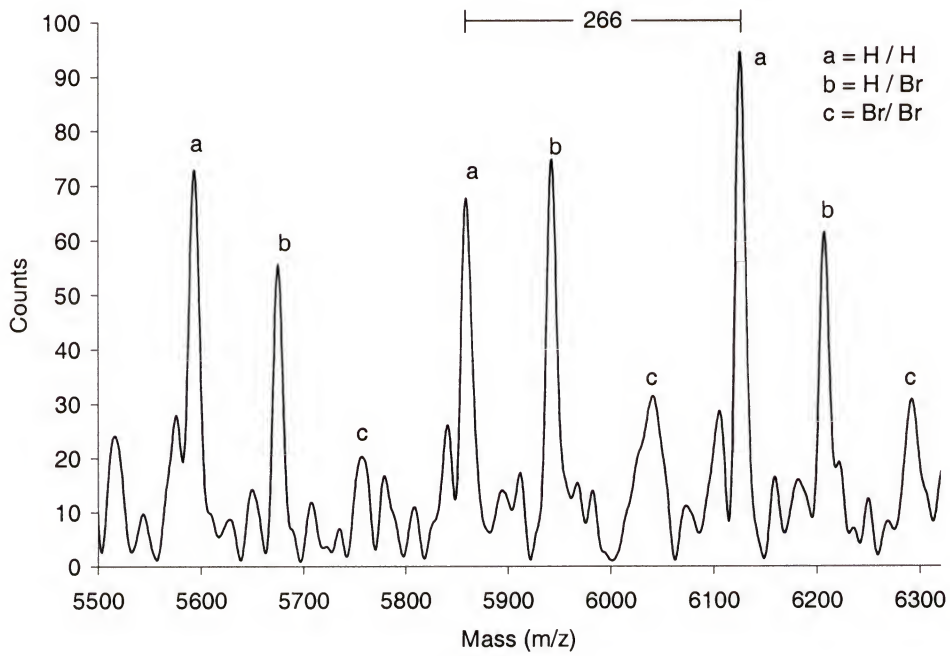

Figure 3.9 Close-up of the MALDI-TOF-MS of **P14** showing the three types of end groups present.

types of end groups could be found.[170] Analysis reveals that the masses of each peak can be represented by (266*n* + 1 + 1), (266*n* + 80 +1), and (266*n* +80 + 80) where *n* is equal to the number of repeat units. From these values, it can be concluded that the three types of end groups correspond to polymer chains that are terminated by two hydrogen atoms, one hydrogen atom and a bromine atom, and two bromine atoms. The McCullough group found that the relative abundances of these types of end groups are variable and depend on small changes in polymerization conditions that cannot be controlled.[170] The limitations of MALDI discussed above should be noted when considering the accuracy of these molecular weights, and even though the PDI value is less than 1.2, these numbers could still be artificially low due to poor detection of larger molecular weights.

The molecular weight can also be estimated from the amount of bromine present in the elemental analysis. If it is assumed that an average of 1 bromine per chain is present, then the molecular weight is 8410 g / mol, which corresponds to a chain length of 32 rings. As shown in the MALDI results, there are chains without bromine and some with two, making this value a very rough estimation.

The relatively low X_n values for these polymers can be attributed to the rigors of step polymerization and the electron-rich nature of the substrate. As previously discussed, monomers **14** and **15** are thick oils that could only be purified by column chromatography, and are difficult to weigh accurately. Small amounts of impurities can limit the conversion of the polymerization reaction, which severely limits the X_n. Also, although the polymerization occurs through an AB-type monomer, that monomer must be generated in-situ with the addition of a solution of MeMgBr in THF. This solution must be titrated (see Section 3.6.1 below) to obtain the proper molarity, and all of these steps

introduce experimental error that can limit X_n. Despite these experimental difficulties, previous work by the McCullough group with GRIM polymerization yielded PDDT with number average molecular weights ranging from 20000 – 30000 g / mol. There are differences between the two monomers; namely 2,5-dibromo-3-dodecyl (DBDT) thiophene is a liquid that can be purified by Kugelrohr distillation. Also, monomer **14** is much more electron-rich than DBDT. In the oxidative addition step of the nickel catalyzed coupling reaction, the metal is being oxidized and the substrate is reduced. Therefore, electron rich substrates are less reactive than electron-poor substrates.[144] Although this electron-rich nature is a hindrance, it is necessary for the final polymer properties that are desired.

The Ni(dppp)Cl_2 catalyst used in the reaction is actually a precatalyst that must be first reduced to the active nickel (0) catalyst, and this occurs by reaction of two molecules of the Grignard compound to yield the active catalyst and a bithiophene. If the stoichiometry is changed to account for this side reaction, then possibly higher molecular weights could be obtained. Many successful cross-couplings have been achieved with Ni(dppp)Cl_2 and this catalysts has many advantages. Namely it is readily available, air-stable, and contains a bidentate ligand, which forces the organic groups to be in a *cis* position on the metal that is necessary for successful transmetallation and reductive elimination.[145] Although a nickel (0) catalyst would eliminate the need for activation of catalyst, they are not desirable as they are air unstable and catalysts such as $Ni(PPh_3)_4$ have been shown to be ineffective for cross-coupling.[145] Other nickel(II) precatalysts may be useful for this reaction, and could be studied to see if molecular weights can be raised.

Some of the available catalysts that have been effective are $Ni(dppp)Br_2$, $Ni(dppf)Cl_2$, and $Ni(dppe)Cl_2$.

Nickel is not the only choice for the cross-coupling of a heteroaryl Grignard and bromide as palladium catalysis can also be used. Nickel catalysts are generally considered to be more reactive and less selective than palladium, which is exhibited by the ability of palladium to tolerate functional groups that nickel cannot (i.e. nitro, cyano, and carboxylic acid).[145] For these reasons, palladium catalysts such as $Pd(PPh_3)Cl_2$ and $Pd(dppf)Cl_2$ should be tried in these reactions to see if polymer properties can be enhanced.

3.4.3 Thermal Analysis

The thermal stability of **P14** was studied by thermogravimetric analysis (TGA) in a nitrogen atmosphere, and the resulting thermogram is displayed in Figure 3.10. The temperature was ramped from 50 to 800 °C at a rate of 20 °C/min, and the weight loss was observed with time. The thermogram for **P14** shows that degradation starts at 250 °C and shows an 8% weight loss before the main weight loss occurs starting at 383 °C with approximately 27% of the material remaining at 800 °C. Differential scanning calorimetry (DSC) analysis showed no transitions in the temperature range from 25 to 300 °C.

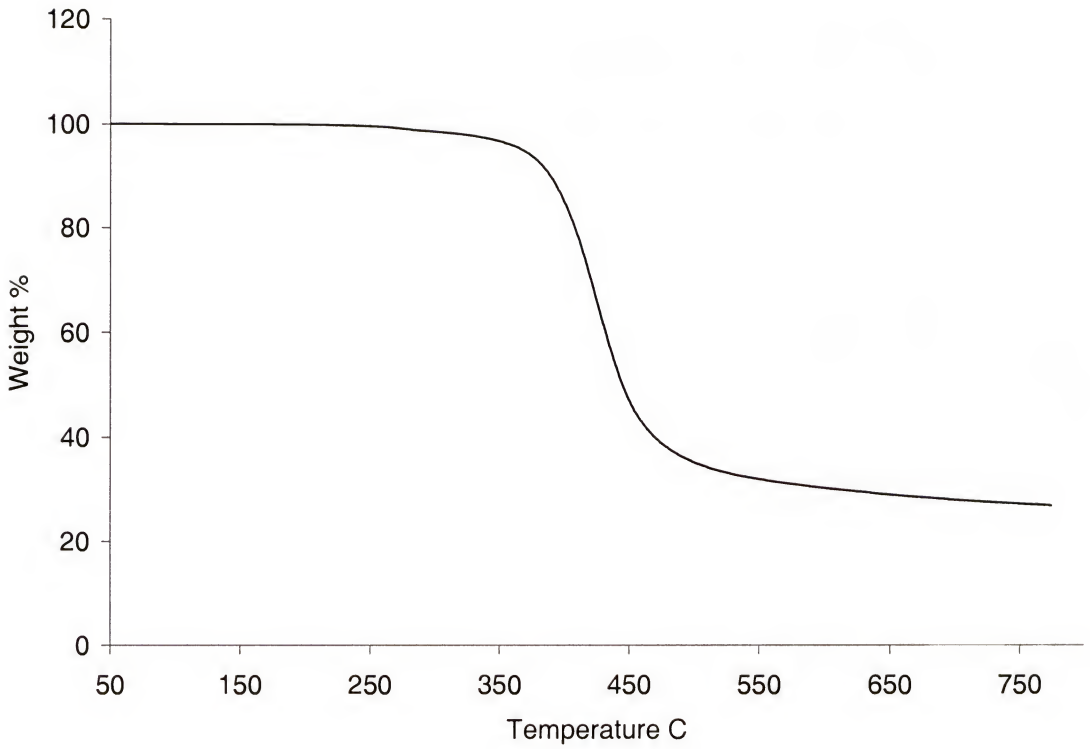

Figure 3.10 TGA thermogram for **P14** under nitrogen at a scan rate of 20 °C/min.

3.4.4 Solution and Solid-State Electronic Spectra

The UV-Vis spectra of **P14** in the solid state before and after electrochemical oxidation and reduction are shown in Figure 3.11. UV-Vis spectroscopy has been used extensively to study the electronic structure of conjugated polymers. Both electronic effects from electron-releasing or withdrawing substituents and bulk effects from chain twisting and packing can help describe the changes in electronic spectra of conjugated polymers. Solution cast films of **P14** are reddish-purple, and have a λ_{max} value of 544 nm, which is almost the same as the solution value (see below). When the films are electrochemically oxidized and then subsequently reduced, they appear as a dark purple color with a λ_{max} that is red shifted to 576 nm and the vibronic fine splitting is more

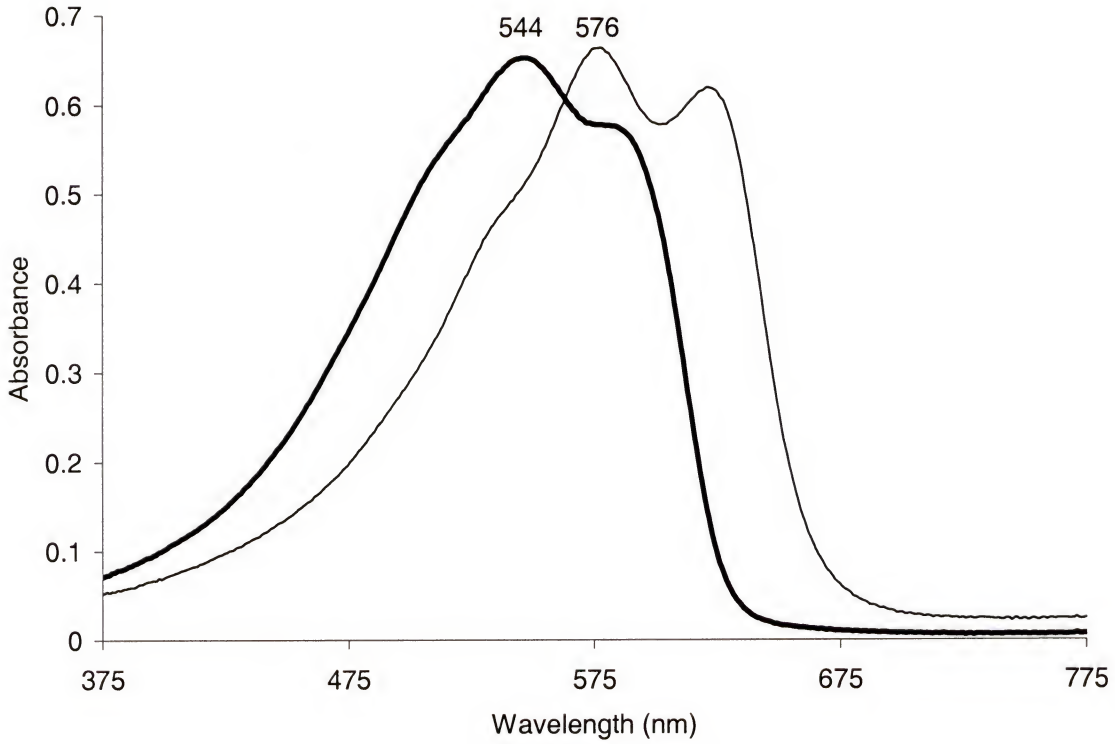

Figure 3.11 UV-Vis spectrum of **P14** in the solid state as cast from toluene (thick line) and after electrochemical oxidation and reduction (thin line).

pronounced thereby exhibiting a spectrum that is very similar to the electrochemically synthesized films discussed in Chapter 2. There is obviously a doping induced ordering of the polymer in the solid state. This type of behavior has been observed in solution with poly(3-octylthiophene) by Apperloo et al.,[171] where the authors attribute this behavior to the partial quinoid geometry of the oxidized state, which reduces conformational disorder along the chain and causes preorganization of the chains. This preorganization is preserved upon dedoping, and thus gives rise to the spectral changes. For comparison, the highest obtained λ_{max} for a regioregular head-to-tail poly(3-alkylthiophene) is 526 nm for thin films of poly(3-dodecylthiophene) (PDDT).[62] This red shift observed for **P14** was expected, because **P14** is much more electron-rich than

PDDT, giving it an elevated HOMO leading to absorption at a higher wavelength and a lower energy.

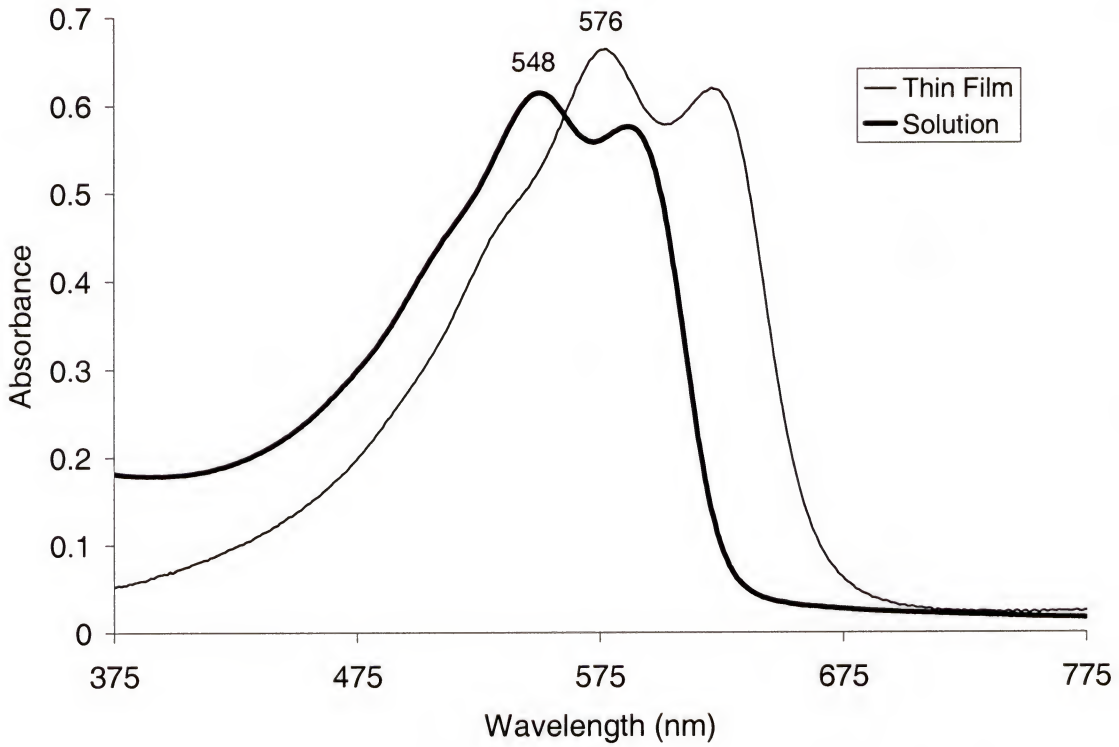

Figure 3.12 UV-Vis spectrum of **P14** in a CH_2Cl_2 solution (thick line) and in the solid state (thin line) after electrochemical oxidation and reduction.

The UV-Vis spectra of neutral **P14** in a methylene chloride solution and in the solid state are compared in Figure 3.12. As seen in other conjugated polymers, the solution λ_{max} (548 nm) is blue shifted (28 nm) when compared to the solid state film, because the chains have more conformational freedom in solution allowing for twisting of the thiophene rings out of plane. The shift from solid state to solution is much smaller in **P14** than PDDT, where λ_{max} of PDDT in solution is 450 nm, which is a 76 nm shift from the solid state value.[62] This fact combined with the fact that the polymer retains its

vibronic fine structure in solution suggests that **P14** is more ordered in solution than PDDT.

3.4.5 Photoluminescence

The absorption and fluorescence spectrum of a THF solution of **P14** is displayed in Figure 3.13. When the polymer solution is excited at 550 nm, a maximum emission wavelength of 615 nm is obtained. The polymer emits in the red region, and when a solution of polymer is placed under a UV lamp, red emission can be observed visually. Most fully conjugated polythiophenes are red emitters, with regioregular PATs exhibiting fluorescence with a maximum emission wavelengths between 550 and 570

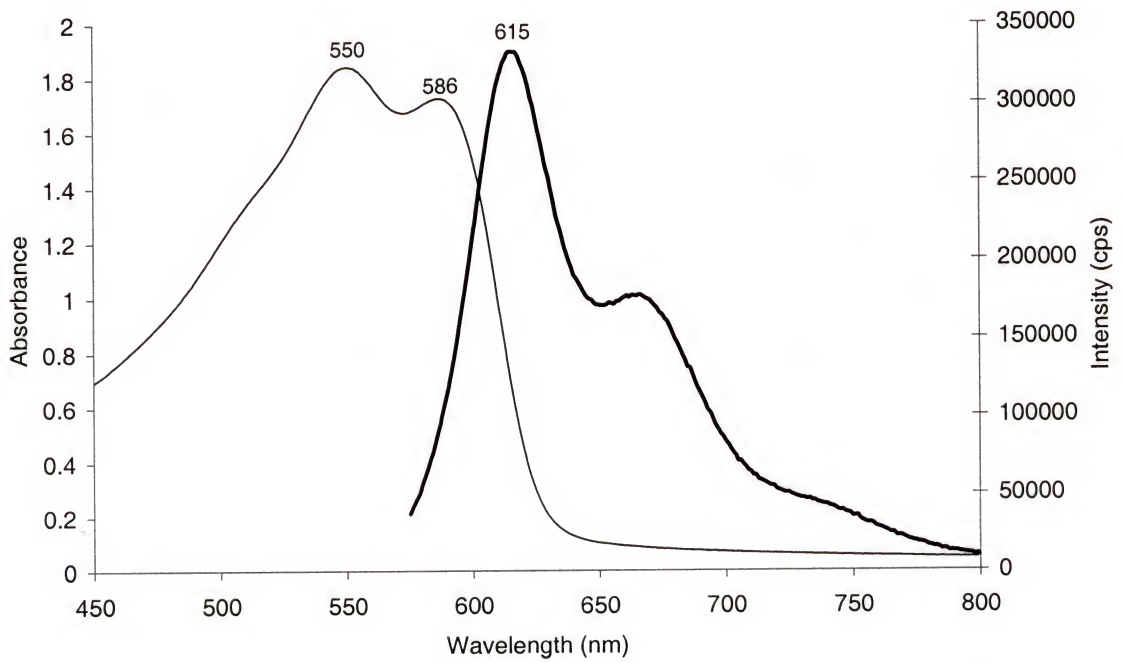

Figure 3.13 UV-Vis absorption (thin line) and photoluminescence emission spectrum (thick line) excited at 550 nm of **P14** in THF.

nm.[59,93] Photoluminescence efficiencies (ϕ_F) were calculated for solutions of **P14** in toluene and THF, and the values obtained were 0.45 and 0.44 respectively. These values are on the high end when compared with other photoluminescence efficiencies previously reported in the literature for polythiophenes. For example, poly(3-octylthiophene) exhibits a ϕ_F value of 0.27 and poly(3-dioctylphenylthiophene) (PDOPT) exhibits a higher value of 0.37.[172] The phenyl group in PDOPT is believed to be ca. 90° out of plane with the polymer chain allowing the octyl groups to force the main chains apart. Close chain contact is believed to lead to excimer formation, which leads to lower luminescence intensity and yield. The seven membered rings and butyl groups in **P14** could also serve to space the main polymer chains apart, which could lead to the high ϕ_F values.

The fluorescence spectrum of a film of **P14** cast from toluene is displayed in

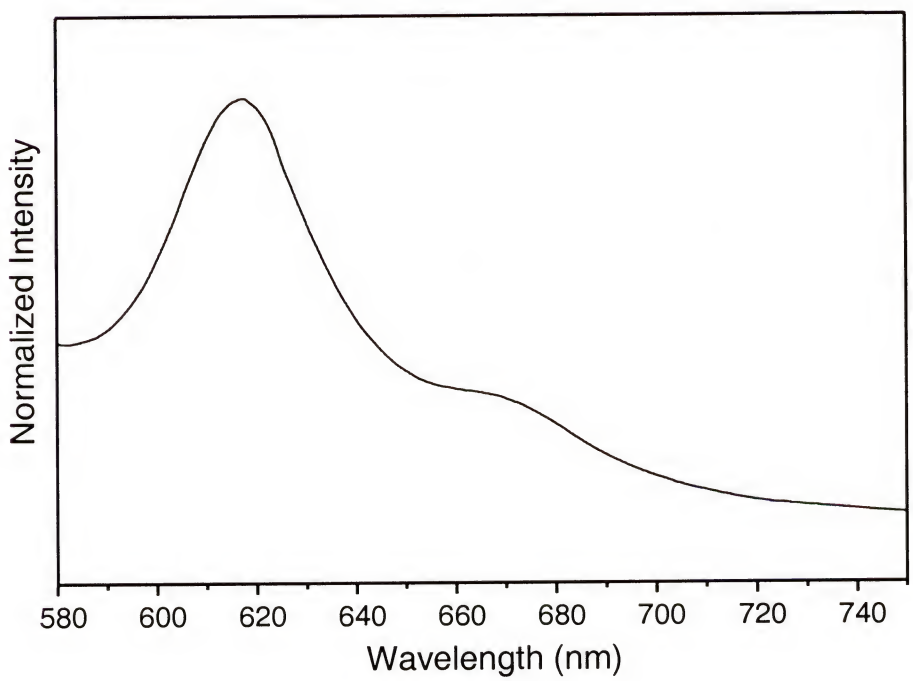

Figure 3.14 Photoluminescence spectrum of a solution cast film from toluene of **P14** excited at 500 nm.

Figure 3.14. The emission wavelength of 617 nm is very close to the value obtained in solution of 615 nm. The films are not visually luminescent, and the intensity is much lower than solution values, which would be expected since the chains are packed closer together in the solid state. More detailed photophysical studies are currently underway.

3.4.6 Polymer Electrochemistry

The cyclic voltammogram for a solution cast film from toluene of **P14** is shown in Figure 3.15. As expected for this electron-rich system, the $E_{1/2}$ is relatively low at 0 V vs.

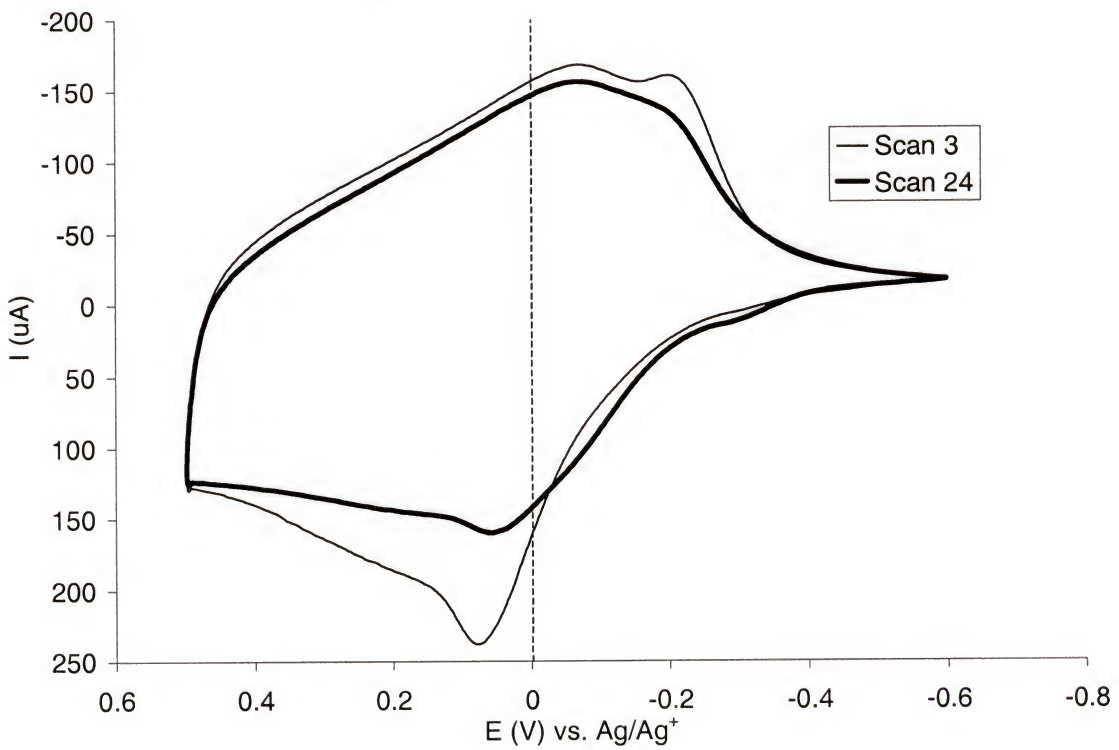

Figure 3.15 Cyclic voltammogram of **P14** as a function of repeated scans at 20 mV/s in 0.1 M TBAP/ACN: after 3 scans (thin line) and 24 scans (thick line). The dotted line shows where $E_{1/2}$ was measured.

Ag/Ag^+. This is much lower than the value of 0.39 V vs. Ag/Ag^+ for regioregular PDDT.[173] Also, the $E_{1/2}$ value is very close to that of PProDOT-Bu_2 synthesized by electrochemical polymerization, showing that soluble polymers can be synthesized with similar characteristics as the electropolymerized versions. Upon repeated scanning, there is a charge loss of 15% from scan 3 to 24. Since no delamination of the polymer from the electrode is evident, this loss of current response could be attributed to the slow dedoping of the polymer, as seen in the electrochromic switching studies (see below). If the polymer is not fully dedoped then in subsequent scans the current response of the polymer oxidation would be lower. This difficulty in reduction could be due to more closely packed chains in the solution cast film as compared to electrochemically polymerized films.

3.4.7 Spectroelectrochemistry and Electrochromic Switching

A spectroelectrochemical series was obtained on a solution cast film of **P14** in 0.1 M TBAP/ACN, and the results are displayed in Figure 3.16. When the polymer is held at a potential of –1.0 V (Figure 3.16b), there is a distinct π to π^* transition with a band gap of 1.8 eV, and two peaks at 2.0 and 2.2 eV. These values are very close to those of the electrochemically synthesized PProDOT polymers discussed in Section 2.6.2 (E_g = 1.75 eV). Notice that the baseline rises as lower energies are approached; this is due to slight oxidation of the polymer and trapped charges. Upon addition of hydrazine to further reduce the polymer (Figure 3.16a), the π to π^* transition increases in intensity

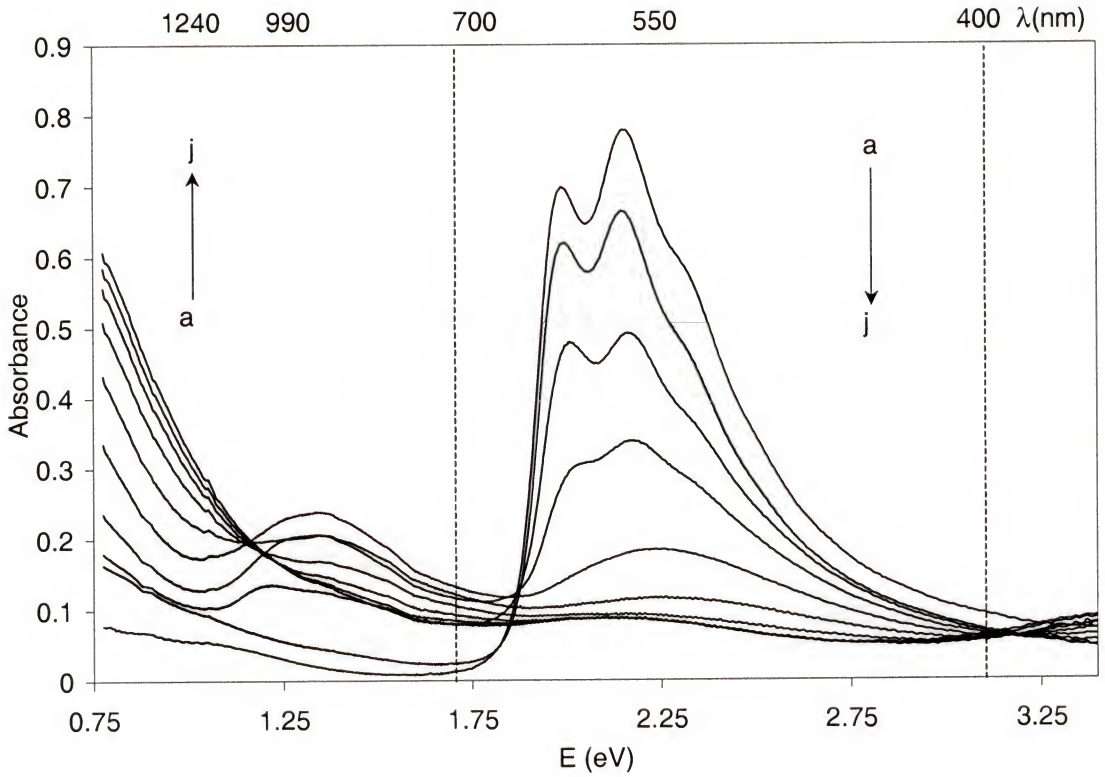

Figure 3.16 Spectroelectrochemistry of a solution cast film of **P14** in 0.1 M TBAP/ACN as a function of applied potential vs. Ag/Ag^+: (a) hydrazine reduced, (b) –1.0 V, (c) –0.2, (d) –0.1, (e) 0.0, (f) +0.1, (g) +0.2, (h) +0.3, (i) +0.4, (j) +0.5 V.

and the intensity of the low energy tail decreases. Upon stepwise oxidation of the polymer, the π to π^* transition decreases and two lower energy transitions increase in intensity at 1.35 and below 0.75 eV. Similar to the electrochemically polymerized films, the peak at 1.35 eV increases until 0 V, and then decreases upon application of more anodic potentials until at 0.5 V one lower energy transition is present, with very little "tailing" through the visible region. The fully oxidized film is a very transmissive sky blue in color, again greatly similar to the electrochemically synthesized films.

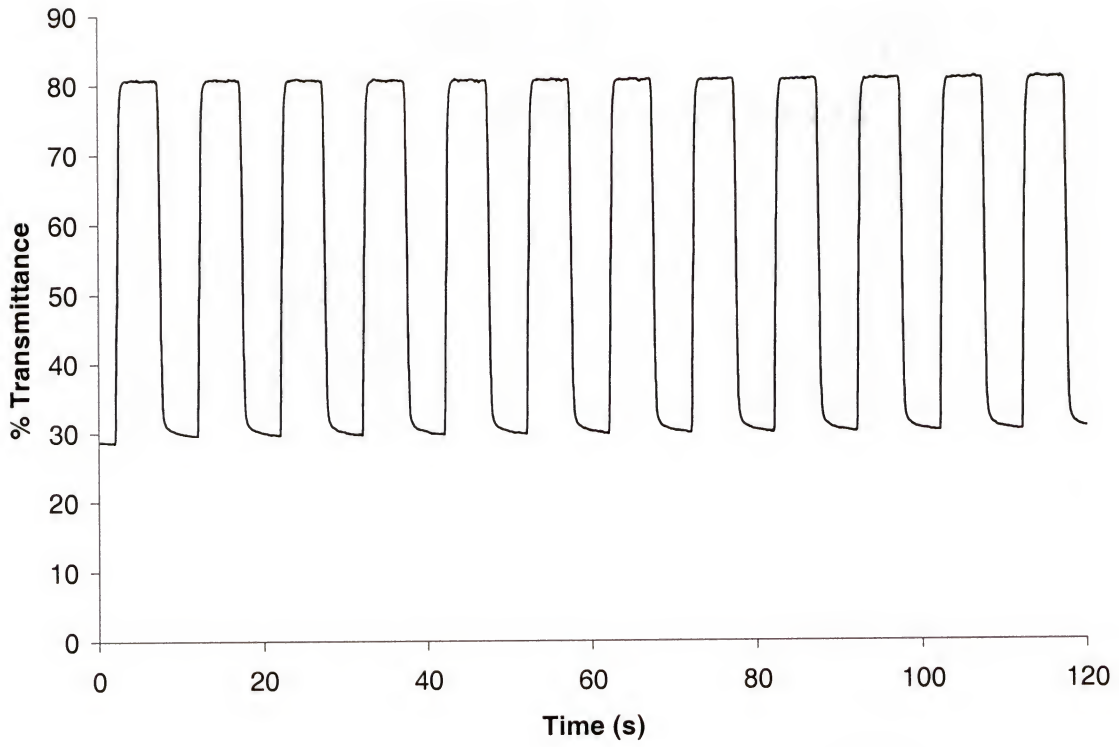

Figure 3.17 Electrochromic switching of **P14** for 12 switches between –1.0 and 0.8 V vs. Ag/Ag^+ in 0.1 M TBAP/ACN at a step time of 10 s.

For electrochromic switching, the same polymer film used for spectroelectrochemistry was switched by repeated potential steps between its reduced (-1.0 V) and oxidized (+0.8 V) states while %T at λmax (574 nm) was monitored vs. time and the results are displayed in Figure 3.17. The film oxidizes quite rapidly with response time to oxidize equal to 0.65 s at 95% of full contrast. Reduction is much slower, and even after 10 s the %T does not fully return to its initial value. This supports the earlier conclusion from spectroelectrochemistry that there are trapped charges in the film. If the film is held at –1.0 V for five minutes, then the film will eventually return to its original %T value. The difference between this film and the electrochemically synthesized film, could be due to morphology. It is generally believed that an

electrochemically polymerized film has an open morphology, while a solution cast film is more compact. This should hinder ion movement in and out of the film, and also introduce sites where charge gets trapped in the film leading to slower response times. The Δ%T value for this film of **P14** is 51%, which is substantially lower than the values for electrochemically synthesized PProDOT-Bu_2. The difference is in the reduced form, which is less absorptive than in the electrochemically synthesized polymer. A film thickness study is the next step in these experiments, to see where the Δ%T value is greatest. Although the electrochromic switching of the cast film is not as rapid, and does not have as high of a contrast as the electrochemically synthesized films, the switching is still quite rapid and reproducible and with more experiments, can be optimized.

3.4.8 Solution Doping

A solution of **P14** in CH_2Cl_2 was doped stepwise by addition of 2.0 μL aliquots of a 0.8 mM solution of $SbCl_5$ in CH_2Cl_2, and the results are displayed in Figure 3.18. The figure is split into the initial and final doping steps for clarity. In Figure 3.18a, the first part of doping shows a π to π* transition with an onset of 1.95 eV, peaks at 2.13 and 2.27 eV, and the reduced solution appears light purple in color. Note that the spectrum with the highest intensity of the peak at 2.27 eV is reduced with hydrazine, and the polymer solution is slightly oxidized with no oxidant addition. Upon oxidation, the π to π* transition decreases with the subsequent increase of two lower energy peaks at 1.3 and 0.9 eV. Similar to the behavior of the film spectroelectrochemistry discussed earlier, at higher doping levels (Figure 3.18b) the peak at 1.3 eV decreases until there appears to be only one transition below 0.9 eV. Again, there is very little tailing in the visible

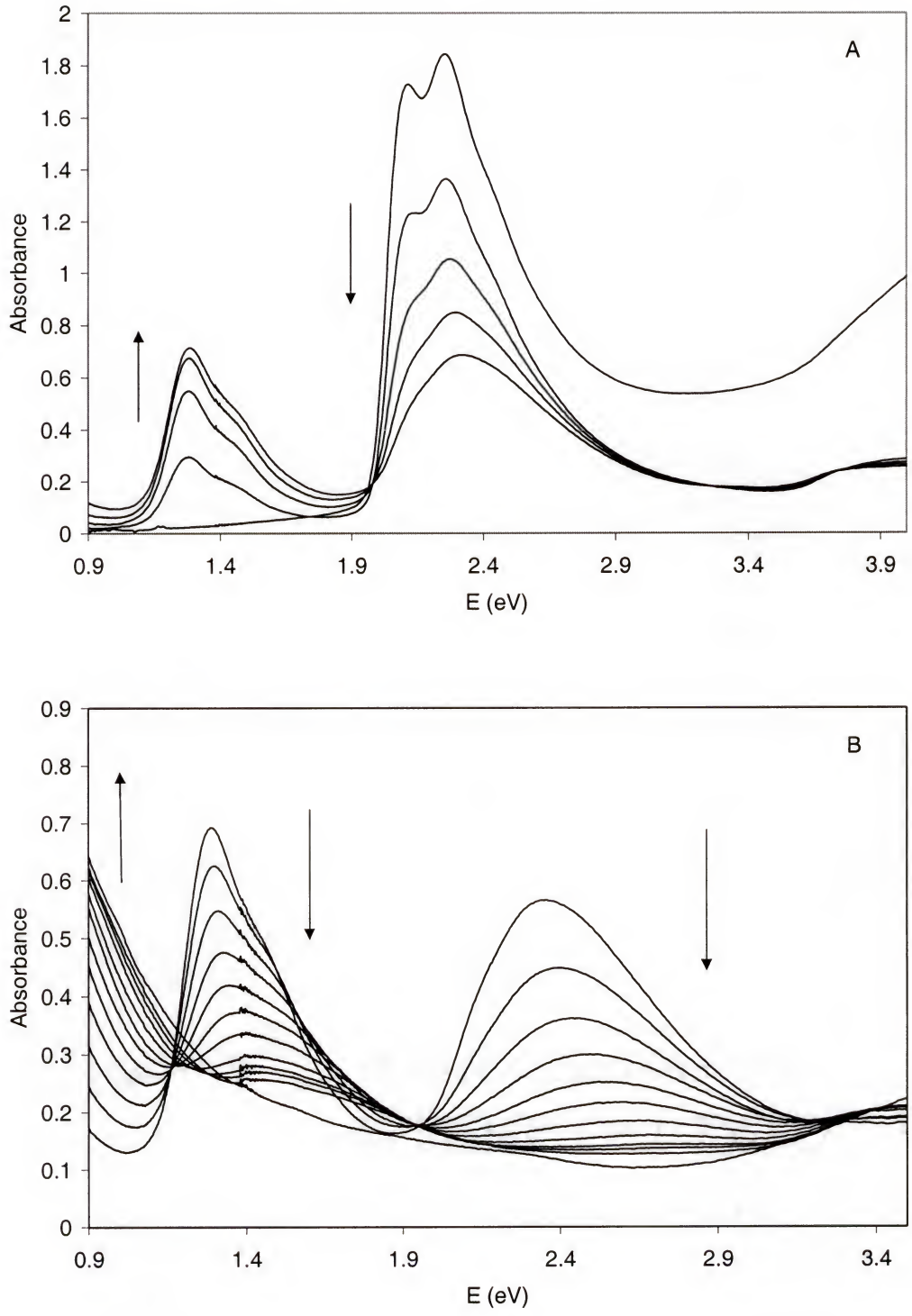

Figure 3.18 UV-Vis-NIR spectra of a solution of **P14** in CH_2Cl_2 as a function of addition of 2.0 μL aliquots of a 0.8 mM solution $SbCl_5$ in CH_2Cl_2. Part A displays initial doping and B displays final doping.

region, and the oxidized solution appears as a very transmissive light blue. The dopant ion is hexachloroantimonate ($SBCl_6^-$), and it should not attribute greatly to the color of the doped solution, as tetramethylammoniumhexachloroantimonate is a colorless solid.[174] These doping trends support the conclusions discussed in Section 2.6, and illustrate the transitions as described by the FBC theory. At low doping levels, polarons are the main charge carriers giving rise to two lower energy transitions, while at high doping levels bipolarons are formed giving rise to a lower energy transition below 0.9 eV. These results are very similar to those obtained by Apperloo, et al.. for poly(3-octylthiophene) doped in solution by thianthrenium perchlorate.[118] The authors did note that their films were unstable, which could possibly be remedied by the electron-rich nature of **P14**.

3.5 Synthesis and Crystal Structure of BiProDOT-Et_2 Model Compound

The Reynolds group has synthesized the dimer of EDOT, and shown through crystal structure data that the thiophene rings are co-planar with a torsional angle of 0 ° within experimental error.[175] It was desirable to obtain the crystal structure of a ProDOT-R_2 compound to probe the dihedral angle between the thiophenes. BiProDOT-Et_2 (**20**) was synthesized as outlined in Figure 3.19 following the $Fe(acac)_3$ route used by Zhu and Swager to synthesize BiEDOT.[176] Originally, the dimer of ProDOT-Oct_2 (**10d**) was synthesized, but it was obtained as an oil. ProDOT-Et_2 was lithiated, and the anion was transferred to a refluxing THF solution of $Fe(acac)_3$ which gives BiProDOT-Et_2 (**20**) in 80% yield. This compound was recrystallized from hexanes / ethyl acetate to yield single crystals for X-ray structure determination.

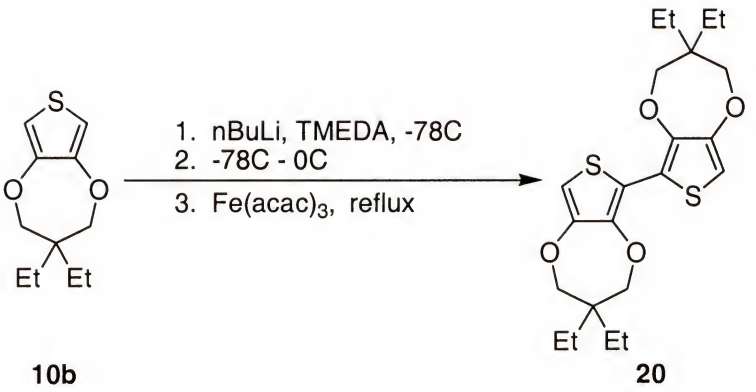

Figure 3.19 Synthesis of BiProDOT-Et_2 (**20**).

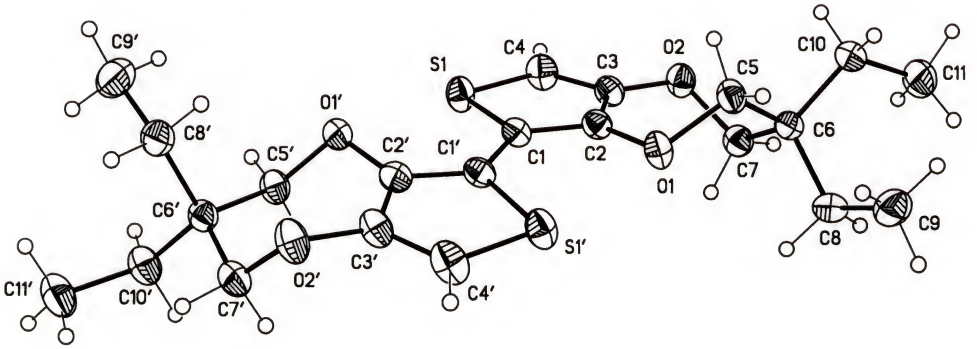

Figure 3.20 Perspective view and atom labeling of the crystal structure of BiProDOT-Et_2 (**20**).

A crystal structure was obtained for this compound and is displayed in Figure 3.20. The dihedral angle between the thiophene rings is 9.37 °, which is close to coplanar, showing that there are not large steric problems with the thiophenes obtaining planarity with respect to each other. An interesting feature of the crystal structure is the conformation of the propylenedioxy seven-membered rings. In the ring on the right side of the structure, the seven-membered ring is in a twist conformation, while the ring on the right is in a chair-like conformation. This shows that the seven-membered ring has

enough conformational freedom to obtain the conformation to allow for planarity between the thiophene rings.

3.6 Conclusions

Electron-rich soluble polymers based on the PProDOT-R_2 structure have been synthesized using the Grignard metathesis reaction. PProDOT-Bu_2 exhibits an X_n value of 20 as determined by MALDI-TOF mass spectrometry, and is thermally stable to 250 °C. Fluorescence spectroscopy shows that PProDOT-Bu_2 emits red light with an emission maximum at 615 nm in solution and 617 nm in the solid state. Solution photoluminescence efficiencies were measured to be 0.45 and 0.44 in toluene and THF respectively. Polymer films cast onto Pt electrodes can be cycled between their reduced and oxidized forms with an $E_{1/2}$ value of 0 V vs. Ag/Ag^+. Spectroelectrochemistry results of cast films of PProDOT-Bu_2 estimate a band gap of 1.8 eV, and when fully oxidized the film shows very little absorbance in the visible region. Electrochromic switching shows that the films can be switched efficiently between their oxidized and reduced forms. The solid state electrochemistry and spectroelectrochemistry results are very similar to the results discussed in Chapter 2 for the electropolymerized version of these polymers, indicating that the chemically polymerized films do behave similarly to the electropolymerized films. Solution doping with $SbCl_5$ was performed, and at high doping levels the solutions are a very transmissive blue with very little absorbance in the visible region. A model compound BiProDOT-Et_2 was synthesized, and the crystal structure indicates that the dihedral angle between the thiophene rings is 9.37°. These results prove that highly electron-rich polymers can be successfully synthesized by chemical

polymerized and fully characterized by traditional techniques used for other synthetic polymers.

3.7 Experimental

3.7.1 Materials

Compounds **8**, **10c**, and **10d** were synthesized as described in Chapter 2. NBS was obtained from Acros, and recrystallized from water prior to use. Methylmagnesium bromide in butyl ether was purchased from Aldrich, and exact molarity was determined by titration with a solution of 0.25 M 2-butanol and 0.005 M N-phenyl-1-napthamine in p-xylene.[177] TBAP was prepared by mixing a 1:1 mole ratio of tetrabutylammonium bromide (Aldrich) dissolved in water with perchloric acid. The precipitate was filtered, recrystallized from ethanol and dried in vacuo. Acetonitrile (Aldrich) was dried over calcium hydride and distilled under argon. Toluene (Fisher) was dried over sodium metal and distilled under argon. Tetrahydrofuran (THF) was dried over NaK and distilled under argon. Anhydrous *N, N*-dimethylforamide (DMF), p-toluenesulfonic acid, 2,2-(bis-bromomethyl)-1,3-propanediol, sodium hydride, 6-phenyl-1-octanol, *N, N, N',N'*-tetramethylethylenediamine, $Fe(acac)_3$, and $Ni(dppp)Cl_2$ were obtained from Aldrich and used as purchased. *n*-BuLi was obtained from Acros and used as purchased. Chloroform and 1-octanol were obtained from Fisher and used as purchased.

3.7.2 Structural Identification of Monomers and Polymers

NMR spectra were recorded on a Gemini 300 FT-NMR, VXR 300 FT-NMR, or a Varian XL-300 FT-NMR. Mass spectrometry was carried out on a Finnigan MAT 95Q mass spectrometer. Elemental analyses were accomplished at Robertson Microlit Laboratories, Inc., Madison, NJ. FT-IR spectra of samples prepared as thin films on NaCl plates were obtained using a Perkin-Elmer 1640 FT-IR spectrometer.

GPC was performed on two 300 x 7.5 mm Polymer Laboratories PLGel 5uM mixed-C columns with a Waters Associates Liquid Chromatography 757 UV absorbance detector at 550 nm. Molecular weights were referenced to polystyrene standards (Polymer Laboratories). Polymer samples were prepared in THF (1 mg/mL), and passed through a 50 uM filter prior to injection. A constant flow rate of 1 mL/min was used.

MALDI-TOF-MS were obtained on a Bruker reflex II mass spectrometer equipped with delayed extraction (Bruker Daltonics, Manning Park, Billerica, MA). The accelerating voltage was 21 KeV with a delay of 50 ns. The system was operated in reflectron mode. Both terthiophene and dithranol were used as matrices with better resolution in terthiophene. Samples were prepared from a 1:1 combination of a THF solution of 0.1M terthiophene and 1 x 10^{-4} M THF solution of polymer. This mixture was then spotted on the MALDI sample plate.

UV-Vis-NIR spectra were recorded using a Varian Cary 5E UV-Vis-NIR spectrophotometer. Fluorescence data were obtained with a Spex F-112 photon counting fluorimeter at room temperature. Emission quantum yields were measured relative to Rhodamine 6G in methanol at 1.00 x 10^{-6} M where $\phi_F = 1.00$[178], and the optical density of the solutions was kept below A=0.1. Thermogravimetric analysis was obtained with a

Perkin-Elmer TGA 7 thermogravimetric analyzer. Differential scanning calorimetry was obtained on a Perkin-Elmer DSC 7 differential scanning calorimeter. Polymer electrochemistry was carried out on a EG&G Princeton Applied Research model 273A potentiostat/galvanostat with a platinum button working electrode, a platinum flag counter electrode, and a Ag/Ag^+ reference electrode. Spectroelectrochemistry was performed using a Varian Cary 5E UV-Vis-NIR spectrophotometer. A three-electrode cell was used with an ITO-coated glass slide as the working electrode, a platinum wire counter electrode, and a Ag/Ag^+ reference electrode all contained in a normal UV-Vis cuvette. Potentials were applied using the same EG&G potentiostat as described above. Polymer films were cast on both the platinum button and ITO slide with a micropipet from a 2% solution of polymer in toluene. The films were dried under a nitrogen blanket prior to use.

3.7.3 Synthesis

6,8-dibromo-3,3-dibutyl-3,4-dihydro-2H-thieno[3,4-b][1,4]dioxepine (ProDOT-Bu_2-Br_2) (14). 1g (3.7 mmol) of compound **10c** was dissolved in 100 mL of chloroform in a two neck flask equipped with an argon inlet. Argon was bubbled through the solution for 20 minutes, and then 2 g (11.1 mmol) of NBS was added. The clear yellow solution was stirred at room temperature for 4 hours after which the solution was a dark brownish-red color. The chloroform was removed under vacuum, and the resulting residue was purified using column chromatography on silica gel with 8:2 hexanes/methylene chloride as the eluent to yield (after two columns) 1.53 g (97%) of compound **14** as a clear viscous oil. ^1H NMR ($CDCl_3$): δ 0.90 (t, 6H), 1.30 (m, 12H),

3.88 (s, 4H). ^{13}C NMR ($CDCl_3$): δ 14.20, 23.52, 26.04, 31.88, 44.21, 78.14, 90.82, 147.29. Elemental Analysis: Calculated for $C_{15}H_{22}Br_2O_2S$: C, 42.27; H, 5.20; S, 7.52. Found: C, 42.47; H, 5.02; S, 7.84.

6,8-dibromo-3,3-dioctyl-3,4-dihydro-2H-thieno[3,4-b][1,4]dioxepine (ProDOT-Oct_2-Br_2) (15). Compound **15** was synthesized using the same procedure as compound **14** using 1 g (2.6 mmol) of compound **10d**, 0.48 g (2.7 mmol) and 25 mL each of chloroform and acetic acid. Yield 0.41 g (35%). A clear viscous oil. ^1H NMR ($CDCl_3$): δ 0.89 (t, 6H), 1.30 (m, 28), 3.85 (s, 4H). 14.15, 22.70, 29.37, 29.51, 30.61, 31.91, 43.76, 78.21, 91.15, 146.89. Elemental Analysis: Calculated for $C_{23}H_{38}Br_2O_2S$: C, 51.31; H, 7.11; S, 5.96. Found: C, 51.52; H, 6.96; S, 6.21.

3,3-bis-bromomethyl-3,4-dihydro-2H-thieno[3,4-b][1,4]dioxepine (ProDOT-($CH_2Br)_2$) (17). 3 g (20.8 mmol) of compound **8**, 10.9 g (41.6 mmol) of compound **16**, 0.4 g (2.1 mmol) of p-toluenesulfonic acid, and 200 mL and toluene were combined in a 2-neck flask equipped with a soxhlet extractor with type 4A molecular sieves in the thimble. The solution was heated to reflux and allowed to reflux for 1 day. The reaction mixture was cooled and washed with water. The toluene was removed under vacuum, and the crude product was purified by column chromatography on silica gel with 3:2 hexanes / methylene chloride as the eluent to yield 4.2 g (59%) of compound **17** as a white solid. mp 66-68 °C. ^1H NMR ($CDCl_3$): δ 3.61 (s, 4H), 4.10 (s, 4H), 6.49 (s, 2H); ^{13}C NMR ($CDCl_3$): δ 34.41, 46.12, 74.15, 105.72, 148.5. Elemental analysis: Calculated

for $C_9H_{10}O_2Br_2S$: C, 31.60%; H, 2.95%; S, 9.37. Found: C, 31.83%; H, 2.99%; S, 9.20%; HRMS calculated for $C_9H_{10}O_2Br_2S$: 339.8768. Found: 341.8730 (M+2).

3,3-bis-octyloxymethyl-3,4-dihydro-2H-thieno[3,4-b][1,4]dioxepine (ProDOT-($CH_2OC_8H_{17}$)$_2$) (18). 0.57 g (4.38 mmol) of 1-octanol was dissolved in 50 mL of DMF in a 2 necked flask equipped with a reflux condenser and argon inlet. 0.21 g (8.76 mmol) of NaH was added and the mixture was heated to 110 °C. After 4 hours, 0.5 g (1.46 mmol) of compound **17** was added and the mixture was heated at 110 °C for 20 hours. The mixture was cooled, poured into 200 mL of brine, and extracted three times with methylene chloride. The combined methylene chloride layers were combined and washed with copious amounts of water. The chloroform was removed under pressure to yield a dark oil. Purification by column chromatography on silica gel with 3:2 hexanes/methylene chloride as eluent yielded 0.25 g (40%) of compound **18** as a slightly yellow oil. ^{1}H NMR ($CDCl_3$): δ 0.85 (m, 6H), 1.29 (m, 20H), 1.55 (m, 4H), 3.39 (t, 4H), 3.50 (s, 4H), 4.05 (s, 4H), 6.45 (s, 2H). Elemental analysis: Calculated for $C_{25}H_{44}O_4S$: C, 68.14%; H, 10.06%. Found: C, 68.47%; H, 10.12%.

3,3-bis-(5-phenyl-hexyloxymethyl)-3,4-dihydro-2H-thieno[3,4-b][1,4]dioxepine (ProDOT-($CH_2OC_6H_{12}Ph$)$_2$) (19). Compound **19** was synthesized using the same procedure as compound **18** using 0.5 g (1.46 mmol) of compound **17**, 0.59 g (3.21 mmol) of 6-phenyl-1-hexanol, 0.24 g (6.42 mmol) of NaH, and 50 mL of DMF. Yield 0.36 g (46%). A yellow oil. ^{1}H NMR ($CDCl_3$): δ 1.35 (m, 8H), 1.60 (m, 8H), 2.65 (t, 4H), 3.40 (t, 4H), 3.52 (s, 4H), 4.05 (s, 4H), 6.46 (s, 2H), 7.25 (m, 10H).

PProDOT-Bu_2 (P14). MeMgBr solution in butyl ether was titrated as described above[177] and the concentration was found to be 0.925 M. 0.400 g (0.939 mmol) of compound **14** was dissolved in 25 mL of freshly distilled THF. 1.02 mL (0.9 mmol) of MeMgBr in butyl ether was added and the colorless solution was heated to reflux. After 1 hour, 0.013 g (2 mol%) of Ni(dppp)Cl_2 was added and the bright red mixture was heated at reflux for 20 hours. The polymer was precipitated into 200 mL of methanol, and filtered into a soxhlet thimble. Soxhlet extractions were performed for 24 hours with methanol and 48 hours with hexanes to remove impurities. A subsequent soxhlet extraction with methylene chloride was used to dissolve the polymer from the thimble, and the methylene chloride was removed to yield a dark purple solid 0.15 g (60%) of **P14**. ^{1}H NMR ($CDCl_3$): δ 0.90 (bm, 6H), 1.20 (bm, 12H), 3.87 (bm, 4H). ^{13}C NMR ($CDCl_3$): δ 13.10, 22.64, 24.14, 30.62, 42.51, 62.80, 77.05, 113.50, 116.42, 120.48, 144.69. Elemental analysis: Calculated for a chain taking into account the bromine content found and assuming one bromine and one hydrogen as endgroups $C_{465}H_{683}O_{62}S_{31}Br$: C, 66.97%; H, 8.26%; S, 11.92% Br 0.95. Found: C, 65.86%; H, 8.23%; S, 11.61%; Br, 0.95%.

PProDOT-Oct_2 (P15). Polymer **P15** was synthesized with the same procedure for **P14** using 0.400 g (0.740 mmol) of compound **15**, 0.74 mL (0.7 mmol) of MeMgBr in butyl ether, 0.004 g (1 mol %) of Ni(dppp)Cl_2, and 30 mL of THF. Yield: 0.11 g (40%). A dark purple solid. ^{1}H NMR ($CDCl_3$): δ 0.88 (bm, 6H), 1.28 (bm, 24H), 1.45 (bm, 4H), 3.93 (bm, 4H).

BiProDOT-Et$_2$ (20). 0.5 g (2.3 mmol) of compound **10b** and 0.53 g (4.6 mmol) of TMEDA was dissolved in 25 mL of THF, cooled to –78 °C where 1.16 mL (2.9 mmol) of 2.5 M nBuLi in hexanes was added and the solution was stirred for 40 minutes. After raising the temperature to 0 °C, the solution was transferred via cannula to a refluxing solution of 0.81 g (2.3 mmol) of $Fe(acac)_3$ in 25 mL of THF, and the red solution was refluxed overnight. The THF was removed under vacuum, and the resulting red solid was run through a plug of silica gel with chloroform as the eluent to yield a green solid. The solid was dissolved in chloroform and two drops of hydrazine hydrate was added, and the chloroform was removed under vacuum to yield 0.4 g (80%) of compound **20** as a yellow solid. mp 121-123 °C. ^{1}H NMR (C_6D_6): δ 0.59 (t, 12H), 1.16 (q, 8H), 3.59 (s, 4H), 3.71 (s, 4H), 6.33 (s, 2H); ^{13}C NMR ($CDCl_3$): δ 7.21, 23.65, 43.90, 77.09, 77.15, 102.82, 115.10, 145.05, 149.57. Elemental analysis: Calculated for $C_{22}H_{30}O_4S_2$: C, 62.53%; H, 7.16%; S, 15.17. Found: C, 62.40%; H, 7.11%; S, 15.00%; HRMS calculated for $C_{22}H_{30}O_4S_2$: 422.1585. Found: 422.1588.

3.7.4 X-Ray Crystallography; Data Collection, Structure Solution, and Refinement

Data were collected at 173 K on a Siemens SMART PLATFORM equipped with A CCD area detector and a graphite monochromator utilizing MoK_α radiation (λ = 0.71073 Å). Cell parameters were refined using up to 8192 reflections. A hemisphere of data (1381 frames) was collected using the ω-scan method (0.3° frame width). The first 50 frames were remeasured at the end of data collection to monitor instrument and crystal

stability (maximum correction on I was < 1 %). Absorption corrections by integration were applied based on measured indexed crystal faces.

The structure was solved by the Direct Methods in *SHELXTL5,* and refined using full-matrix least squares. The non-H atoms were treated anisotropically, whereas the hydrogen atoms were calculated in ideal positions and were riding on their respective carbon atoms. The thiophene rings are planar and have a dihedral angle of 9.37(9)° between them. The S1 seven membered ring adopts a twist conformation with C5 and C7 located at distances of 0.815(3) and -0.779(3)Å, respectively, of the plane of atoms C2, C3, O1 and O2; atom C6 lies within 2σ of the same plane. On the other hand, the S1' seven membered ring adopts a chair conformation where atoms C5', C6' and C7' are located at distances of -1.126(3), -1.046(3) and -1.133(3)Å, respectively, from the plane of C2', C3' O1' and O4'. A total of **184** parameters were refined in the final cycle of refinement using 3085 reflections with $I > 2\sigma(I)$ to yield R_1 and wR_2 of **3.78**% and **9.08**%, respectively. Refinement was done using F^2.[179]

CHAPTER 4
CARBAZOLE-BASED POLYMERS

4.1 Introduction

Up to now, the polymers discussed in this dissertation were cathodically coloring and only able to switch between two different color states, the importance of which has been discussed previously. For device applications, polymers that exhibit three or more color states are also important with ultimate applicability to large signs and camouflage. Unfortunately, there are relatively few polymers that exhibit multiple color states. Polyaniline (PANI) is the most studied of these polymers, and until recently was thought to be the most industrially viable. PANI exhibits three color states, yellow in the neutral form, green in the mildly oxidized state, and blue in the fully oxidized state.[180,181,182] With continuous cycling, PANI tends to lose its ability to access its different color states, thus leading to a need for a more stable polychromic polymer.

Polycarbazole is another polychromic polymer that is colorless when neutral, green in an intermediate oxidized state (0.7 V vs. SCE), and blue in the fully oxidized state (1.0 V vs. SCE).[183,184,185,186] The first study on the electrochemical polymerization of carbazoles showed that the polymerization primarily occurs through the 3 and 6 positions.[187] These carbazole-based polymers form three distinct color states, because there is a break in conjugation along the polymer chain. Figure 4.1 shows the three separate redox states that are formed in a carbazole polymer and,unlike polythiophene

and other polyheterocycles, polycarbazole is not fully conjugated, because the nitrogen atom breaks the conjugation. Therefore, the radical cations and dications that are formed upon oxidation are not free to move along the polymer chain.

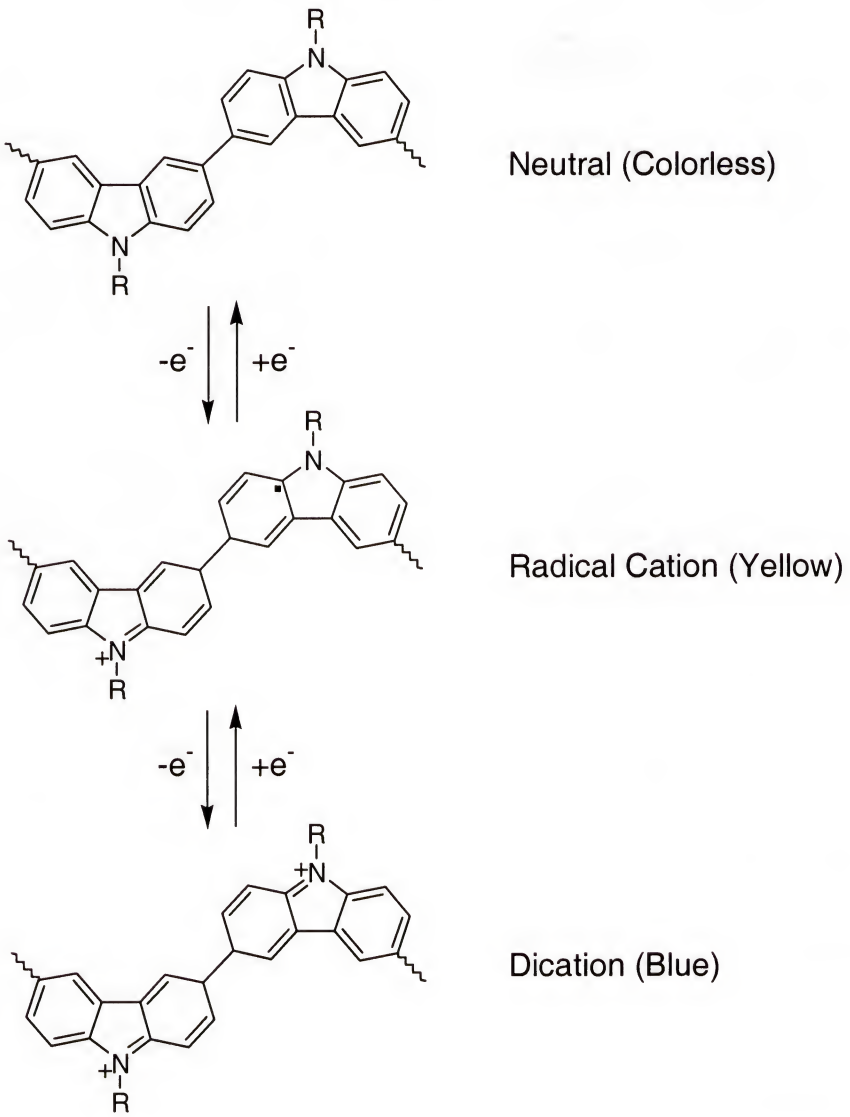

Figure 4.1 The three discrete color states of polycarbazole illustrating the break in conjugation of the molecule.

Recently, the Reynolds group has reported on the synthesis and electropolymerization of bisheterocycle-*N*-substituted carbazoles, where the heterocycle

was either EDOT or pyrrole.[188,189] As previously discussed in Chapter 1, multi-ring monomers with terminal electron-rich heterocyles such as EDOT and pyrrole considerably lower the oxidation potential of the monomer by increasing electron density and conjugation length. The bisheterocycle carbazoles exhibit $E_{p,m}$ values that range from 0.15 to 0.43 vs. Ag/Ag^+ which is substantially lower than the value for carbazole (0.95 V) under the same conditions. As proven by the slow increase in current response of the polymer redox during electropolymerization of carbazole, it was concluded that the polymerization is more sluggish than the bisheterocycle carbazoles. The poly(bisEDOT-*N*-R-carbazole) polymers exhibit two distinct redox processes with band gaps of 2.4 – 2.5 eV, and three distinct color states are obtainable, yellow in the neutral form, green in the mildly oxidized form, and blue when fully oxidized. The ability of these polymers to switch rapidly and reproducibly between these color states has made them useful as anodically coloring polymers (see Chapter 1) for dual-polymer electrochromic devices.[101,102]

Although these polymers are very useful for device applications, the unsubstituted bisEDOT-carbazole (BEDOT-Cz) monomer could not be synthesized with the Grignard coupling method used. The unsubstituted monomer would be very useful as it would prove very versatile as both a monomer and polymer, in that many different derivatives could be synthesized from one molecule. Figure 4.2 shows the possible utility of such an unsubstituted derivative, in that the monomer could be first substituted with various R groups and then polymerized or the unsubstituted monomer could be polymerized followed by macromolecular substitution. In this chapter, the synthesis of two new

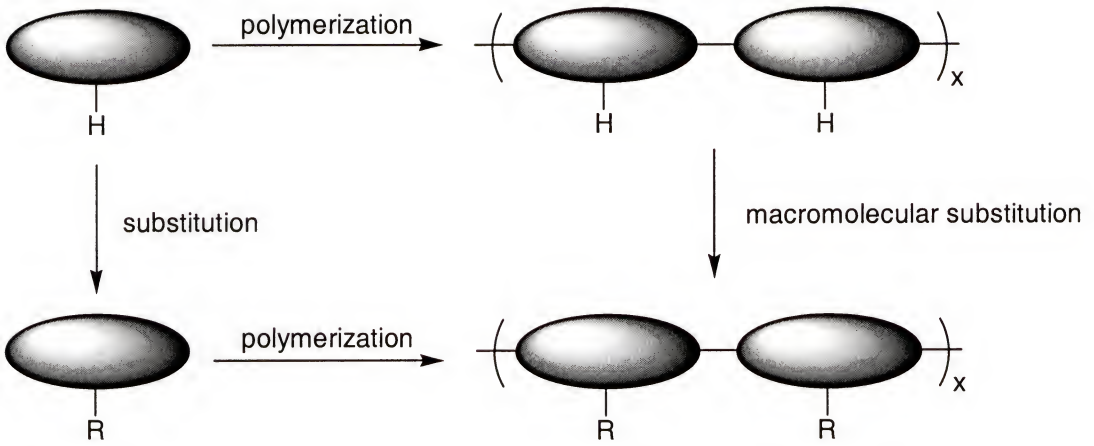

Figure 4.2 Schematic demonstrating the versatility of an unsubstituted monomer in synthesizing a variety of substituted polymers.

unsubstituted monomers that yield three color polymers are presented, BEDOT-Cz, and BEDOT-diphenylamine (BEDOT-DPA) (see Figure 4.3).

As discussed in Chapter 1, anodically coloring or high gap polymers are used along with cathodically coloring polymers in the fabrication of dual-polymer electrochromic devices. Although the PBEDOT-NRCz polymers have been useful as anodically coloring polymers in devices, they exhibit a yellow color in their reduced form. The ideal anodically coloring polymer would exhibit a colorless neutral form and a deeply colored oxidized form. In order to achieve this colorless neutral form, the band gap of BEDOT-NRCz monomers would need to be raised from 2.5 eV to close to 3.0 eV where all of the absorbance would occur in the UV region. Two molecules will be discussed as attempts to raise the band gap of BEDOT-Cz, and they are bisthienyl-*N*-dodecylcarbazole (BTh-NC12Cz) and BEDOT-DPA (see Figure 4.3).

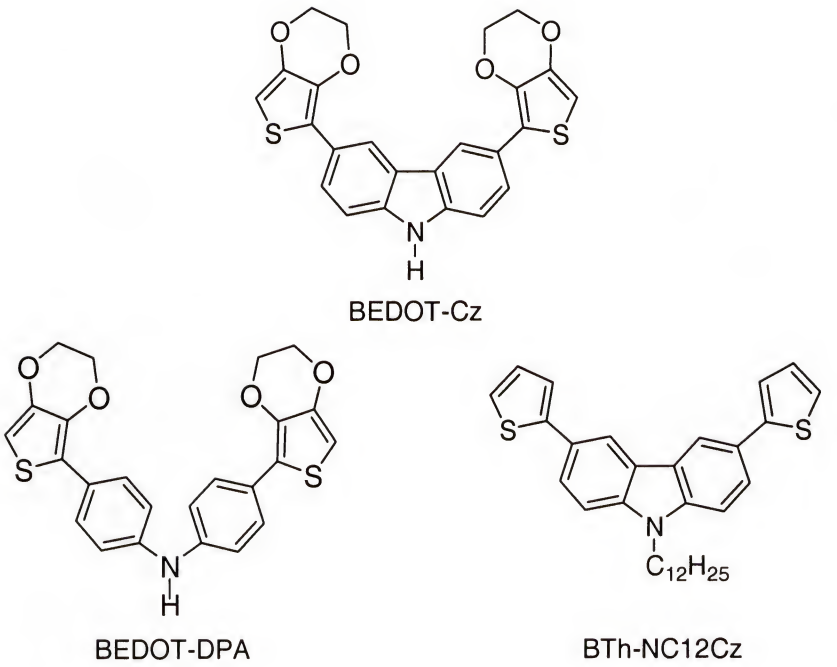

Figure 4.3 The monomer structures discussed in this chapter.

4.2 Monomer Synthesis

4.2.1 Synthesis of 3,6-bis(2-(3,4-ethylenedioxy)-thienyl)carbazole (BEDOT-Cz) (**15**)

A new synthetic method based on the Stille coupling reaction was used to synthesize the unsubstituted BEDOT-Cz (**15**) monomer, and this method is detailed in Figure 4.4. In the first step, EDOT is lithiated and the anion is trapped with trimethyl-silylchloride, followed by another lithiation and trapping with trimethylstannylchloride to yield compound **11** in 95% yield. Carbazole is deprotonated with NaH and treated with benzoyl chloride to yield the benzoyl protected carbazole compound **13** in 75% yield. Compounds **11** and **13** are combined in a Stille coupling reaction under Pd catalysis to yield compound **14** in 72% yield. The TMS groups are included to help in purification of compound **14** by facilitating separation of the mono and dicoupled product by column

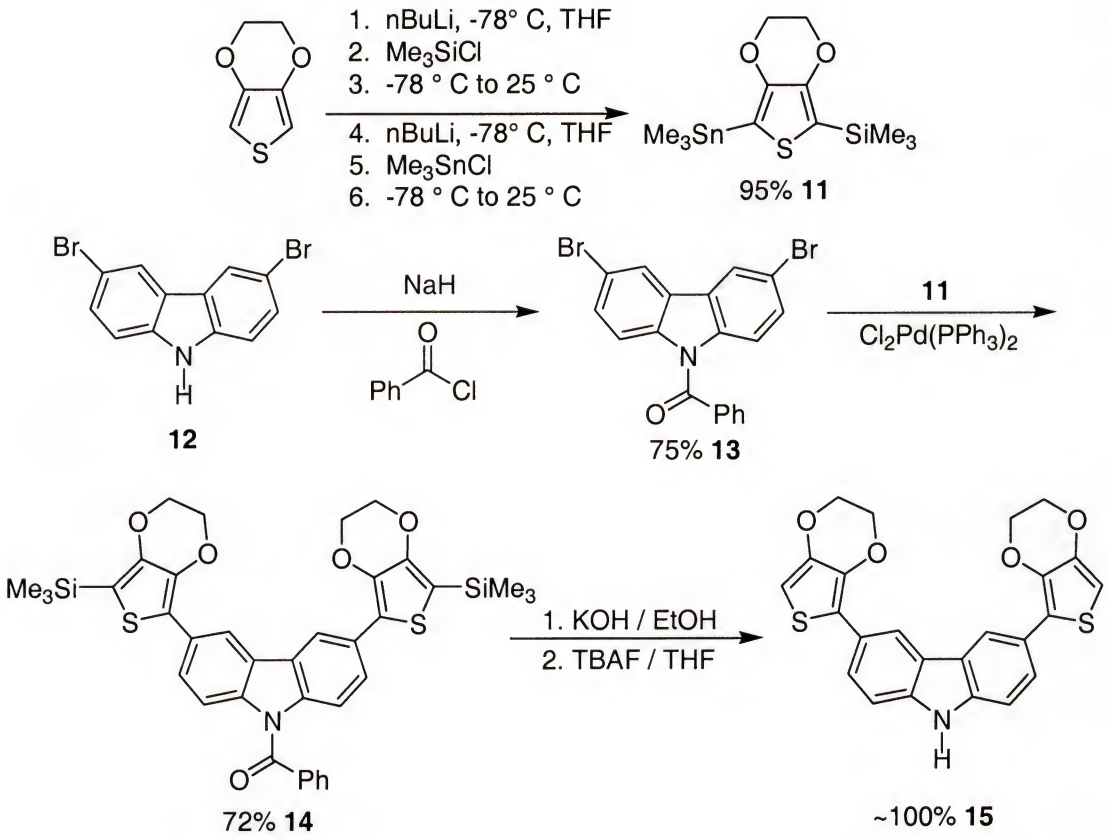

Figure 4.4 Synthesis of BEDOT-Cz.

chromatography. The benzoyl group is removed with base, and it should be noted that some of the TMS groups are removed in this step. Finally, the rest of the TMS groups are removed with TBAF to yield the final monomer BEDOT-Cz as a slightly yellow-green solid in an overall yield of 68% based on EDOT.

4.2.2 Synthesis of Substituted BEDOT-Cz Derivatives (**16-18**)

Substitution of BEDOT-Cz is important, because many different derivatives can be synthesized from one compound. Particularly interesting is the substitution of BEDOT-Cz with electron withdrawing groups. These groups may serve to lower the electron density of the backbone, which lowers the LUMO energy but also lowers the

HOMO energy to a greater extent, thereby raising the band gap of the system. Figure 4.5 details the substitution reactions used to synthesize BEDOT-Cz derivatives with electron withdrawing groups. BEDOT-Cz was treated with NaH and then treated with an appropriate aryl halide. Compounds **16** and **17** were synthesized from the corresponding fluoro compounds in a nucleophilic aromatic substitution reaction. Compound **16** is an off-white solid, and **17** is a bright yellow solid. The synthesis of compound **18** was attempted with treatment of the BEDOT-Cz anion with triflic anhydride. Unfortunately, the product **18** could not be isolated from the reaction.

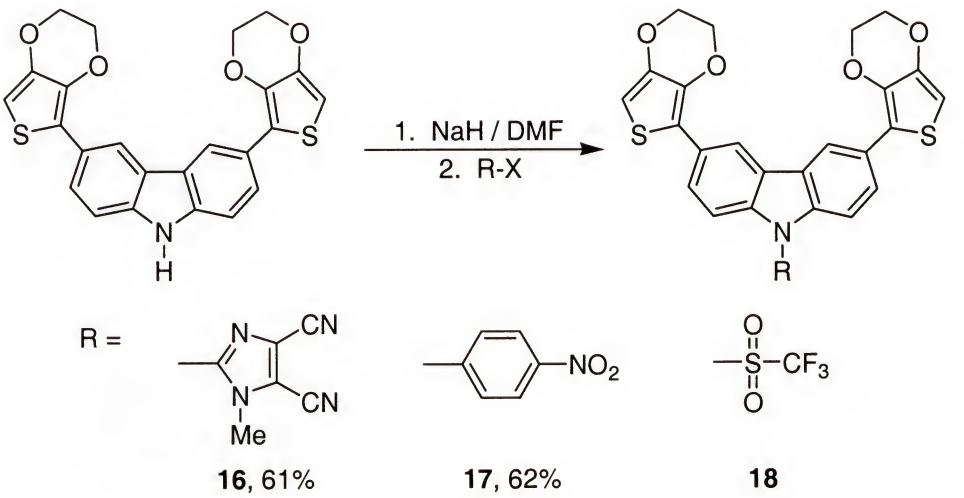

Figure 4.5 Synthesis of substituted BEDOT-Cz derivatives.

4.2.3 Synthesis of 3,6-bis(2-thienyl)-*N*-dodecylcarbazole (BTh-NC12Cz) (**21**)

In order to compare the effect of the electron rich character of the terminal heterocycle on electropolymerization, switching potentials and band gap, the EDOT in BEDOT-Cz was replaced by thiophene. In this monomer, higher polymerization and switching potentials should occur with the possibility of an elevated band gap when

compared to BEDOT-Cz. Polythiophene has a band gap of 2.2 eV, while the electron rich nature of EDOT raises the HOMO leading to a lower band gap of 1.6 eV. Therefore, the band gap should increase when replacing EDOT with thiophene. Although the monomer will not be as electron rich as BEDOT-Cz, because it is an extended conjugation monomer the oxidation potential should still be rather low. Figure 4.6 shows the synthesis of BTh-NC12Cz. Thiophene was lithiated and the anion was trapped with trimethylstannyl-chloride to yield compound **19**. Compound **19** was combined with compound **20** under Stille coupling conditions to yield compound **21** as a slightly yellow oil.

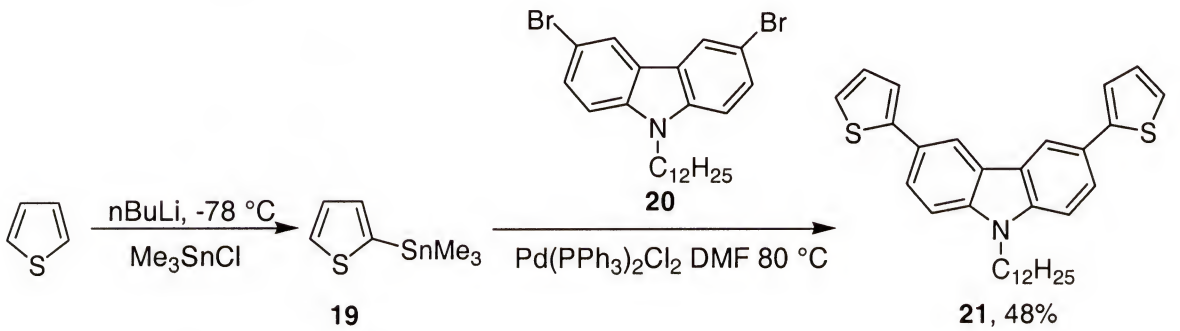

Figure 4.6 Synthesis of BTh-NC12Cz.

4.2.4: Synthesis of 4,4'-bis(2-(3,4-ethylenedioxy)-thienyl)diphenylamine (BEDOT-DPA) (**26**)

Examination of the structure of 3,6-linked carbazole shows it to be a functionalized diphenyl amine held in a planar conformation by the fused rings. In order to examine the effect of opening up the skeleton to conformational disorder, we have synthesized BEDOT-DPA. This monomer should have low monomer and polymer switching potetials, and if the benzene rings twist out of plane, the mean conjugation

length of the monomer could be shortened leading to an increase in expected band gap. Figure 4.7 shows the synthesis of BEDOT-DPA, and it is very similar to that of BEDOT-Cz. Diphenylamine was brominated using NBS to yield the dibrominated compound **23** in good yield. This was followed by protection of the amine with an acetyl group to yield compound **24**. Compound **24** was combined with compound **11** to yield the dicoupled product **25**. Base was used to remove the acetyl group, and TBAF was used to remove the TMS groups to yield the final monomer **26** in an overall yield based on EDOT of 40% as an off-white solid.

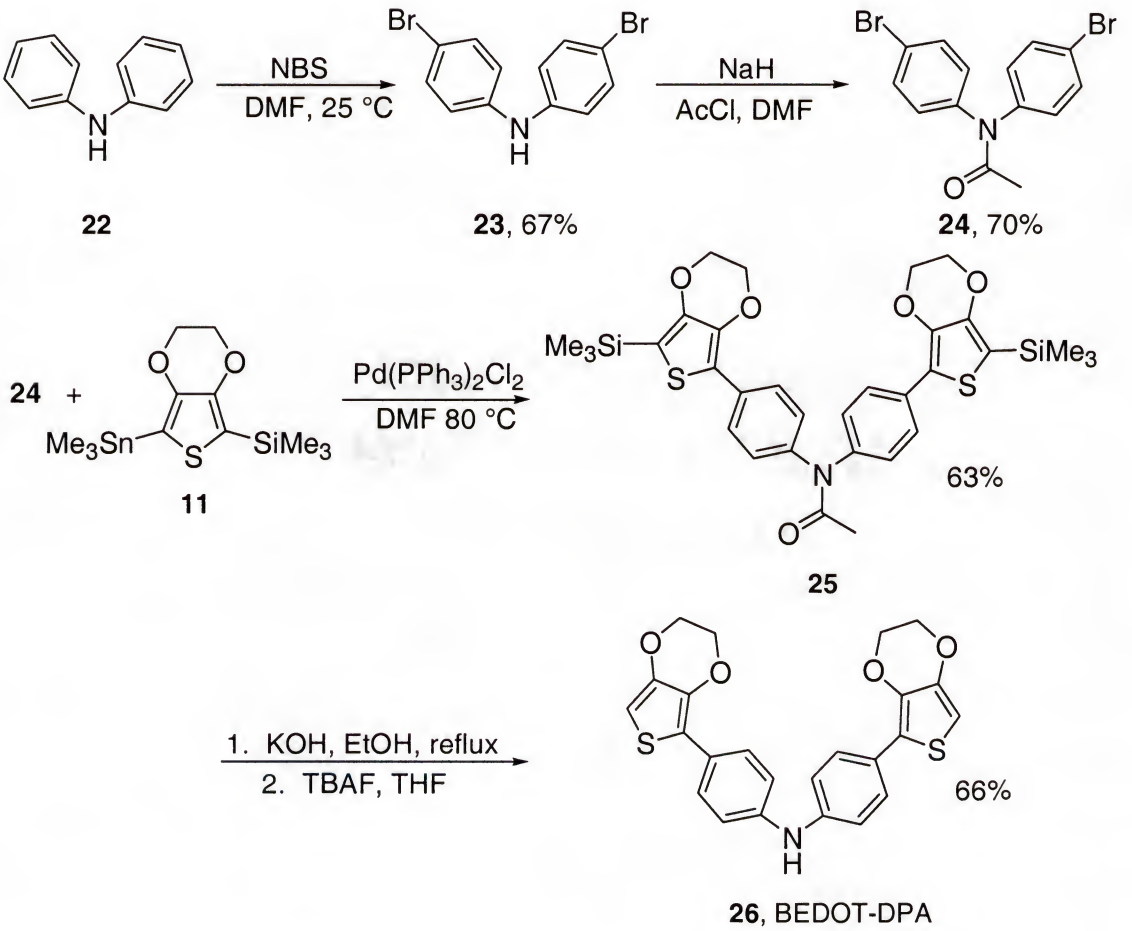

Figure 4.7 Synthesis of BEDOT-DPA.

4.3 Electropolymerization

4.3.1 Electropolymerization of BEDOT-Cz (**15**) and Substituted BEDOT-Cz (**16-17**)

The repeated scan electropolymerization of BEDOT-Cz was studied using a standard three-electrode set-up. A schematic diagram representing the oxidative electropolymerization of BEDOT-Cz and the subsequent polymer redox switching is shown in Figure 4.8. Because the nitrogen breaks the conjugation, the polymer is expected to have two distinct redox processes, first is oxidation to the radical cation, and the second is oxidation to the dication. Because the external rings are highly electron rich, the polymerization should take place through these positions and at a low potential.

The repeated scan electropolymerization of BEDOT-Cz was studied on a 10 mM solution of monomer in 0.1 M TBAP / 10:1 ACN:CH_2Cl_2 and the results are displayed in Figure 4.9. Starting at –1.0 V, the potential is scanned anodically at a scan rate of 100 mV/s. At 0.36 V there is an onset of monomer oxidation ($E_{on,m}$) with a peak at 0.44 V ($E_{p,m}$). Polymerization occurs and upon scanning cathodically, the reduction or dedoping of the polymer is observed with a peak at 0.1 V ($E_{p,c}$). Upon repeated scanning, oxidation of the polymer occurs at 0.17 V ($E_{p,a}$) and the peak for monomer oxidation shows an increased current response. This shows that porous conducting polymer has formed on the electrode surface and therefore the surface area of the working electrode has increased. The current response of the polymer oxidation and reduction also increases upon repeated scanning, indicating that electroactive polymer is being deposited on the electrode. The potentials for polymerization are much lower than that of EDOT or

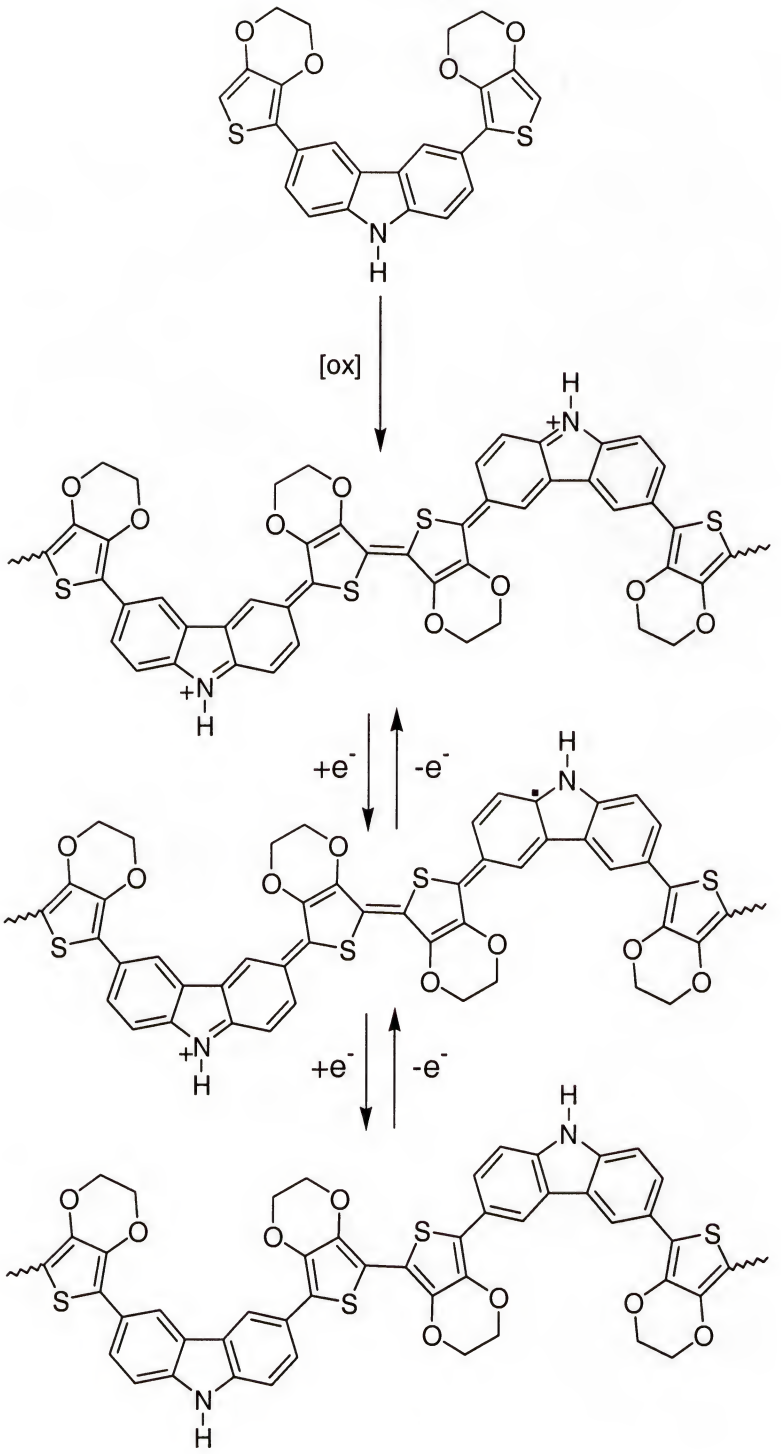

Figure 4.8 Representation of the repeated scan electropolymerization of BEDOT-Cz (**15**) including redox switching of the polymer.

carbazole, and the values are similar to those of the N-substituted BEDOT-Cz derivatives previously studied in the Reynolds group.[189]

The inset of Figure 4.9 shows the first scan of the electropolymerization of BEDOT-Cz, and illustrates a frequently mentioned feature of the first potential cycle of electropolymerization called the "nucleation loop" or "trace-crossing".[190] This effect is similar in respect to the deposition of metal on a substrate, where an overpotential is required for nucleation to occur, followed by further deposition of the metal at the redox potential of the metal now on the electrode resulting in the crossing of the reverse trace

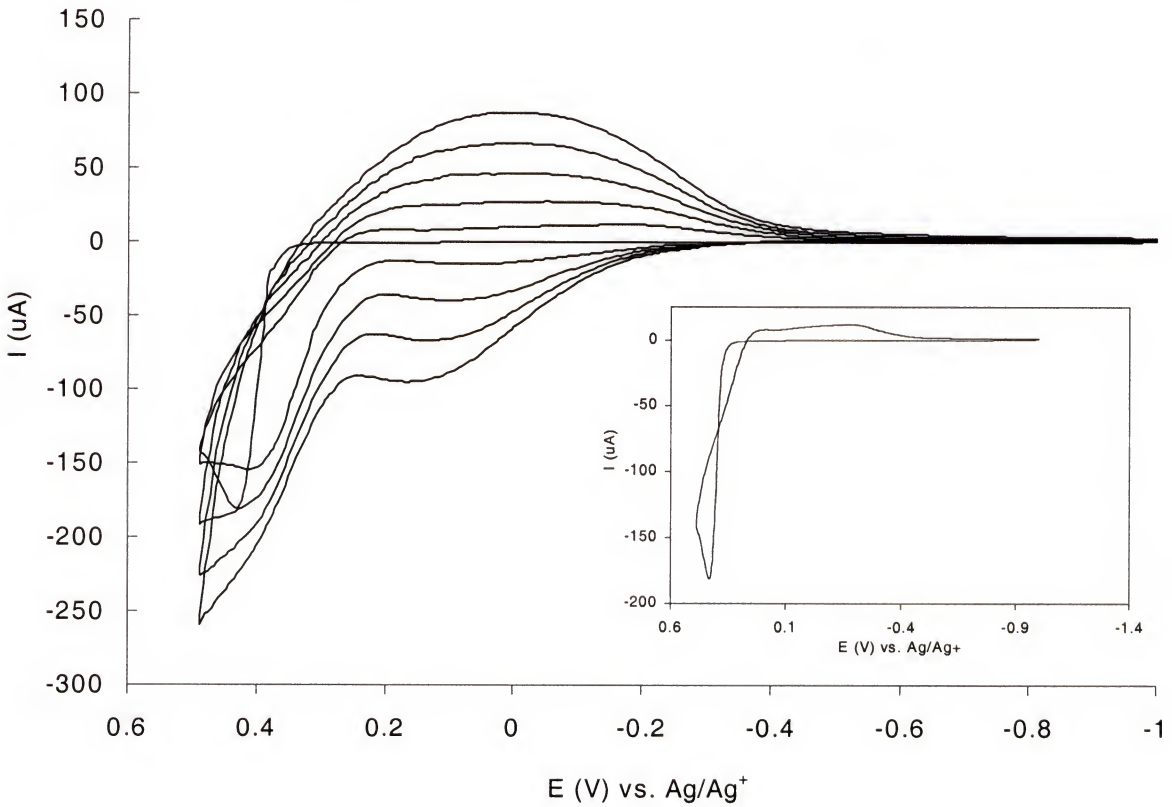

Figure 4.9 Repeated scan electropolymerization from a 0.01 M solution of BEDOT-Cz (**15**) in 0.1 M TBAP / 10:1 ACN / CH_2Cl_2 at a scan rate of 100 mV/s on a platinum button. The inset shows the first scan.

over the forward trace. It is believed that the same type of overpotential is necessary in the nucleation of conducting polymers, resulting in the formation of the nucleation loop. More recently, Zhou and Heinze have shown that, at least in the case of polypyrrole, the nucleation –growth mechanism can explain trace-crossing in the first potential cycle, but not all trace-crossing is due to this process.[191] Other processes, such as the swelling of the existing polymer and follow-up reactions, should be taken into account.

Electropolymerization of compound **16** (BEDOT-N-DCI-Cz) was attempted in 0.1 M TBAP/ACN and 0.1 M TBAP / CH_2Cl_2. In both solvent systems, polymerization did not occur. There is an irreversible oxidation at 0.8 V with no polymer redox observed and deposition of a non-electroactive red solid on the working electrode. Unfortunately, the same type of behavior was observed for compound **17** (BEDOT-N-pNO_2Ph-Cz). An irreversible oxidation was observed followed by deposition of a red solid on the electrode that was non-electroactive. The substitution of electron-withdrawing groups on the carbazole nitrogen was then abandoned as a method to raise the band-gap of PBEDOT-Cz. It may be that the electron-withdrawing groups stabilize the radical formed through resonance, and a radical-cation salt is precipitated on the electrode surface, or some sort of charge transfer complex is formed between the electron-rich and electron-poor sections of the monomer inhibiting polymerization.

4.3.2: Electropolymerization of BTh-NC12Cz (**21**) and BEDOT-DPA (**26**)

The repeated scan electropolymerization of BTh-NC12Cz was studied with a 2.5 mM solution of monomer in 0.1 M TBAP / 3:1 ACN: CH_2Cl_2, and the results are displayed in Figure 4.10. Starting at –0.2 V, the potential is scanned anodically at a scan

rate of 100 mV/s. The $E_{on,m}$ occurs at 0.57 V with $E_{p,m}$ at 0.67 V where polymerization occurs and upon scanning cathodically $E_{p,c}$ is observed at 0.22 V. Upon repeated scanning, $E_{p,a}$ occurs at 0.38 V, and the peak monomer oxidation increases in current response with repeating scanning, indicating that the electrode surface area is increasing. The peak polymer oxidation and reduction potentials do shift slightly upon repeated scanning, indicating that the polymer is slightly harder to oxidize and reduce when more material is deposited on the electrode. The $E_{p,m}$ is 0.23 V higher than BEDOT-Cz, and 0.21 V higher than BEDOT-NC20Cz as reported by the Reynolds group[189]; this is expected since thiophene is less electron rich than EDOT. This value also compares well

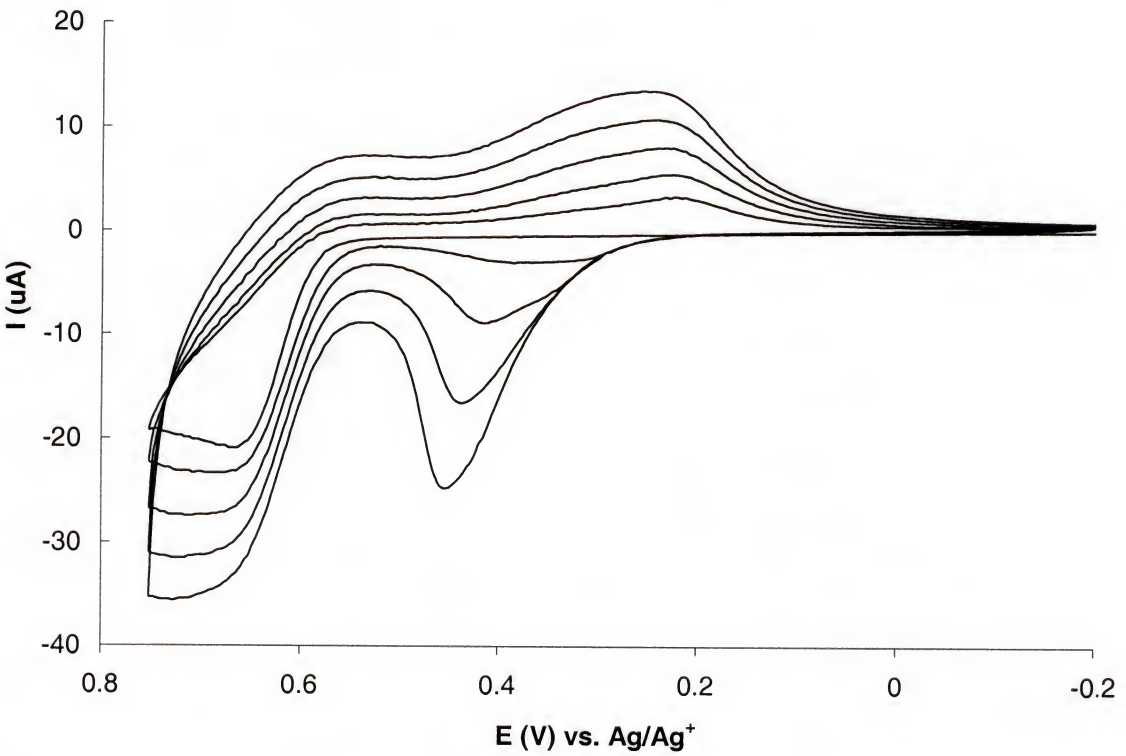

Figure 4.10 Repeated scan electropolymerization from a 0.01 M solution of of BTh-NC12Cz (**21**) in 0.1 M TBAP / 3:1 ACN / CH_2Cl_2 at a scan rate of 100 mV/s on a platinum button.

with a value 0.849 V vs. Fc/Fc^+ reported in the literature for BTh-NC2Cz by Sezer et al..[192] Although the potential is higher, it is still relatively low when compared to thiophene or carbazole alone.

The repeated scan electropolymerization behavior of BEDOT-DPA (**26**) was studied with a 10 mM solution of monomer in 0.1 M TBAP / CAN, and the results are shown in Figure 4.11. Starting at –0.5 V, the potential is scanned anodically at a scan rate of 100 mV/s, where $E_{on,m}$ is observed at 0.17 V, and $E_{p,m}$ at 0.32 V. Polymerization occurs and, upon scanning cathodically, two peaks are observed for polymer reduction or dedoping at 0.12 and –0.14 V. Upon repeated scanning, a current response is observed

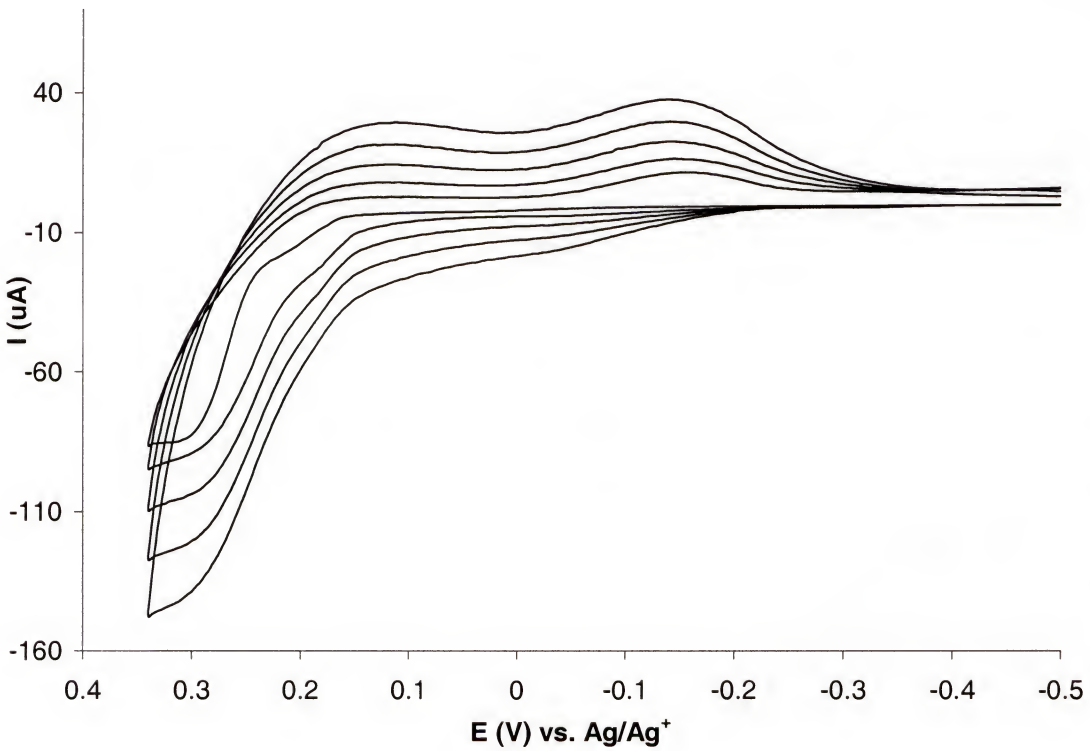

Figure 4.11 Repeated scan electropolymerization from a 0.01 M solution of BEDOT-DPA (**26**) in 0.1 M TBAP/ACN at a scan rate of 100 mV/s on a platinum button.

for polymer oxidation. The peak monomer oxidation increases in current response with repeating scanning, indicating that the electrode surface area is increasing. Compared to BEDOT-Cz, the $E_{p,m}$ of BEDOT-DPA is 0.12 V lower, exhibiting that the benzene rings are probably not very far out of plane with the thiophene rings. In fact, they may be more in plane than BEDOT-Cz as crystal structures obtained previously by the Reynolds group on BEDOT-*N*-methyl-Cz show that while one of the thiophene rings is approximately coplanar with the plane of the carbazole, the other EDOT is twisted 26.2 ° out of plane.[189] Upon electropolymerization, the rings in the oxidized polymer are forced into a planar structure, because of the quinoidal geometry of the doped form, therefore monomers that are planar will oxidize at lower potentials than those that are twisted out of plane.[78] This hypothesis about BEDOT-DPA could be supported by X-ray crystal data, but unfortunately attempts at growing a proper crystal failed.

4.4 Polymer Electrochemistry

4.4.1 Polymer Electrochemistry of PBEDOT-Cz (**P15**)

The electrochemistry of PBEDOT-Cz was studied in 0.1 M TBAP/ACN at various scan rates in order to study the redox switching of the polymer, and the results are displayed in Figure 4.12. Each voltammogram represents the third scan of the polymer at a specific scan rate. There are two distinct oxidation and reduction processes, with $E_{1/2}$ values of 0.15 ($E_{1/2,p1}$) and 0.48 ($E_{1/2,p2}$) V. This is consistent with the fact that these polymers have a break in conjugation at the nitrogen, and that two separate redox processes are involved. These values correlate well with the previously reported *N*-

substituted PBEDOT-Cz polymers reported by the Reynolds group, where $E_{1/2,p1}$ ranged from 0.19 to 0.23 V and $E_{1/2,p2}$ ranged from 0.46 to 0.55 V.[189] It is important to note that the unsubstituted nitrogen does not greatly effect the polymer redox properties, with no crosslinking reactions evident in the scanned potential window. Finally, the peak current of each redox process scales linearly with scan rate, indicating that the electroactive centers are adhered to the electrode surface.

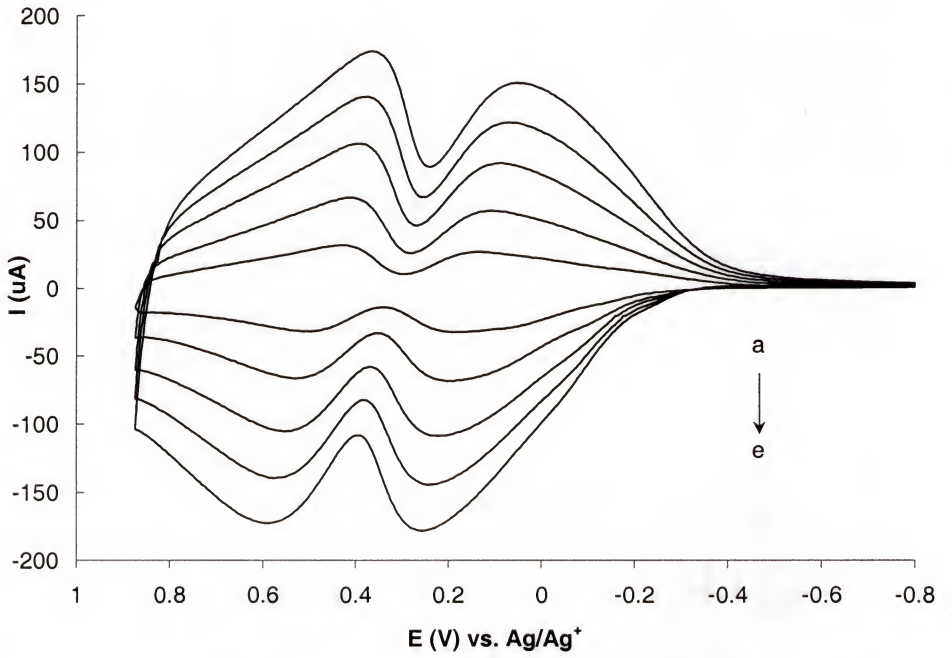

Figure 4.12 Scan rate dependence of BEDOT-Cz (**P15**) in 0.1 M TBAP/ACN at the following scan rates: a) 50 b) 100 c) 150 d) 200 e) 250 mV/s.

4.4.2 Polymer Electrochemistry of PBTh-NC12Cz (**P21**) and PBEDOT-DPA (**P26**)

The electrochemistry of PBTh-NC12Cz was studied in 0.1 M TBAP/ACN at various scan rates in order to study the redox switching of the polymer, and the results are displayed in Figure 4.13. Each voltammogram represents the third scan of the polymer at a specific

scan rate. Although there are two redox processes evident, they are not as well defined as in the PBEDOT-Cz case. There are two oxidation processes centered at 0.5 and 0.74 V, and two reduction processes at 0.62 and 0.31 V. These values are much higher than the potentials observed for BEDOT-Cz. This is expected, because thiophene is less electron-rich than EDOT and thiophene also has open β-positions where crosslinking can occur, and therefore the oxidation potentials are greater. Again, the peak

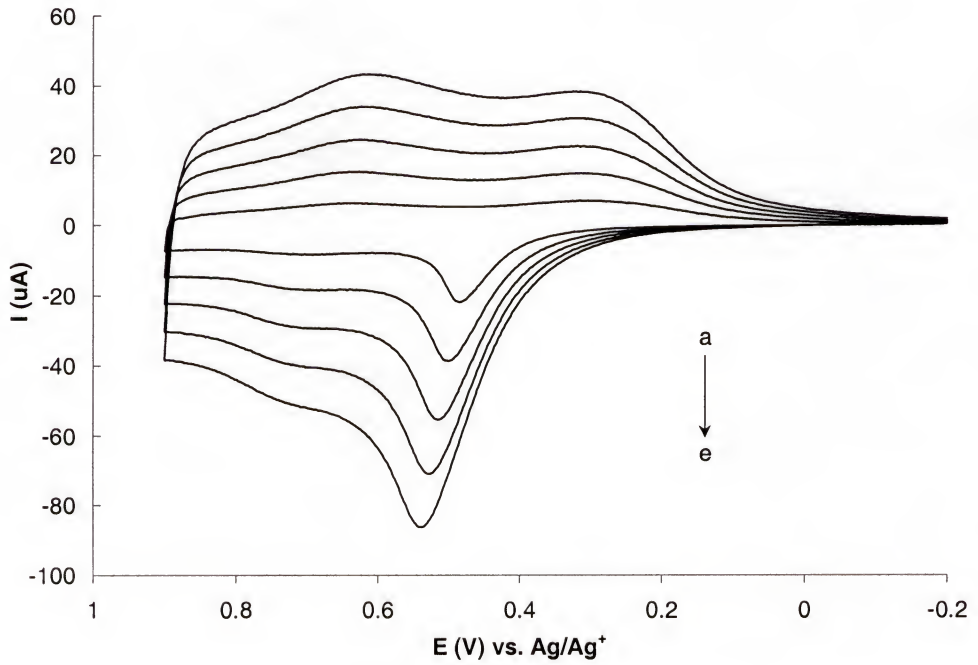

Figure 4.13 Scan rate dependence of PBTh-NC12Cz (**P21**) in 0.1 M TBAP/ACN at the following scan rates: a) 100 b) 200 c) 300 d) 400 e) 500 mV/s.

current scales linearly with the scan rate indicating that the electroactive centers are adhered to the electrode surface.

The electrochemistry of PBEDOT-DPA was studied in 0.1 M TBAP/ACN at various scan rates in order to study the redox switching of the polymer, and the results are displayed in Figure 4.14. Each voltammogram represents the third scan of the polymer at

a specific scan rate. The peak shape is very broad for this polymer when compared to PBEDOT-Cz. Although there is some evidence of two separate redox processes, they are not well defined. There are two oxidation processes evident centered at 0.06 and 0.35 V. At faster scan rates these peaks are combined into one peak. The reduction processes are not as well defined, there is one predominant process at 0.1V and also a shoulder at –0.18 V. The reason for the more ill-defined processes is not clear, although it may be that the

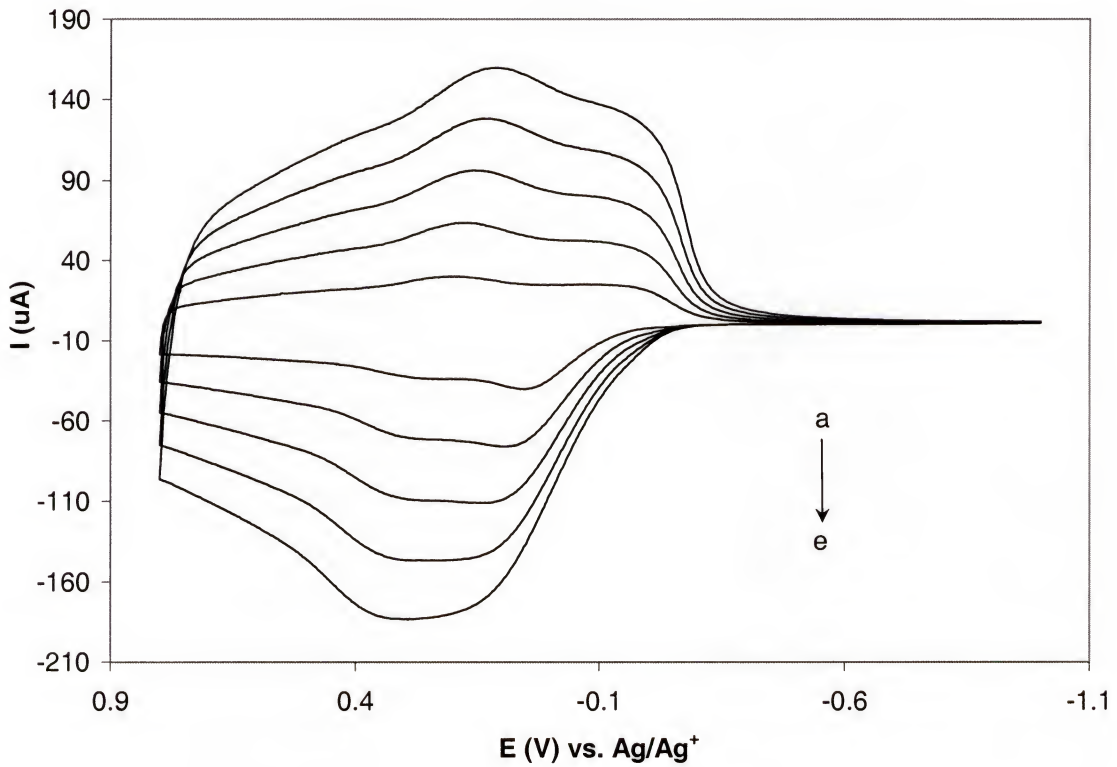

Figure 4.14 Scan rate dependence of PBEDOT-DPA (**P26**) in 0.1 M TBAP/ACN at the following scan rates: a) 100 b) 200 c) 300 d) 400 e) 500 mV/s.

freedom of the benzene rings to rotate may result in many different conjugation lengths and therefore more ill-defined peaks. The polymer oxidation potential is comparable to that of BEDOT-Cz. Again, the peak current scales linearly with the scan rate indicating that the electroactive centers are adhered to the electrode surface.

4.5 Spectroelectrochemistry

4.5.1 Spectroelectrochemistry of PBEDOT-Cz (**P15**)

To elucidate the electronic structure of the polymers, spectroelectrochemical analysis was performed. A spectroelectrochemical series for PBEDOT-Cz in 0.1 M TBAP/ACN is displayed in Figure 4.15. The results are very similar to that of the previously reported *N*-substituted PBEDOT-Cz polymers.[189] The polymer exhibits a band

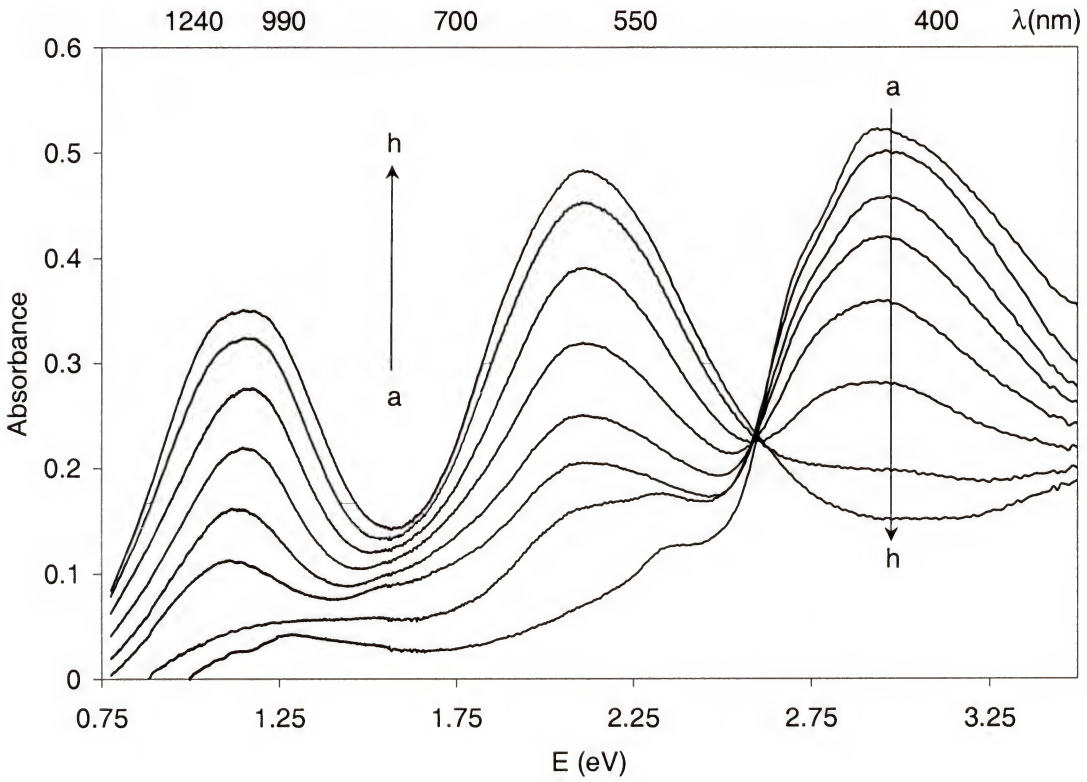

Figure 4.15 Spectroelectrochemistry of BEDOT-Cz in 0.1 M TBAP/ACN at applied potentials of: (a) –1.0 V, (b) –0.5, (c) –0.2, (d) –0.1, (e) 0, (f) +0.1, (g) +0.2, (h) +0.2 V vs. Ag/Ag^{+}.

gap (measured as the onset of the π to π* absorption) of 2.5 eV with a peak at 2.9 eV. Similar to the *N*-substituted polymers, these polymers are not fully reduced at –1.0 V, and require addition of hydrazine for further reduction. This has been attributed to charge trapping in the polymer. Upon oxidation, the peak at 2.9 eV decreases in intensity and two new lower energy transitions increase in intensity at 2.1 and 1.1 eV. The unsubstituted amine has little effect on the optical properties of the polymer, and the polymer exhibits three color states: yellow, green, and blue, the same as the colors for the *N*-substituted derivatives.

4.5.2 Spectroelectrochemistry of PBTh-NC12Cz (**P21**)

A spectroelectrochemical series for PBTh-NC12Cz in 0.1 M TBAP/ACN is displayed in Figure 4.16. The polymer exhibits a band gap of 2.5 eV and a λ_{max} value of 3.1 eV. Upon oxidation the π to π* transition centered at 3.1 eV decreases in intensity as two lower energy intragap transitions increase in intensity at 2.2 and 1.2 eV. Starting at 0.7 eV (Figure 4.16h), the peak at 2.2 eV starts to decrease and the peak at 1.2 eV shifts to slightly higher energy (1.4 eV). The polymer exhibits three color states: yellow, green, and blue similar to BEDOT-Cz.

It was a surprise that the band gap of PBEDOT-Cz and PBTh-NC12Cz were the same, and this result needed to be rationalized. The classical way of modifying the band gap of a conjugated polymer is to use electron releasing or withdrawing substituents to increase the HOMO or lower the LUMO levels respectively. This is the method used to lower the polythiophene band gap from 2.2 eV to 1.6 eV in PEDOT. There are several other factors that affect the band gap of a conjugated polymer, and Roncali summarized

these factors in a recent review article.[193] According to the article, there are five factors that affect the band gap of a polymer: the energy related to bond length alternation, the mean deviation from planarity, the aromatic resonance energy of the cycle, the electronic effects of the substituents, and the intermolecular interactions in the solid state. This

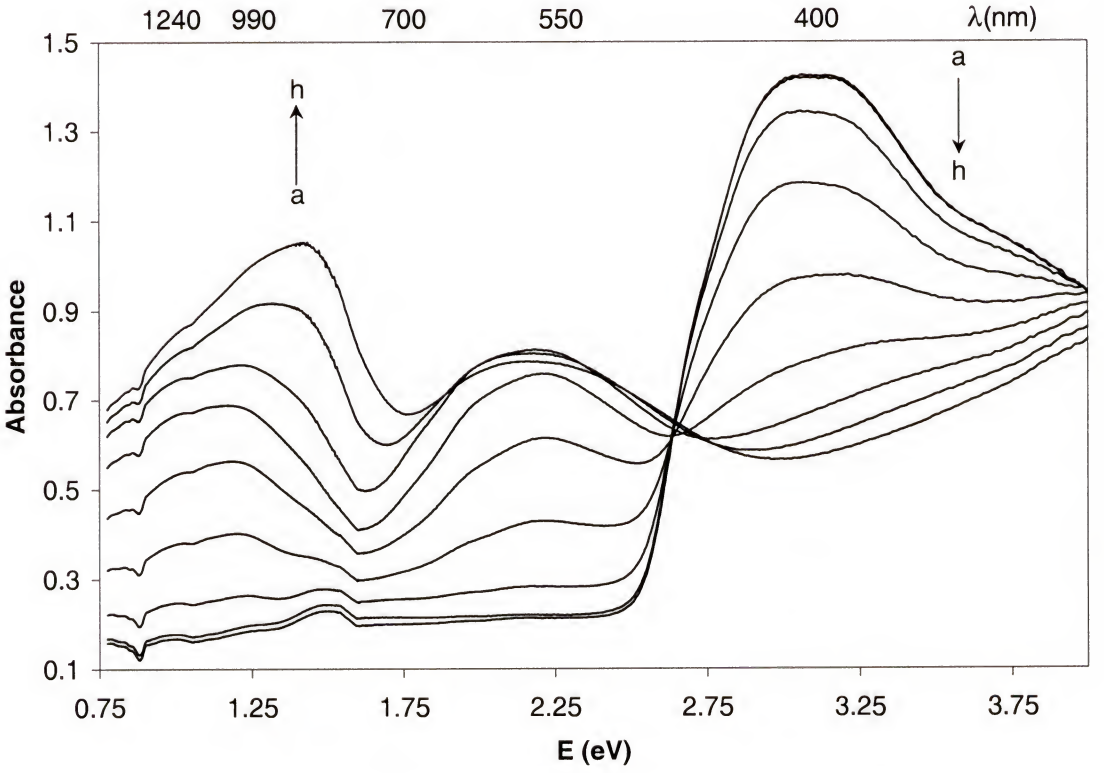

Figure 4.16 Spectroelectrochemistry of BTh-NC12Cz in 0.1 M TBAP/ACN at applied potentials of: (a) –0.7 V, (b) 0, (c) +0.2, (d) +0.3, (e) +0.4, (f) +0.5, (g) +0.6, (h) +0.7, (i) +0.8 V vs. Ag/Ag^{+}.

shows that just one component cannot be weighed when comparing band gaps of polymers. In the case of BEDOT-Cz and BTh-NC12Cz, it is obvious that the substituent effect does not influence the band gap, but the main effect in this case is believed to be conjugation length. When the conjugation length is longer, the band gap is lower. In

normal fully conjugated polymers, this effect is nominal, because the band gap levels off after 10 to 12 rings. Because the nitrogen breaks the conjugation, BEDOT-Cz and BTh-NC12Cz have the same short conjugation length of four rings. When comparing PEDOT and polythiophene, the band gap is lowered dramatically with addition of the ethylene-dioxy substituent because long runs of rings are in conjugation, and therefore the substituent effects add up to a larger change. However, in the case of the carbazole based polymers, the short conjugation length means that the substituent effect is minimized. Model compounds that contain either the biEDOT or bithiophene unit with two capped terminal carbazoles could be synthesized, and UV-vis spectra of these two molecules should be similar if this hypothesis is correct.

4.5.3 Spectroelectrochemistry of PBEDOT-DPA (**P26**)

A spectroelectrochemical series for PBEDOT-DPA in 0.1 M TBAP/ACN is displayed in Figure 4.17. The polymer exhibits a band gap of 2.3 eV, with a λ_{max} value of 2.75 eV. The π to π^* transition decreases in intensity upon oxidation, while two intraband transitions at 1.95 and 0.91 eV increase in intensity at lower energy. Starting at +0.5 V (Figure 4.16h), the peak at 1.95 eV decreases, and at +1.0 V only a single bipolaron peak at 0.97 eV is present. The band gap and λ_{max} values of BEDOT-DPA are lower than those of BEDOT-Cz and BTh-NC12Cz, substantiating the argument put forth in Section 4.3.2 that the ring system of BEDOT-DPA may be more planar than the carbazole based systems. Three color states are obtained for BEDOT-DPA which are yellow, green, and blue.

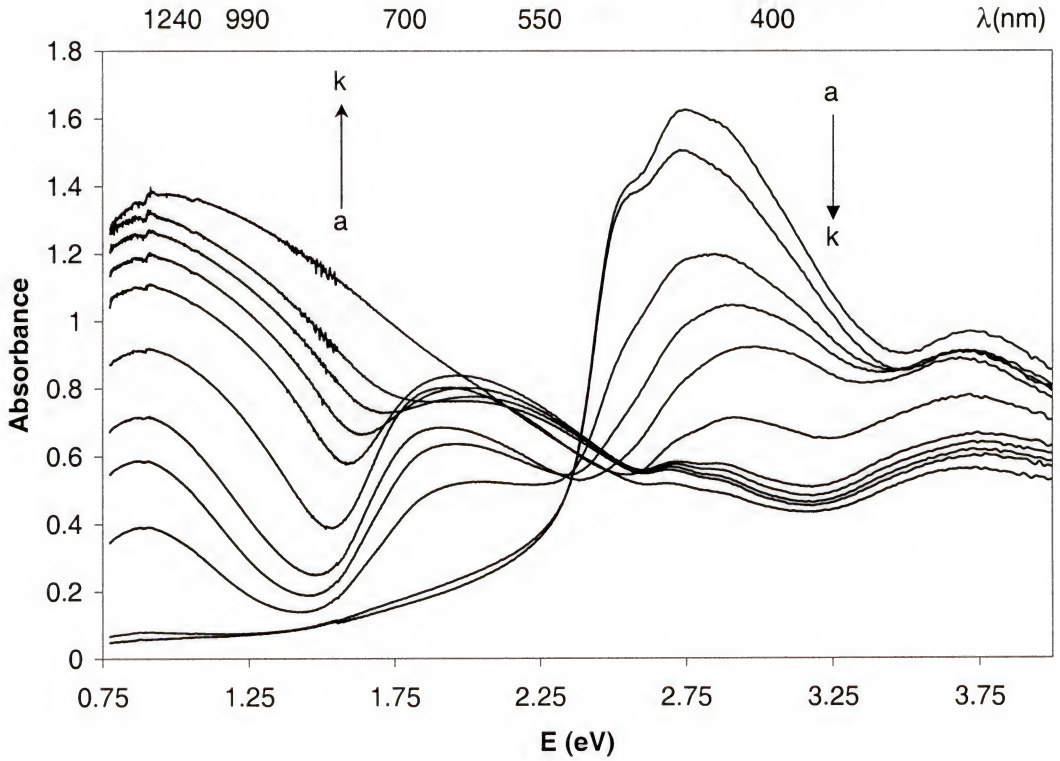

Figure 4.16 Spectroelectrochemistry of PBEDOT-DPA in 0.1 M TBAP/ACN at applied potentials of: (a) –1.0 V, (b) –0.2, (c) 0, (d) +0.1, (e) +0.2, (f) +0.3, (g) +0.4, (h) +0.5, (i) +0.6, (j) +0.7, (k) +1.0 V vs. Ag/Ag^{+}.

4.6 Conclusions

BEDOT-Cz and PBEDOT-Cz were successfully synthesized as a versatile unsubstituted monomer and three-color (yellow, green, and blue) electroactive polymer that makes the synthesis of different derivatives via *N*-substitution more facile. The monomer polymerization potential, polymer switching potentials and spectroelectrochemical results are very similar to that of the previously reported *N*-substituted analogues, proving that the unsubstituted amine does not interfere with the polymer redox. Substitution with electron withdrawing groups was attempted but failed to yield electroactive polymer.

The thiophene analogue of BEDOT-Cz was synthesized as BTh-NC12Cz, and subsequently electropolymerized to form a three-color (yellow, green, and blue) electroactive polymer with switching potentials somewhat higher than BEDOT-Cz. Spectroelectrochemical results show that the band gap of the polymer is 2.5 eV, which is the same as BEDOT-Cz. This surprising result was probably due to an attenuated substituent effect in the shorter conjugation length carbazole based polymers compared to fully conjugated polymers like polythiophene or PEDOT.

Finally, a novel three-color (yellow, green, and blue) electrochromic polymer based on a diphenylamine unit was synthesized as BEDOT-DPA, and also yielded a monomer and polymer with an unsubstituted amine site allowing for the easy synthesis of many different derivatives. Although it was hypothesized that the opening up of the carbazole structure to diphenylamine might raise the band gap because of an increase in conformational disorder, BEDOT-DPA actually exhibited a lower $E_{p,mon}$ and band gap than BEDOT-Cz indicating that the ring system may actually be more planar than the carbazole system.

4.7 Experimental

4.7.1 Materials

EDOT was provided by Bayer and was purified by vacuum distillation (65 °C at 0.2 mmHg) prior to use. N-methyl-2-fluoro-4,5-dicyanoimidazole was kindly provided by Professor Paul Rasmussen from the University of Michigan. Compound **20** was synthesized as described previously.[189] 2-trimethylstannylthiophene was prepared as described previously.[194] TBAP was prepared by mixing a 1:1 mole ratio of

tetrabutylammonium bromide (Aldrich) dissolved in water with perchloric acid. The precipitate was filtered, recrystallized from ethanol and dried in vacuo. NBS was obtained from Acros, and recrystallized from water prior to use. Acetonitrile (Aldrich) and methylene chloride (Fisher) were dried over calcium hydride and distilled under argon. Anhydrous *N,N*-dimethylformamide (DMF), 3,6-dibromocarbazole, trimethyltinchloride, sodium hydride, tetrabutylammoniumfluoride, p-fluoronitrobenzene, diphenylamine, and thiophene were obtained from Aldrich and used as purchased. Potassium hydroxide, nBuLi, trimethylsilylchloride, benzoyl chloride, ethanol, triflic anhydride, acetyl chloride were obtained from Fisher and used as purchased. $Pd(PPh_3)_2Cl_2$ was purchased from Strem and used as purchased. Prior to all experimentation, the glassware was flame dried under vacuum, and back-filled with argon. All reactions were performed under argon.

4.7.2 Structural Identification of Monomers and Polymers

NMR spectra were recorded on a Gemini 300 FT-NMR, VXR 300 FT-NMR, or a Varian XL-300 FT-NMR. Mass spectrometry was carried out on a Finnigan MAT 95Q mass spectrometer. Elemental analyses were accomplished at Robertson Microlit Laboratories, Inc., Madison, NJ.

Electropolymerization and polymer electrochemistry was carried out on an EG&G Princeton Applied Research model 273A potentiostat/galvanostat employing a platinum button working electrode, a platinum plate counter electrode, and a Ag/Ag^+ reference electrode. The monomer concentration for polymerization is 10mM in all cases, and the supporting medium is 0.1 M TBAP/ACN.

For spectroelectrochemistry, spectra were recorded using a Varian Cary 5E UV-Vis-NIR spectrophotometer. Polymers were prepared using a constant potential of 1.2 V vs. Ag/Ag^+. The working electrodes were ITO coated glass slides (7 x 50 x 0.6 mm, 20 Ω/□) from Delta Technologies. The reference electrode was Ag/Ag^+, and the counter electrode was a platinum wire. Polymer synthesis and electrochemistry were controlled by an EG&G Princeton Applied Research model 273A potentiostat / galvanostat.

4.7.3 Synthesis

3,6-dibromo-N-benzoyl carbazole (13). To a solution of 6 g (18.5 mmol) of 3,6-dibromocarbazole in 75 mL of DMF, 0.8 g (20 mmol) of NaH was added. Upon addition, the reaction turned yellow with gas evolution evident. After stirring for 15 min., 2.81 g (20 mmol) of benzoyl chloride was added via syringe. After addition, the reaction immediately turned white. The reaction was stirred overnight at room temperature, and the mixture was poured into water. The white solid was collected by filtration and washed with water and dried to yield 6 g (75%) of product. mp= 213-216 °C. (lit.[195] 215 – 216 °C) ^{1}H-NMR ($CDCl_3$): δ 7.32 (d, 2H), 7.42 (dd, 2H), 7.52 (t, 2H), 7.68 (t, 3H), 8.05 (s, 2H).

2-(trimethyl)stannyl-5-(trimethyl)silyl-(3,4-ethylenedioxy)thiophene (11). 5 g (35.2 mmol) of EDOT was dissolved in 150mL of THF in a two-neck flask equipped with an argon inlet, and the flask was cooled to –78 °C. After cooling for 20 minutes, 14.08 mL (35.2 mmol) of 2.5M nBuLi in hexanes was added slowly via syringe, and the solution was stirred for 1 hour. To this pale yellow solution, 3.8 g (35.2 mmol) of

trimethylsilylchloride was added via syringe. The flask was warmed to room temperature, and stirred for one hour. The flask was cooled to –78 °C, and 14.08 mL (35.2 mmol) of 2.5M nBuLi in hexanes was added slowly via syringe. After stirring for 1 hour, 35.2 mL (35.2 mmol) of 1.0 M trimethyltinchloride in hexanes was added via syringe, and the flask was warmed to room temperature and stirred overnight. The solution was concentrated to 30 mL under vacuum, and poured into 200 mL of water. The water was extracted with pentane three times, and the combined pentane layers were washed with water. The pentane was removed under vacuum to yield 13.0 g (98%) of pure compound **11**. mp = 64-65. ^{1}H-NMR ($CDCl_3$): δ 0.23 (s, 9H), 0.28 (s, 9H), 4.19 (s, 4H). Elemental analysis: calculated for $C_{12}H_{22}O_2SiSnS$: C, 38.22%; H, 5.88%; S, 8.50. Found: C, 37.93%; H, 5.74%; S, 8.70%..

3,6-Bis(2-(3,4-ethylenedioxy)-(5-trimethylsilyl)-thienyl)-*N*-benzoylcarbazole (14). To a 3-necked round bottom flask, 6.22 g (16.5mmol) of compound **11**, 3.08 g of compound **13**, and 0.2 g (2 mol %) of $Pd(PPh_3)_2Cl_2$ were added and exposed to vacuum for 10 min, backfilled with argon, and 100 mL of DMF was added via syringe. The reaction was heated to 90 °C, and after 2 hours turned black. Heating was continued overnight, and the mixture was cooled and poured into 1 L of brine. A dark brown solid was collected by filtration. It was purified using column chromatography on grade (III) alumina with a mixture of chloroform and hexanes (3:1) as eluent to yield 3.6 g (72%) of a bright yellow solid, which was deprotected without any further purification.

3-6-Bis(2-(3,4-ethylenedioxy)thienyl)-carbazole (15). 3.5 g (5.04 mmol) of compound **14** was added to a round bottom flask, and dissolved in 350 mL of ethanol. 3 g (54 mmol) of KOH was added, and the reaction was heated to reflux and left overnight. The mixture was cooled and poured into 500 mL of water. A white solid was collected by filtration, and ^{1}H-NMR indicated that the amide had been cleaved, but approximately 15% of the TMS groups were still present. The resulting product was then dissolved in THF and stirred with 2 equivalents of TBAF for 2 hours. The resulting product contained no TMS groups, and was obtained as 2.2 g (99%) of a white solid. mp = 314-316 °C. ^{1}H-NMR (d_6-DMSO): δ 4.28 (d, 8H), 6.48 (s, 2H), 7.45 (d, 2H), 7.70 (d, 2H), 8.30 (s, 2H), 11.4 (s, 1H). Elemental analysis: calculated for: $C_{24}H_{17}O_4S_2N$: H, 3.83; C, 64.41; S, 14.33. Found: H, 3.62; C, 64.51; S, 14.31.

3,6-Bis(2-(3,4-ethylenedioxy)thienyl)-*N*-dicyanoimidazolecarbazole (16). In a schlenk flask, 0.2 g (0.45 mmol) of compound **15** was dissolved in 30 mL of DMF. 0.011 g (0.47 mmol) of NaH was added in one portion, and the reaction immediately turned yellow with gas evolution evident. After 15 min, 0.07 g (0.47 mmol) of fluoro-N-methyl dicyanoimidazole was added, and the reaction immediately turned colorless. The solution was allowed to stir at room temperature overnight, and 100 mL of water was added to yield a white solid that was collected by filtration. The solid was purified on basic alumina to yield 0.16 g (61 %) of a white solid. ^{1}H-NMR ($CDCl_3$): δ 3.68 (s, 3H), 4.38 (d, 8H), 6.35 (s, 2H), 7.20 (d, 2H), 7.88 (d, 2H), 8.45 (s, 2H). Elemental analysis: calculated for $C_{30}H_{19}O_4S_2N_5$: C, 62.38; H, 3.32; S, 11.10. Found: C, 61.99; H, 3.05; S, 11.03.

3,6-Bis(2-(3,4-ethylenedioxy)thienyl)-*N*-(p-nitrophenyl)carbazole (17). In a Schlenk flask, 0.39 g (0.88 mmol) of compound **15** was dissolved in 30 mL of anhydrous DMF. After addition of .025 g (1.06 mmol) of NaH, the solution turned yellow and bubbling was evident. The solution was stirred for 15 minutes, and 0.15 g (1.06 mmol) of p-fluoronitrobenzene was added via syringe. The orange solution was stirred for 15 hours after which time a yellow precipitate was observed in the flask. The mixture was poured into 100 mL of water and the yellow solid was collected via filtration, washed with water, and dried to yield 0.31 g (62%) of a highly fluorescent yellow solid. mp = 322-324 (d). ^{1}H-NMR (DMSO-d_6) δ 6.6 (s, 2H), 7.58 (d, 2H), 7.78 (d, 2H), 7.98 (m, 2H), 8.5 (m, 4H) Elemental Analysis: Calculated for $C_{30}H_{20}N_2O_6S_2$: C, 63.37%; H, 3.55%; N, 4.93%. Found: C, 62.94%; H, 3.72%; N, 5.27%. FAB-HRMS calculated for $C_{30}H_{20}N_2O_6S_2$: 568.0763. Found: 569.0818 (M+1).

3-6-Bis(2-thienyl)-*N*-dodecyl-carbazole (21). 1 g (2.95 mmol) of compound **20** and 0.08 g (2 mol %) of $Pd(PPh_3)Cl_2$ were combined in a schlenk flask with an argon inlet. The contents were placed under vacuum for 10 minutes and backfilled with argon. 50 mL of DMF and 1.53 g (6.19 mmol) of compound **19** were added via syringe, and the reaction was heated to 80 °C for 24 hours. The dark black mixture was poured into water, and extracted three times with chloroform. The combined chloroform layers were washed with copious amounts of water. The chloroform was removed under vacuum and purified with column chromatography on silica gel with chloroform as the eluent to yield 0.7 g (48%) of a slightly yellow oil as product **21**. ^{1}H-NMR ($CDCl_3$): δ 0.90 (t, 3H), 1.35

(m, 18H), 1.91 (p, 2H), 4.25 (t, 2H), 7.14 (m, 2H), 7.29 (m, 2H), 7.40 (m, 4H), 7.76 (dd, 2H), 8.37 (s, 2H). ^{13}C NMR ($CDCl_3$) : δ 14.2, 22.7, 27.4, 29.0, 29.3, 29.5, 29.7, 31.9, 43.2, 109.2, 117.9, 122.2, 123.3, 123.8, 124.5, 125.9, 128.0, 140.4, 145.6. Elemental Analysis: Calculated for $C_{32}H_{37}S_2N$: C, 76.91; H, 7.46; S, 12.83. Found: C, 76.56; H, 7.55; S, 12.90. FAB-HRMS calculated for $C_{32}H_{37}S_2N$: 499.2367. Found: 499.2341.

4,4'-dibromodiphenylamine (23). A solution of 10.53 g (59.0 mmol) of NBS in 50 mL of DMF was added via cannula to a solution of 5 g (29.6 mmol) of diphenylamine in 50 mL of DMF in a round bottom flask. Heat evolution was detected upon mixture of the two solutions. The pale yellow solution was stirred at room temperature for 18 hours. The faint red solution was poured into water, and extracted three times with methylene chloride. The combined organic layers were washed with copious amounts of water, dried with $MgSO_4$, and the methylene chloride was removed under vacuum to yield a brown oil. Purification on silica gel with chloroform as the eluent yielded 6.5 g (67%) of a white solid as product **23**. mp = 102-104 °C. (lit[196] 100-102 °C) ^{1}H-NMR ($CDCl_3$): δ 5.67 (s, 1H), 6.93 (d, 4H), 7.37 (d, 4H).

4,4'-*N*-acetyl-diphenylamine (24). 4.5 g (13.8 mmol) of compound **23** was dissolved in 50 mL of DMF. 0.5 g (20.6 mmol) of NaH was added, and the reaction immediately turned yellow with gas evolution evident. After stirring for 15 minutes, 1.6 g (20.6 mmol) of benzoyl chloride was added, and the reaction was stirred overnight. The reaction mixture was poured into water, and extracted three times with chloroform. The combined organic layers were washed with copious amounts of water, dried with

$MgSO_4$, and the chloroform was removed under vacuum. Further purification with column chromatography on silica gel with chloroform as eluent yielded 3.69 g (70%) of a honey colored thick oil. ^{1}H-NMR ($CDCl_3$): δ 2.05 (s, 3H), 7.15 (d, 2H), 7.48 (m, 2H).

4,4'-Bis(2-(3,4-ethylenedioxy)-(5-trimethylsilyl)-thienyl)-*N*-acetyl-diphenylamine (25). 1.86 g (4.95 mmol) of compound **11** and 0.7 g (2mol%) of $Pd(PPh_3)Cl_2$ were combined in a schlenk flask equipped with an argon inlet. The contents were placed under vacuum for 10 minutes and backfilled with argon. A solution of 0.87 g (2.36 mmol) of compound **24** in 30 mL of DMF was added via syringe along with an additional 30 mL of DMF. The flask was heated to 80 °C and stirred overnight. The black mixture was poured into 200 mL of brine, and a tan solid was collected via filtration and washed with water. Further purification with column chromatography on silica with 3:1 chloroform/hexanes as the eluent yielded 0.95 g (63%) of a yellow solid, which was deprotected without any further purification. ^{1}H-NMR ($CDCl_3$): δ 0.3 (s, 18H), 2.1 (s, 3H), 4.25 (m, 8H), 7.25 (d, 4H), 7.7 (s, 4H).

4,4'-Bis(2-(3,4-ethylenedioxy)-thienyl)diphenylamine (26). Compound **26** was synthesized using the same procedure to synthesize compound **15** using 0.62 g (0.97 mmol) of compound **25**, 0.55 g (0.97 mmol) of KOH, 150 mL of Ethanol, and 2 eq. TBAF. Yield 0.29g (66%). mp = 157 –159 °C. ^{1}H-NMR (d_6-DMSO): δ 4.28 (d, 8H), 6.48 (s, 2H), 7.10 (d, 4H), 7.55 (d, 4H), 8.58 (s, 1H). Elemental Analysis: Calculated for $C_{24}H_{19}O_4S_2N$: C, 64.12; H, 4.26; S, 14.26. Found: C, 64.33; H, 3.98; S, 14.11. FAB-HRMS calculated for $C_{24}H_{19}O_4S_2N$: 449.0755. Found: 450.0798 (M+1).

APPENDIX
CRYSTALLOGRAPHIC DATA

Table A-1: Crystallographic data and structure refinement for ProDOT (**4e**).

Empirical formula	$C_7H_8O_2S$
Formula weight	156.19
Temperature	173(2) K
Wavelength	0.71073 Å
Crystal system	Monoclinic
Space group	P2 (1) / n
Unit cell dimensions	a = 8.1108(2) Å $\alpha = 90°$ b = 10.2518(3) Å $\beta = 92.695(1)°$ c = 8.6934(1) Å $\gamma = 90°$
Volume, Z	722.06(3) $Å^3$, 4
Density (calculated)	1.437 Mg/m^3
Absorption coefficient	0.378 mm^{-1}
F(000)	328
Crystal size	0.38 x 0.28 x 0.17 mm
Theta range for data collection	3.07 to 27.48°
Limiting indices	$-10 \leq h \leq 9$, $-13 \leq k \leq 7$, $-11 \leq l \leq 11$
Reflections collected	4957
Independent reflections	1648 [R(int) = 0.0228]
Absorption correction	Empirical
Min. and Max. Transmission	0.713, 0.952
Refinement method	Full-matrix least-squares on F^2
Data / restraints / parameters	1648 / 0 / 124
Goodness-of-fit on F^2	1.084
Final R indices [I>2sigma(I)]	R1 = 0.0278, wR2 = 0.0657 [1468]
R indices (all data)	R1 = 0.0312, wR2 = 0.0669

Extinction coefficient	0.050(3)
Largest diff. peak and hole	0.280 and -0.295 e.Å^{-3}

Table A-2: Atomic coordinates (x 10^4) and equivalent isotropic displacement parameters (A^2 x 10^3) for ProDOT (**4e**). U(eq) is defined as one third of the trace of the orthogonalized U_{ij} tensor.

	x	y	z	U(eq)
S	1328(1)	4939(1)	6996(1)	28(1)
O1	5618(1)	6250(1)	8394(1)	28(1)
O2	4219(1)	7670(1)	5636(1)	30(1)
C3	3476(1)	6633(1)	6313(1)	22(1)
C4	1951(2)	6192(1)	5851(2)	28(1)
C6	7161(2)	7354(1)	6395(2)	33(1)
C7	5848(2)	7390(2)	5101(2)	33(1)
C5	7046(2)	6199(1)	7459(2)	30(1)
C1	3133(2)	4984(1)	8106(2)	26(1)
C2	4152(1)	5938(1)	7629(1)	22(1)

Table A-3: Bond lengths (Å) and angles (°) for ProDOT (**4e**).

S-C4	1.7151(14)
S-C1	1.7155(13)
O1-C2	1.3722(14)
O1-C5	1.447(2)
O2-C3	1.369(2)
O2-C7	1.450(2)
C3-C4	1.360(2)
C3-C2	1.434(2)
C4-H4	0.94(2)
C6-C5	1.508(2)
C6-C7	1.512(2)
C6-H6B	0.97(2)
C6-H6A	0.97(2)
C7-H7B	0.97(2)
C7-H7A	1.01(2)
C5-H5B	0.98(2)
C5-H5A	0.94(2)
C1-C2	1.358(2)
C1-H1	0.94(2)
C4-S-C1	92.28(6)
C2-O1-C5	114.72(9)
C3-O2-C7	114.24(10)
C4-C3-O2	122.94(11)
C4-C3-C2	112.26(11)
O2-C3-C2	124.70(11)
C3-C4-S	111.46(10)
C3-C4-H4	126.4(11)
S-C4-H4	122.1(11)
C5-C6-C7	114.47(11)
C5-C6-H6B	109.0(10)
C7-C6-H6B	110.5(10)
C5-C6-H6A	107.8(9)
C7-C6-H6A	106.8(10)
H6B-C6-H6A	108.1(14)
O2-C7-C6	112.76(12)
O2-C7-H7B	104.8(11)
C6-C7-H7B	110.4(11)
O2-C7-H7A	107.5(9)
C6-C7-H7A	110.8(9)
H7B-C7-H7A	110.4(14)
O1-C5-C6	112.98(11)
O1-C5-H5B	108.6(9)
C6-C5-H5B	110.8(9)

O1-C5-H5A	106.5(10)
C6-C5-H5A	111.0(10)
H5B-C5-H5A	106.7(13)
C2-C1-S	111.28(10)
C2-C1-H1	128.3(10)
S-C1-H1	120.4(10)
C1-C2-O1	123.10(11)
C1-C2-C3	112.70(11)
O1-C2-C3	124.08(11)

Table A-4: Anisotropic displacement parameters (A^2 x 10^3) for ProDOT **(4e)**. The anisotropic displacement factor exponent takes the form: -2 pi^2 [h^2 a*^2 U11 + ... + 2 h k a* b* U12]

	U11	U22	U33	U23	U13	U12
S	21(1)	33(1)	31(1)	-4(1)	1(1)	-4(1)
O1	22(1)	40(1)	22(1)	-3(1)	-4(1)	-4(1)
O2	27(1)	27(1)	37(1)	9(1)	5(1)	3(1)
C3	23(1)	23(1)	22(1)	0(1)	3(1)	3(1)
C4	24(1)	34(1)	24(1)	-1(1)	-2(1)	4(1)
C6	24(1)	34(1)	40(1)	-4(1)	6(1)	-5(1)
C7	30(1)	38(1)	33(1)	8(1)	9(1)	-1(1)
C5	21(1)	37(1)	31(1)	-4(1)	-3(1)	2(1)
C1	25(1)	28(1)	24(1)	1(1)	1(1)	1(1)
C2	21(1)	24(1)	20(1)	-4(1)	-1(1)	1(1)

Table A-5: Hydrogen coordinates (x 10^4) and isotropic displacement parameters (A^2 x 10^3) for ProDOT (**4e**).

	x	y	z	U(eq)
H4	1278(22)	6520(17)	5033(21)	45(5)
H6B	7138(21)	8146(17)	6994(20)	43(5)
H6A	8218(21)	7309(15)	5918(19)	35(4)
H7B	6066(23)	8087(19)	4393(22)	52(5)
H7A	5783(20)	6527(16)	4542(18)	36(4)
H5B	7014(19)	5380(15)	6875(17)	28(4)
H5A	7978(21)	6154(15)	8149(19)	37(4)
H1	3300(20)	4409(16)	8935(19)	39(4)

Table A-6: Crystallographic data and structure refinement for EDOT-Ph (**4d**).

Empirical formula	$C_{12}H_{10}O_2S$
Formula weight	218.26
Temperature	173(2) K
Wavelength	0.71073 Å
Crystal system	Monoclinic
Space group	P2(1)/c
Unit cell dimensions	a = 9.1090(1) Å α = 90° b = 16.8237(4) Å β = 92.774(1)° c = 6.6466(1) Å γ = 90°
Volume, Z	1017.42(3) $Å^3$, 4
Density (calculated)	1.425 Mg/m^3
Absorption coefficient	0.291 mm^{-1}
F(000)	456
Crystal size	0.20 x 0.19 x 0.13 mm
Theta range for data collection	2.24 to 27.49 °
Limiting indices	$-12 \leq h \leq 12$, $-23 \leq k \leq 19$, $-8 \leq l \leq 7$
Reflections collected	6895
Independent reflections	2331 [R(int) = 0.0297]
Absorption correction	None
Refinement method	Full-matrix least-squares on F^2
Data / restraints / parameters	2330 / 0 / 177
Goodness-of-fit on F^2	1.052
Final R indices [I>2sigma(I)]	R1 = 0.0368, wR2 = 0.0823 [1871]
R indices (all data)	R1 = 0.0494, wR2 = 0.0875

Extinction coefficient	0.0054(13)
Largest diff. peak and hole	0.571 and -0.209 e.Å^{-3}

Table A-7: Atomic coordinates (x 10^4) and equivalent isotropic displacement parameters (A^2 x 10^3) for EDOT-Ph (**4d**). U(eq) is defined as one third of the trace of the orthogonalized U_{ij} tensor.

	x	y	z	U(eq)
S	3666(1)	2024(1)	8102(1)	31(1)
O1	3331(1)	414(1)	3933(2)	26(1)
C1	4274(2)	1278(1)	6598(3)	29(1)
O2	599(1)	1283(1)	4304(2)	29(1)
C2	3185(2)	1018(1)	5296(2)	23(1)
C3	1846(2)	1441(1)	5487(2)	24(1)
C4	1935(2)	2000(1)	6961(3)	29(1)
C5	1918(2)	99(1)	3228(3)	28(1)
C6	896(2)	770(1)	2623(3)	31(1)
C7	2207(2)	-451(1)	1504(3)	26(1)
C8	3028(2)	-209(1)	-97(3)	30(1)
C9	3360(2)	-744(1)	-1592(3)	37(1)
C10	2858(2)	-1518(1)	-1514(3)	41(1)
C11	2010(2)	-1758(1)	41(3)	40(1)
C12	1691(2)	-1227(1)	1561(3)	32(1)

Table A-8: Bond lengths (Å) and angles (°) for EDOT-Ph (**4d**).

S-C1	1.712(2)
S-C4	1.717(2)
O1-C2	1.372(2)
O1-C5	1.448(2)
C1-C2	1.357(2)
C1-H1	0.92(2)
O2-C3	1.376(2)
O2-C6	1.448(2)
C2-C3	1.423(2)
C3-C4	1.358(2)
C4-H4	0.94(2)
C5-C6	1.505(2)
C5-C7	1.506(2)
C5-H5	1.06(2)
C6-H6A	0.99(2)
C6-H6B	1.06(2)
C7-C12	1.389(3)
C7-C8	1.391(2)
C8-C9	1.385(3)
C8-H8	1.00(2)
C9-C10	1.382(3)
C9-H9	0.97(2)
C10-C11	1.379(3)
C10-H10	0.99(2)
C11-C12	1.389(3)
C11-H11	0.97(2)
C12-H12	0.95(2)
C1-S-C4	92.36(9)
C2-O1-C5	111.85(12)
C2-C1-S	111.20(14)
C2-C1-H1	129.2(13)
S-C1-H1	119.6(13)
C3-O2-C6	112.05(13)
C1-C2-O1	124.7(2)
C1-C2-C3	112.7(2)
O1-C2-C3	122.65(14)
C4-C3-O2	124.4(2)
C4-C3-C2	112.9(2)
O2-C3-C2	122.72(14)
C3-C4-S	110.85(14)
C3-C4-H4	129.3(12)
S-C4-H4	119.8(12)
O1-C5-C6	109.89(14)

O1-C5-C7	106.62(14)
C6-C5-C7	112.7(2)
O1-C5-H5	107.8(11)
C6-C5-H5	108.1(11)
C7-C5-H5	111.6(11)
O2-C6-C5	112.16(14)
O2-C6-H6A	106.4(11)
C5-C6-H6A	111.8(11)
O2-C6-H6B	109.7(13)
C5-C6-H6B	104.8(13)
H6A-C6-H6B	112(2)
C12-C7-C8	119.4(2)
C12-C7-C5	119.0(2)
C8-C7-C5	121.5(2)
C9-C8-C7	120.1(2)
C9-C8-H8	122.0(13)
C7-C8-H8	117.8(13)
C10-C9-C8	120.1(2)
C10-C9-H9	121.8(13)
C8-C9-H9	118.0(13)
C11-C10-C9	120.1(2)
C11-C10-H10	121.5(13)
C9-C10-H10	118.4(13)
C10-C11-C12	120.1(2)
C10-C11-H11	120.3(14)
C12-C11-H11	119.6(14)
C11-C12-C7	120.1(2)
C11-C12-H12	120.0(14)
C7-C12-H12	119.9(14)

Table A-9: Anisotropic displacement parameters (A^2 x 10^3) for EDOT-Ph (**4d**). The anisotropic displacement factor exponent takes the form: -2 pi^2 [h^2 a*^2 U11 + ... + 2 h k a* b* U12].

	U11	U22	U33	U23	U13	U12
S	37(1)	30(1)	26(1)	-5(1)	-4(1)	-3(1)
O1	23(1)	30(1)	25(1)	-7(1)	-3(1)	2(1)
C1	28(1)	32(1)	26(1)	-2(1)	-3(1)	1(1)
O2	23(1)	32(1)	30(1)	-8(1)	-1(1)	3(1)
C2	27(1)	24(1)	19(1)	1(1)	1(1)	0(1)
C3	24(1)	24(1)	24(1)	1(1)	0(1)	-2(1)
C4	30(1)	26(1)	30(1)	-3(1)	2(1)	1(1)
C5	28(1)	31(1)	26(1)	-1(1)	0(1)	-2(1)
C6	28(1)	33(1)	31(1)	-9(1)	-5(1)	4(1)
C7	22(1)	30(1)	27(1)	-4(1)	-3(1)	3(1)
C8	30(1)	29(1)	31(1)	1(1)	-2(1)	-3(1)
C9	30(1)	52(1)	29(1)	-4(1)	2(1)	2(1)
C10	39(1)	44(1)	40(1)	-18(1)	-8(1)	14(1)
C11	43(1)	22(1)	54(1)	-1(1)	-14(1)	1(1)
C12	30(1)	35(1)	31(1)	7(1)	-3(1)	-1(1)

Table A-10: Hydrogen coordinates (x 10^4) and isotropic displacement parameters (A^2 x 10^3) for EDOT-Ph (**4d**).

	x	y	z	U(eq)
H1	5219(24)	1096(13)	6786(30)	38(6)
H4	1221(22)	2361(12)	7357(30)	34(5)
H5	1467(22)	-207(12)	4439(30)	34(5)
H6A	-66(21)	572(12)	2087(28)	31(5)
H6B	1457(26)	1093(14)	1534(35)	57(7)
H8	3400(25)	348(14)	-90(34)	51(6)
H9	3999(24)	-568(13)	-2630(34)	46(6)
H10	3094(24)	-1886(13)	-2619(34)	48(6)
H11	1649(26)	-2299(14)	93(35)	53(7)
H12	1120(24)	-1395(13)	2636(33)	45(6)

Table A-11: Crystallographic data and structure refinement for BiProDOT-Et_2 (**20**).

Empirical formula	$C_{22}H_{30}O_4S_2$	
Formula weight	422.58	
Temperature	173(2) K	
Wavelength	0.71073 Å	
Crystal system	Orthorhombic	
Space group	P2(1)2(1)2(1)	
Unit cell dimensions	a = 7.7486(4) Å	α = 90°.
	b = 9.9587(5) Å	β = 90°.
	c = 27.327(1) Å	γ = 90°.
Volume	2108.7(2) $Å^3$	
Z	4	
Density (calculated)	1.331 Mg/m^3	
Absorption coefficient	0.278 mm^{-1}	
F(000)	904	
Crystal size	0.20 x 0.19 x 0.19 mm^3	
Theta range for data collection	2.18 to 27.50°.	
Index ranges	$-10 \le h \le 10$, $-12 \le k \le 9$, $-35 \le l \le 28$	
Reflections collected	14839	
Independent reflections	4829 [R(int) = 0.0322]	
Completeness to theta = 27.50°	100.0 %	
Absorption correction	Integration	
Max. and min. transmission	0.9629 and 0.9193	
Refinement method	Full-matrix least-squares on F^2	
Data / restraints / parameters	4829 / 0 / 257	
Goodness-of-fit on F^2	1.050	
Final R indices [I>2sigma(I)]	R1 = 0.0302, wR2 = 0.0718 [4477]	
R indices (all data)	R1 = 0.0342, wR2 = 0.0741	
Absolute structure parameter	0.05(5)	
Largest diff. peak and hole	0.236 and -0.163 $e.Å^{-3}$	

$R1 = \Sigma(||F_o| - |F_c||) / \Sigma|F_o|$

$wR2 = [\Sigma[w(F_o^2 - F_c^2)^2] / \Sigma[w(F_o^2)^2]]^{1/2}$

$S = [\Sigma[w(F_o^2 - F_c^2)^2] / (n-p)]^{1/2}$

$w= 1/[\sigma^2(F_o^2)+(0.0370*p)^2+0.31*p]$, $p = [\max(F_o^2,0)+ 2* F_c^2]/3$

Table A-12: Atomic coordinates (x 10^4) and equivalent isotropic displacement parameters ($Å^2$x 10^3) for BiProDOT-Et_2 (**20**). U(eq) is defined as one third of the trace of the orthogonalized U^{ij} tensor.

	x	y	z	U(eq)
S1	2203(1)	5889(1)	1129(1)	30(1)
O1	6327(2)	5984(1)	330(1)	28(1)
O2	3543(2)	4303(1)	-114(1)	30(1)
C1	4309(2)	6310(2)	979(1)	23(1)
C2	4743(2)	5775(2)	534(1)	24(1)
C3	3401(2)	4978(2)	323(1)	27(1)
C4	1951(2)	4968(2)	602(1)	32(1)
C5	6284(2)	6121(2)	-197(1)	28(1)
C6	6476(2)	4759(2)	-452(1)	25(1)
C7	5242(2)	3754(2)	-209(1)	28(1)
C8	8309(2)	4203(2)	-383(1)	31(1)
C9	9742(2)	5028(2)	-618(1)	39(1)
C10	5991(2)	4969(2)	-992(1)	31(1)
C11	6441(3)	3821(2)	-1337(1)	42(1)
S1'	7605(1)	7267(1)	1185(1)	31(1)
O1'	3321(1)	7765(1)	1898(1)	27(1)
O2'	6305(2)	9001(1)	2401(1)	33(1)
C1'	5417(2)	7070(2)	1304(1)	24(1)
C2'	4990(2)	7689(2)	1734(1)	25(1)
C3'	6425(2)	8288(2)	1973(1)	28(1)
C4'	7916(2)	8133(2)	1723(1)	35(1)
C5'	3050(2)	7213(2)	2382(1)	27(1)
C6'	3639(2)	8109(2)	2804(1)	25(1)
C7'	5600(2)	8257(2)	2807(1)	30(1)
C8'	2800(3)	9503(2)	2774(1)	34(1)
C9'	848(3)	9532(3)	2828(1)	53(1)
C10'	3141(3)	7339(2)	3275(1)	34(1)
C11'	3401(3)	8083(2)	3758(1)	44(1)

Table A-13: Bond lengths [Å] and angles [°] for BiProDOT-Et_2 (**20**).

S1-C4	1.7187(18)
S1-C1	1.7340(17)
O1-C2	1.3635(19)
O1-C5	1.4472(19)
O2-C3	1.3745(19)
O2-C7	1.448(2)
C1-C2	1.370(2)
C1-C1'	1.449(2)
C2-C3	1.431(2)
C3-C4	1.359(2)
C5-C6	1.532(2)
C6-C7	1.536(2)
C6-C8	1.536(2)
C6-C10	1.537(2)
C8-C9	1.522(3)
C10-C11	1.522(3)
S1'-C4'	1.7197(18)
S1'-C1'	1.7376(17)
O1'-C2'	1.3710(19)
O1'-C5'	1.446(2)
O2'-C3'	1.370(2)
O2'-C7'	1.443(2)
C1'-C2'	1.367(2)
C2'-C3'	1.421(2)
C3'-C4'	1.351(3)
C5'-C6'	1.530(2)
C6'-C7'	1.527(2)
C6'-C8'	1.535(2)
C6'-C10'	1.547(2)
C8'-C9'	1.520(3)
C10'-C11'	1.526(3)
C4-S1-C1	92.18(8)
C2-O1-C5	113.62(12)

C3-O2-C7	114.36(13)
C2-C1-C1'	127.00(15)
C2-C1-S1	110.31(12)
C1'-C1-S1	122.63(12)
O1-C2-C1	121.65(14)
O1-C2-C3	125.00(15)
C1-C2-C3	113.33(15)
C4-C3-O2	123.48(15)
C4-C3-C2	112.19(15)
O2-C3-C2	124.32(15)
C3-C4-S1	111.93(13)
O1-C5-C6	111.59(14)
C5-C6-C7	108.61(13)
C5-C6-C8	110.68(14)
C7-C6-C8	106.71(13)
C5-C6-C10	107.05(14)
C7-C6-C10	110.61(14)
C8-C6-C10	113.12(14)
O2-C7-C6	113.38(14)
C9-C8-C6	115.34(14)
C11-C10-C6	115.86(15)
C4'-S1'-C1'	91.91(9)
C2'-O1'-C5'	114.44(12)
C3'-O2'-C7'	114.61(13)
C2'-C1'-C1	128.23(15)
C2'-C1'-S1'	110.25(12)
C1-C1'-S1'	121.50(12)
C1'-C2'-O1'	122.26(14)
C1'-C2'-C3'	113.23(15)
O1'-C2'-C3'	124.44(15)
C4'-C3'-O2'	123.31(16)
C4'-C3'-C2'	112.87(15)
O2'-C3'-C2'	123.76(16)
C3'-C4'-S1'	111.71(13)
O1'-C5'-C6'	115.13(13)
C7'-C6'-C5'	110.93(14)

C7'-C6'-C8'	109.54(15)
C5'-C6'-C8'	111.17(14)
C7'-C6'-C10'	106.94(14)
C5'-C6'-C10'	105.36(13)
C8'-C6'-C10'	112.79(14)
O2'-C7'-C6'	114.97(15)
C9'-C8'-C6'	115.66(18)
C11'-C10'-C6'	116.48(15)

Symmetry transformations used to generate equivalent atoms:

Table A-14: Anisotropic displacement parameters ($Å^2 x\ 10^3$) for BiProDOT-Et_2 (**20**). The anisotropic displacement factor exponent takes the form: $-2\pi^2[\ h^2\ a^{*2}U^{11} + ... + 2\ h\ k\ a^*\ b^*\ U^{12}\ ]$

	U^{11}	U^{22}	U^{33}	U^{23}	U^{13}	U^{12}
S1	26(1)	38(1)	26(1)	-5(1)	2(1)	-6(1)
O1	27(1)	37(1)	22(1)	-4(1)	2(1)	-9(1)
O2	27(1)	36(1)	26(1)	-8(1)	-2(1)	-4(1)
C1	24(1)	24(1)	21(1)	1(1)	-2(1)	-2(1)
C2	23(1)	26(1)	23(1)	1(1)	-2(1)	-2(1)
C3	28(1)	28(1)	24(1)	-2(1)	-3(1)	-3(1)
C4	28(1)	37(1)	31(1)	-6(1)	-2(1)	-8(1)
C5	35(1)	26(1)	23(1)	2(1)	4(1)	0(1)
C6	27(1)	25(1)	22(1)	1(1)	-1(1)	3(1)
C7	31(1)	26(1)	27(1)	-2(1)	-1(1)	0(1)
C8	29(1)	32(1)	31(1)	3(1)	-5(1)	3(1)
C9	27(1)	46(1)	44(1)	3(1)	1(1)	1(1)
C10	31(1)	39(1)	25(1)	2(1)	-2(1)	5(1)
C11	43(1)	54(1)	29(1)	-10(1)	-5(1)	3(1)
S1'	28(1)	41(1)	24(1)	-2(1)	2(1)	-11(1)
O1'	27(1)	31(1)	23(1)	-2(1)	-2(1)	3(1)
O2'	41(1)	31(1)	27(1)	-7(1)	1(1)	-13(1)
C1'	26(1)	24(1)	23(1)	4(1)	-2(1)	-3(1)
C2'	27(1)	21(1)	25(1)	3(1)	-1(1)	-3(1)
C3'	36(1)	25(1)	24(1)	-1(1)	-1(1)	-8(1)
C4'	35(1)	40(1)	29(1)	-2(1)	-2(1)	-16(1)
C5'	31(1)	25(1)	25(1)	-3(1)	0(1)	-4(1)
C6'	31(1)	22(1)	23(1)	-2(1)	-2(1)	0(1)
C7'	35(1)	32(1)	23(1)	-2(1)	-4(1)	-2(1)
C8'	45(1)	27(1)	30(1)	-5(1)	-4(1)	6(1)
C9'	47(1)	61(2)	52(1)	-18(1)	-11(1)	22(1)
C10'	43(1)	32(1)	26(1)	1(1)	1(1)	-6(1)
C11'	60(1)	46(1)	26(1)	0(1)	1(1)	-2(1)

Table A-15: Hydrogen coordinates (x 10^4) and isotropic displacement parameters ($Å^2$x 10^3) for BiProDOT-Et_2 (**20**).

	x	y	z	U(eq)
H4A	921	4507	517	38
H5A	7230	6722	-303	34
H5B	5178	6537	-296	34
H7A	5123	2957	-423	33
H7B	5752	3452	105	33
H8A	8545	4132	-28	37
H8B	8349	3283	-521	37
H9A	9526	5109	-970	59
H9B	10853	4581	-564	59
H9C	9769	5924	-470	59
H10A	4732	5130	-1012	38
H10B	6576	5791	-1111	38
H11A	7696	3702	-1346	63
H11B	6019	4029	-1666	63
H11C	5896	2992	-1220	63
H4'A	9003	8462	1830	42
H5'A	3671	6346	2404	32
H5'B	1804	7023	2422	32
H7'A	5946	8709	3115	36
H7'B	6121	7350	2809	36
H8'A	3306	10076	3033	41
H8'B	3106	9909	2455	41
H9'1	325	8969	2573	80
H9'2	435	10457	2793	80
H9'3	526	9187	3151	80
H10C	1911	7081	3251	41
H10D	3824	6500	3287	41
H11D	4629	8288	3801	66
H11E	3004	7517	4029	66

H11F	2737	8920	3754	66

Table A-16: Torsion angles [°] for BiProDOT-Et_2 (**20**).

C4-S1-C1-C2	1.43(13)
C4-S1-C1-C1'	-175.92(14)
C5-O1-C2-C1	-144.05(16)
C5-O1-C2-C3	37.3(2)
C1'-C1-C2-O1	-4.0(3)
S1-C1-C2-O1	178.81(12)
C1'-C1-C2-C3	174.78(15)
S1-C1-C2-C3	-2.42(18)
C7-O2-C3-C4	-144.83(17)
C7-O2-C3-C2	35.6(2)
O1-C2-C3-C4	-178.84(16)
C1-C2-C3-C4	2.4(2)
O1-C2-C3-O2	0.7(3)
C1-C2-C3-O2	-177.97(15)
O2-C3-C4-S1	179.12(13)
C2-C3-C4-S1	-1.3(2)
C1-S1-C4-C3	-0.05(15)
C2-O1-C5-C6	-89.39(17)
O1-C5-C6-C7	47.50(18)
O1-C5-C6-C8	-69.34(17)
O1-C5-C6-C10	166.96(13)
C3-O2-C7-C6	-86.17(17)
C5-C6-C7-O2	43.57(18)
C8-C6-C7-O2	162.93(13)
C10-C6-C7-O2	-73.64(17)
C5-C6-C8-C9	-64.3(2)
C7-C6-C8-C9	177.65(15)
C10-C6-C8-C9	55.8(2)
C5-C6-C10-C11	167.89(16)
C7-C6-C10-C11	-73.95(19)
C8-C6-C10-C11	45.7(2)
C2-C1-C1'-C2'	175.33(17)
S1-C1-C1'-C2'	-7.8(2)

C2-C1-C1'-S1'	-6.4(2)
S1-C1-C1'-S1'	170.44(10)
C4'-S1'-C1'-C2'	1.62(14)
C4'-S1'-C1'-C1	-176.90(14)
C1-C1'-C2'-O1'	-6.2(3)
S1'-C1'-C2'-O1'	175.44(13)
C1-C1'-C2'-C3'	176.87(16)
S1'-C1'-C2'-C3'	-1.52(18)
C5'-O1'-C2'-C1'	123.77(16)
C5'-O1'-C2'-C3'	-59.6(2)
C7'-O2'-C3'-C4'	-124.08(19)
C7'-O2'-C3'-C2'	58.9(2)
C1'-C2'-C3'-C4'	0.6(2)
O1'-C2'-C3'-C4'	-176.34(16)
C1'-C2'-C3'-O2'	177.81(15)
O1'-C2'-C3'-O2'	0.9(3)
O2'-C3'-C4'-S1'	-176.57(13)
C2'-C3'-C4'-S1'	0.7(2)
C1'-S1'-C4'-C3'	-1.33(16)
C2'-O1'-C5'-C6'	77.50(18)
O1'-C5'-C6'-C7'	-67.18(18)
O1'-C5'-C6'-C8'	54.96(19)
O1'-C5'-C6'-C10'	177.45(14)
C3'-O2'-C7'-C6'	-78.64(19)
C5'-C6'-C7'-O2'	67.80(19)
C8'-C6'-C7'-O2'	-55.28(19)
C10'-C6'-C7'-O2'	-177.81(14)
C7'-C6'-C8'-C9'	-173.18(17)
C5'-C6'-C8'-C9'	63.9(2)
C10'-C6'-C8'-C9'	-54.2(2)
C7'-C6'-C10'-C11'	68.6(2)
C5'-C6'-C10'-C11'	-173.32(16)
C8'-C6'-C10'-C11'	-51.9(2)

Symmetry transformations used to generate equivalent atoms

REFERENCES

[1] Shirakawa, H.; Lewis, E. J.; MacDiarmid, A. G.; Chiang, C. K.; Heeger, A. J. *J. Chem. Soc., Chem. Commun.* **1977**, 578.

[2] *Handbook of Conducting Polymers*, 2nd ed.; Skotheim, T. A.; Elsenbaumer, R. L.; Reynolds, J. R., Eds.; Marcel Dekker: New York, **1998**.

[3] Reddinger, J. L.; Reynolds, J. R. *Adv. Polym. Sci.* **1999**, *145*, 57.

[4] Shirakawa, H., in *Handbook of Conducting Polymers*, 2nd ed.; Skotheim, T. A.; Elsenbaumer, R. L.; Reynolds, J. R., Eds.; Marcel Dekker: New York, 1998, pp. 197 208.

[5] Chien, J. C. W. *Polyacetylene: Chemistry, Physics, and Materials Science*, Academic: Orlando, **1984**.

[6] Diaz, A. F. *Chem. Scr.* **1981**, *17*, 142.

[7] Tourillon, G.; Garnier, F. J. *J. Electroanal. Chem.* **1982**, *135*, 173.

[8] Diaz, A. F.; Kanazawa, K. K.; Gardini, G. P. *J. Chem. Soc., Chem. Commun.* **1979**, 635.

[9] Grem, G.; Leditzky, G.; Ullrich, B.; Leising, G. *Adv. Mater.* **1992**, *4*, 36.

[10] Burroughes, J. H.; Bradley, D. D. C.; Brown, A. R.; Marks, R. N.; MacKay, K.; Friend, R. H.; Burn, P. L.; Holmes, A. B. *Nature* **1990**, *347*, 539.

[11] Rault-Berthelot, J.; Simonet, J. *J. Electrochem. Soc.* **1985**, *182*, 187.

[12] MacDiarmid, A. G.; Epstein, A. J. *Faraday Discuss. Chem. Soc.* **1989**, *88*, 317.

[13] Asavapiriyanont, S.; Chandler, G. K.; Gunawardena, G. A.; Pletcher, D. *J. Electroanal. Chem.* **1984**, *177*, 229.

[14] Inoue, T.; Yamase, T. *Bull. Chem. Soc. Jpn.* **1983**, *56*, 985.

[15] Genies, E.; Bidan, G.; Diaz, A. F. *J. Electroanal. Chem.* **1983**, *149*, 113.

[16] Diaz, A. F.; Bargon, J. In *Handbook of Conducting Polymers*; Skotheim, T. A., Ed.; 1986; Vol. 1, p. 82.

[17] Waltman, R. J.; Bargon, J. *Tetrahedron* **1984**, *40*, 3963.

[18] Okada, T.; Ogata, T.; Ueda, M. *Macromolecules* **1996**, *29*, 7645.

[19] Toshima, N.; Hara, S. *Prog. Polym. Sci.* **1995**, *20*, 155.

[20] Yoshino, K.; Hayashi, R.; Sugimoto, R. *Jpn. J. Appl. Phys.* **1984**, *23*, L899.

[21] Sugimoto, R.; Takeda, S.; Gu, H. B.; Yoshino, K. *Chem. Express* **1986**, *1*, 635.

[22] Pomerantz, M.; Tseng, J. J.; Zhu, H.; Sproull, S. J.; Reynolds, J. R.; Uitz, R.; Arnott, H. J. *Synth. Met.* **1991**, *41-43*, 825.

[23] Kovacic, P.; Jones, M. B. *Chem. Rev.* **1987**, *87*, 357.

[24] Baughman, R. H.; Bredas, J. L.; Chance, R. R.; Elsenbaumer, R. L.; Shacklette, L. W. *Chem. Rev.* **1982**, *82*, 209.

[25] Waltman, R. J.; Bargon, J.; Diaz, A. F. *J. Phys. Chem.* **1983**, *87*, 1459.

[26] Roncali, J.; Lemaire, M.; Garreau, R.; Garnier, F. *Synth. Met.* **1987**, *18*, 139.

[27] Edwards, J. H.; Feast, W. J. *Polymer* **1980**, *21*, 595.

[28] Edwards, J. H.; Feast, W. J. *Polymer* **1984**, *25*, 395.

[29] Swager, T. M.; Dougherty, D. A.; Grubbs, R. H. *J. Am. Chem. Soc.* **1988**, *110*, 2973.

[30] Swager, T. M.; Grubbs, R. H. *J. Am. Chem. Soc.* **1989**, *111*, 7807.

[31] Ballard, D. G. H.; Courtis, A.; Shirley, I. M.; Taylor, S. C. *J. Chem. Soc., Chem. Commun.* **1983**, 954.

[32] Ballard, D. G. H.; Courtis, A.; Shirley, I. M.; Taylor, S. C. *Macromolecules* **1988**, *21*, 294.

[33] McKean, J. R.; Stille, J. K. *Macromolecules* **1987**, *20*, 1787.

[34] Gin, D. L.; Conticello, V. P.; Grubbs, R. H. *J. Am. Chem. Soc.* **1992**, *114*, 3167.

[35] Schlüter, A. -D. in *Handbook of Conducting Polymers*, 2nd ed.; Skotheim, T. A.; Elsenbaumer, R. L.; Reynolds, J. R., Eds.; Marcel Dekker: New York, 1998, pp. 209 -224.

[36] Wessling, R. A.; Zimmerman, R. G. *J. Poly. Sci., Polym. Symp.* **1985**, *72*, 55.

[37] Lenz, R. W.; Han, C. C.; Stenger-Smith, J. D.; Karasz, F. E. *J. Poly. Sci., Polym. Chem. Ed.* **1988**, *26*, 3241.

[38] Burn, P. L.; Bradley, D. D. C.; Brown, A. R.; Friend, R. H.; Holmes, A. B. *Synth. Met.* **1991**, *41-43*, 261.

[39] Moratti, S. C. in *Handbook of Conducting Polymers*, 2nd ed.; Skotheim, T. A.; Elsenbaumer, R. L.; Reynolds, J. R., Eds.; Marcel Dekker: New York, 1998, pp. 341 -361.

[40] Jen, K. Y.; Eckhardt, H.; Jen, T. R.; Shacklette, L. W.; Elsenbaumer, R. L. *J. Chem. Soc., Chem. Commun.* **1988**, 217.

[41] Odian, G. *Principles of Polymerization*, 3rd ed.; John Wiley & Sons: New York, 1991; pp. 78-83.

[42] Bredas, J. L.; Street, G. B. *Acc. Chem. Res.* **1985**, *18*, 309.

[43] Hoier, S. N.; Park, S.-M. *J. Phys. Chem.* **1992**, *96*, 5188.

[44] Oudard, J. F.; Allendoerfer, R. D.; Osteryoung, R. A. *J. Electroanal. Chem.* **1988**, *241*, 231.

[45] Hill, M. G.; Penneau, J. F.; Zinger, B.; Mann, K. R.; Miller, L. L. *Chem. Mater.* **1992**, *4*, 1106.

[46] Bauerle, P.; Segelbacher, U.; Maier, A.; Mehring, M. *J. Am. Chem. Soc.* **1993**, *115*, 10217.

[47] Furukawa, Y. *J. Phys. Chem.* **1996**, *100*, 15644.

[48] Krische, B.; Zagorska, M. *Synth. Met.* **1989**, *28*, C263.

[49] Waltman, R. J.; Bargon, J. *J. Can. J. Chem.* **1986**, *64*, 76.

[50] Tourillon, G.; Garnier, F. *J. Phys. Chem.* **1983**, *87*, 2289.

[51] Dian, G.; Barbey, G.; Decroix, B. *Synth. Met.* **1986**, *13*, 281.

[52] Tourillon, G.; Garnier, F. *J. Electroamal. Chem.* **1984**, *161*, 51.

[53] Daoust, G.; Leclerc, M. *Macromolecules* **1991**, *24*, 455.

[54] Roncali, J.; Garnier, F.; Garreau, R.; Lemaire, M. *J. Chem. Soc., Chem. Commun.* **1987**, 1500.

[55] Kaneto, K.; Kohno, Y.; Yoshino, K. *Mol. Cryst. Liq. Cryst.* **1985**, *118*, 217.

[56] Jen, K. Y.; Oboodi, R.; Elsenbaumer, R. L. *Polym. Mater. Sci. Eng.* **1985**, *53*, 79.

[57] Elsenbaumer, R. L.; Jen, K. Y.; Oboodi, R. *Synth. Met.* **1986**, *15*, 169.

[58] Miller, G. G.; Elsenbaumer, R. L. *J. Chem. Soc., Chem. Commun.* **1986**, 1346.

[59] McCullough, R. D.; Ewbank, P. C., in *Handbook of Conducting Polymers*, 2nd ed.; Skotheim, T. A.; Elsenbaumer, R. L.; Reynolds, J. R., Eds.; Marcel Dekker: New York, 1998, Chapter 9.

[60] McCullough, R. D. *Adv. Mater.* **1998**, *10*, 93.

[61] McCullough, R. D.; Lowe, R. D. *J. Chem. Soc., Chem. Commun.* **1992**, 70.

[62] McCullough, R. D.; Lowe, R. D.; Jayaraman, M.; Anderson, D. L. *J. Org. Chem.* **1993**, *58*, 904.

[63] Chen, T.-A.; Rieke, R. D. *Synth. Met.* **1993**, *69*, 175.

[64] Chen, T.-A.; O'Brien, R. A.; Rieke, R. D. *Macromolecules* **1993**, *26*, 3462.

[65] Loewe, R. S.; Khersonsky, S. M.; McCullough, R. D. *Adv. Mater.* **1999**, *11*, 250.

[66] Dong, X. Y. M.; Tyson, J. C.; Collard, D. M. *Macromolecules* **2000**, *33*, 3502.

[67] Hong, X. Y. M.; Collard, D. M. *Macromolecules* **2000**, *33*, 6916.

[68] Wang, F.; Wilson, M. S.; Rauh, R. D.; Schottland, P.; Thompson, B. C.; Reynolds J. R. *Macromolecules* **2000**, *33*, 2083.

[69] Jonas, F.; Schrader, L. *Synth. Met.* **1991**, *41-43*, 831.

[70] Heywang, G.; Jonas, F. *Adv. Mater.* **1992**, *4*, 116.

[71] Groenedaal, L.; Jonas, F.; Freitag, D.; Pielartzik, H.; Reynolds, J. R. *Adv. Mater.* **2000**, *12*, 481.

[72] Dietrich, M.; Heinze, J.; Heywang, G.; Jonas, F. *J. Electroanal. Chem.* **1994**, *369*, 87.

[73] Jonas, F.; Krafft, W.; Muys, B. *Macromol. Symp.* **1995**, *100*, 169.

[74] Glenis, S.; Benz, M.; LeGoff, E.; Schindler, J. L.; Kannewurf, C. R.; Kanatzidis, M. G. *J. Am. Chem. Soc.* **1993**, *115*, 12519.

[75] Diaz, A. F.; Crowley, J. I.; Bargon, J.; Gardini, G. P.; Torrance, J. B. *J. Electroanal. Chem.* **1981**, *121*, 355.

[76] Sotzing, G. A.; Reynolds, J. R.; Steel, P. J. *Adv. Mater.* **1997**, *9*, 795.

[77] Akoudad, S.; Roncali, J. *Synth. Met.* **1998**, *93*, 111.

[78] Sotzing, G. A.; Reynolds, J. R.; Steel, P. J. *Chem. Mater.* **1996**, *8*, 882.

[79] Child, A. D.; Reynold, J. R. *J. Chem. Soc., Chem. Commun.* **1991**, 1779.

[80] Reynolds, J. R.; Ruiz, J. P.; Child, A. D.; Nayak, K.; Marynick, D. S. *Macromolecules* **1991**, *24*, 678.

[81] Ruiz, J. P.; Dharia, J. R.; Reynolds, J. R.; Buckley, L. J. *Macromolecules* **1992**, *25*, 849.

[82] Child, A. D.; Sankaran, B.; Larmat, F.; Reynolds, J. R. *Macromolecules* **1995**, *28*, 6571.

[83] Tanaka, S.; Kaeriyama, K.; Hiraide, T. *Makromol. Chem., Rapid Commun.* **1988**, *9*, 743.

[84] Reynolds, J. R.; Child, A. D.; Ruiz, J. P.; Hong, S. Y.; Marynick, D. S. *Macromolecules* **1993**, *26*, 2095.

[85] Irvin, J. A.; Reynolds, J. R. *Polymer* **1998**, *39*, 2339.

[86] Irvin, D. J.; Reynolds, J. R. *Polymers for Advanced Technologies* **1998**, *9*, 260.

[87] Tsuie, B.; Reddinger, J. L.; Sotzing, G. A.; Soloducho, J.; Katritzky, A. R.; Reynolds, J. R. *J. Mater. Chem.* **1999**, *9*, 1289.

[88] Sotzing, G. A.; Reynolds, J. R.; *J. Chem. Soc., Chem. Commun.* **1995**, 703.

[89] Cheng, Y.; Elsenbaumer, R. L. *J. Chem. Soc., Chem. Commun.* **1995**, 1451.

[90] Sotzing, G. A.; Thomas, C. A.; Reynolds, J. R.; Steel, P. J. *Macromolecules* **1998**, *31*, 3750.

[91] *Handbook of Conducting Polymers*, 2nd ed.; Skotheim, T. A.; Elsenbaumer, R. L.; Reynolds, J. R., Eds.; Marcel Dekker: New York, 1998, Chapters 29-38.

[92] Dodabalapur, A.; Torsi, L.; Katz, H. E. *Science* **1995**, *268*, 270.

[93] Kraft, A.; Grimsdale, A. C.; Holmes, A. B. *Angew. Chem. Int. Ed.* **1998**, *37*, 402.

[94] Jonas, F.; Heywang, G.; Schmidtberg, W.; Heinze, J.; Dietrich, M. Europ. Pat. Appl. 339 340, 1988.

[95] DuBois, J. C.; Sagnes, O.; Henry, F. *Synth. Met.* **1989**, *28*, C871.

[96] Novak, P.; Muller, K.; Santhanam, K. S. V.; Haas, O. *Chem. Rev.* **1997**, *97*, 207.

[97] Otero, T. F.; Grande, H.-J. in *Handbook of Conducting Polymers*, 2nd ed.; Skotheim, T. A.; Elsenbaumer, R. L.; Reynolds, J. R., Eds.; Marcel Dekker: New York, 1998, Chapter 36.

[98] McQuade, D. T.; Pullen, A. E.; Swager, T. M. *Chem. Rev.* **2000**, *100*, 2537.

[99] Pernaut, J.-M.; Reynolds J. R. *J. Phys. Chem. B.* **2000**, *104*, 4080.

[100] Monk, P. M. S.; Mortimer, R. J.; Rosseinsky, D. R. *Electrochromism: Fundamentals and Applications*; VCH: Weinheim, 1995.

[101] Sapp, S. A.; Sotzing, G. A.; Reynolds, J. R. *Chem. Mater.* **1998**, *10*, 2101.

[102] Sapp, S. A.; Sotzing, G. A.; Reddinger, J. L.; Reynolds, J. R. *Adv. Mater.* **1996**, *8*, 808.

[103] Wegener, P.; Feldhues, M.; Litterer, H. Ger. Offen. DE 3, 804, 522 A1, 1989; *Chem. Abstr.*, **1990**, *114*, 98369f.

[104] Langeveld-Voss, B. M. W.; Janssen, R. A. J.; Christiaans, M. P. T.; Meskers, S. C. J.; Dekkers, H. P. J. M.; Meijer, E. W. *J. Amer. Chem. Soc.* **1996**, *118*, 4908.

[105] Sawyer, D. T.; Sobkowiak, A.; Roberts Jr., J. L. *Electrochemistry for Chemists*, 2nd ed.; John Wiley & Sons: New York, 1995; Chapter 3.

[106] Abruna, H. *Coordination Chemistry Reviews* **1998**, *86*, 135.

[107] Lane, R. F.; Hubbard, A. T. *J. Phys. Chem.* **1973**, *77*, 1401.

[108] Laviron, E. *J. Electroanal. Chem.* **1972**, *39*, 1.

[109] Patil, A. O.; Heeger, A. J.; Wudl, F. *Chem. Rev.* **1988**, *88*, 183.

[110] Furukawa, Y. *J. Phys. Chem.* **1996**, *100*, 15644.

[111] Cornil, J.; Beljonne, D.; Bredas, J. L. *J. Chem. Phys.* **1995**, *103(2)*, 834.

[112] Fesser, K.; Bishop, A. R.; Campbell, D. K. *Phys. Rev. B* **1983**, *27*, 4804.

[113] Sankaran, B.; Reynolds, J. R. *Macromolecules* **1997**, *30*, 2582.

[114] Havinga, E. E.; Mutsaers, C. M. J.; Jenneskens, L. W.; *Chem. Mater.* **1996**, *8*, 769.

[115] Rughooputh, S. D. D. V.; Heeger, A. J.; Wudl, F. *J. Polym. Sci.* **1987**, *25*, 1071.

[116] Doblhofer, K.; Rajeshwar, K. in *Handbook of Conducting Polymers,* Second Edition (Eds: Skotheim, T. A., Elsenbaumer, R. L., Reynolds, J. R.), Marcel Dekker, New York **1998**, pp. 531-588.

[117] Mastragostino, M.; Arbizzani, C.; Ferloni, P.; Marinangeli, A. *Solid State Ionics* **1992**, *53-56*, 471.

[118] Apperloo, J. J.; van Haare, J. A. E. H.; Janssen, R. A. J. *Synth. Met.* **1999**, *101*, 417.

[119] Bange, K.; Gambke, T. *Adv. Mater.* **1990**, *2*, 10.

[120] Hitchman, M. J. *J. Electroanal. Chem.* **1977**, *85*, 135.

[121] Dautremont-Smith, W. C. *Displays I*, **1982**, 3.

[122] Michalak, F.; Aldebert, P. *Solid State Ionics* **1996**, *85*, 265.

[123] Habib, M. A.; Maheswari, S. P.; Carpenter, M. K. *J. Appl. Electrochem.* **1991**, *21*, 203.

[124] Choy, J.; Kim, Y.; Kim, B.; Park, N.; Campet, G.; Grenier, J.-C. *Chem. Mater.* **2000**, *12*, 2950.

[125] Cummins, D.; Boschloo, G.; Ryan, M.; Corr, D.; Rao, S. N.; Fitzmaurice, D. *J. Phys. Chem. B* **2000**, *104*, 11449.

[126] Paoli, M.-A.; Casalbore-Miceli, G.; Girotto, E. M.; Gazotti, W. A. *Electrochim. Acta* **1999**, *44*, 2983.

[127] Kuehni, R. G. *Color: an Introduction to Practice and Principles*; Wiley: New York, 1996.

[128] CIE. *Colorimetry (Official Recommendations of the International Commission on Illumination);* CIE Publication No. 15, CIE: Paris **1971**.

[129] Brotherson, I. D.; Mudigonda, D. S. K.; Osborn, J. M.; Belk, J.; Chen, J.; Loveday, D. C.; Boehme, J. L.; Ferraris, J. P.; Meeker, D. L. *Electrochim. Acta* **1999**, *44*, 2993.

[130] Mudigonda, D. S. K.; Meeker, D. L.; Loveday, D. C.; Osborn, J. M.; Ferraris, J. P. *Polymer* **1999**, *40*, 3407.

[131] Hyodo, K. *Electrochim. Acta* **1994**, *39*, 265.

[132] De Paoli, M. A.; Casallbore-Miceli, G.; Girotto, E. M.; Gazotti, W. A. *Electrochim. Acta* **1999**, *44*, 2983.

[133] Hyodo, K.; Omae, M. *J. Electroanal. Chem.* **1990**, *292*, 93.

[134] Granstrom, M.; Inganäs, O. *Appl. Phys. Lett.* **1996**, *68*, 147.

[135] Granstrom, M.; Berggren, M.; Pede, D.; Inganäs, O.; Anderson, M. R.; Hjertberg, T.; Wennerstrom, O. *Supramol. Sci.* **1997**, *4*, 27.

[136] Wang, Y. Z.; Sun, R. G.; Epstein, A. J. *Appl. Phy. Lett.* **1999**, *74*, 3613.

[137] Thompson, B. C.,; Schottland, P.; Zong, K.; Reynolds, J. R. *Chem. Mater.* **2000**, *12*, 1563.

[138] Schwendeman, I.; Hwang, J.; Welsh, D. M.; Tanner, D. B.; Reynolds. J. R. *Adv. Mater.* Accepted for publication.

[139] Gogte, V. N.; Shah, L. G.; Tilak, B. D.; Gadekar, K. N.; Sahasrabudhe, M. B.; *Tetrahedron* **1967**, *23*, 2437.

[140] Leznoff, C. C.; Drew, D. M. *Can. J. Chem.* **1996**, *74*, 307.

[141] Gronowitz, S.; Moses, P.; Hakansson, R. *Arkiv. Kemi.* **1966**, *16*, 267.

[142] Goldoni, F.; Langeveld-Voss, B. M. W.; Meijer, E. W. *Synth. Commun.* **1998**, *28*, 2237.

[143] Sheldrick, G. M. *SHELXTL5*. **1995**, Siemens Analytical Instrumentation, Madison, Wisconsin, USA.

[144] Hegedus, L. S. *Transition Metals in the Synthesis of Complex Molecules*, 2nd ed; University Science Books: Sausalito, 1999; Chapter 4.

[145] Brandsma, L.; Vasilevsky, S. F.; Verkruijsse *Application of Transition Metal Catalysts in Organic Synthesis*; Springer-Verlag: Berlin, 1998.

[146] Schlüter, A. –D.; Wegner, G. *Acta Polymer.* **1993**, *30*, 645.

[147] Bochmann, M.; Kelly, K.; Lu, J. *J. Polym. Sci., Polym. Chem. Ed.* **1992**, *30*, 2511.

[148] Stille, J. K. *Angew. Chem. Int. Ed. Engl.* **1986**, *25*, 508.

[149] Mitchell, T. M. *Synthesis* **1992**, 803.

[150] Negishi, E. *Am. Chem. Soc. Div. Pet. Chem. Prepr.* **1979**, *24*, 226.

[151] Negishi, E. *Acc. Chem. Res.* **1982**, *15*, 340.

[152] Miyaura, N.; Suzuki, A. *Chem. Rev.* **1995**, *95*, 2457.

[153] Tamao, K.; Sumitani, K.; Kumada, M. *J. Am. Chem. Soc.* **1972**, *94*, 4376.

[154] Tamao, K.; Kodama, S.; Nakajima, I.; Kumada, M.; Minato, A.; Suzuki, K. *Tetrahedron* **1982**, *38*, 3347.

[155] Kalinin, V. N. *Synthesis* **1992**, 413.

[156] Yamamoto, T.; Yamamoto, A. *Chem. Lett.* **1977**, 353.

[157] Balanda, P. B.; Ramey, M. B.; Reynolds, J. R. **1999**, *32*, 3970.

[158] Bao, Z.; Chan, W.K.; Yu, L. *J. Am. Chem. Soc.* **1995**, *117*, 12426.

[159] Zhang, Q. T.; Tour, J. M. *J. Am. Chem. Soc.* **1997**, *119*, 9624.

[160] Pelter, A.; Jenkins, I.; Jones, D. E. *Tetrahedron* **1997**, *53*, 10357.

[161] Yamamoto, T.; Sanechika, K.; Yamamoto, A. *J. Poly. Sci., Polym Lett. Ed.* **1980**, *18*, 9.

[162] Yamamoto, T.; Morita, A.; Miyazaki, Y.; Maruyama, T.; Wakayama, H.; Zhou, Z.; Nakamura, Y.; Kanbara, T.; Sasaki, S.; Kubota, K. *Macromolecules* **1992**, *25*, 1214.

[163] Mori, S; Barth, H. G. *Size Exclusion Chromatography*; Springer-Verlag: Berlin, 1999.

[164] Vanhee, S.; Rulkens, R.; Lehmann, U.; Rosenauer, C.; Schulze, M.; Kohler, W.; Wegner, G. *Macromolecules* **1996**, *29*, 5136.

[165] Nielen, M. W. F. *Mass Spectrom. Rev.* **1999**, *18*, 309.

[166] Zenobi, R.; Knochenmuss, R. *Mass Spectrom. Rev* **1998**, *17*, 337.

[167] Hanton, S. D. *Chem. Rev.* **2001**, *101*, 527.

[168] Murray, K. K. *Mass Spectrom. Rev.* **1997**, *16*, 283.

[169] Pavia, D.L.; Lampman, G. M.; Kriz, G. S. *Introduction to Spectroscopy* 2nd ed.; Saunder: Fort Worth, 1996.

[170] Liu, J.; Loewe, R. S.; McCullough, R.D. *Macromolecules* **1999**, *32*, 5777.

[171] Apperloo, J. J.; Janssen, R. A. J.; Nielsen, M. M.; Bechgaard, K. *Adv. Mater.* **2000**, *12*, 1594.

[172] Andersson, M. R.; Thomas, O.; Mammo, W.; Svensson, M.; Theander, M.; Inganäs, O. *J. Mater. Chem.* **1999**, *9*, 1933.

[173] McCullough, R. D.; Tristram-Nagle, S.; Williams, S. P.; Lowe, R. S.; Jayaraman, M. *J. Am. Chem. Soc.* **1993**, *115*, 4910.

[174] *Dictionary of Inorganic Compounds*; Chapman and Hall: London, 1992; Vol. 3.

[175] Sotzing, G. A.; Reynolds, J. R.; Steel, P. J. *Adv. Mater.* **1997**, *9*, 795.

[176] Zhu, S. S.; Swager, T. M. *J. Am. Chem. Soc.* **1997**, *119*, 12568.

[177] Furniss, B. S.; Hannaford, A. J.; Smith, P. W. G.; Tatchell, A. R. *Vogel's Textbook of Practical Organic Chemistry*, 5th ed.; John Wiley & Sons: New York, 1989; pp. 444-445.

[178] Murov, S. L.; *Handbook of Photochemistry*, 2nd ed.; Marcel Dekker: New York, 1993.

[179] Sheldrick, G. M. **1998**. *SHELXTL5*. Bruker-AXS, Madison, Wisconsin, USA.

[180] Huang, W.-S.; Humprey, B. D.; MacDiarmid, A. G. *J. Chem. Soc., Faraday Trans. 1* **1986**, *82*, 2385.

[181] Chinn, D.; DuBow, J.; Liess, M.; Josowicz, M.; Janata, J. *Chem. Mater.* **1995**, *7*, 1504.

[182] Kobayashi, T.; Yoneyama, H.; Tamura, H. *J. Electroanal. Chem.* **1984**, *161*, 419.

[183] Faid, K.; Ades, D.; Siove, A.; Chevrot, C. *J. Chim. Phys.* **1992**, *89*, 1019.

[184] Faid, K.; Siove, A.; Ades, D.; Chevrot, C. *Synth. Met.* **1993**, *55-57*, 1656.

[185] Faid, K.; Ades, D.; Siove, A.; Chevrot, C. *Synth. Met.* **1994**, *63*, 89.

[186] Qui, Y.-J.; Reynolds, J. R.; *J. Electrochem. Soc.* **1990**, *137*, 900.

[187] Ambrose, J. G.; Nelson, R. F. *J. Electrochem. Soc.* **1968**, *115*, 1159.

[188] Reddinger, J. L.; Sotzing, G. A.; Reynolds, J. R. *J. Chem. Soc., Chem. Commun.* **1996**,1777.

[189] Sotzing, G. A.; Reddinger, J. L.; Katritzky, A. R.; Soloducho, J.; Musgrave, R.; Reynolds, J. R.; Steel, P. J. *Chem. Mater.* **1997**, *9*, 1578.

[190] Asavapiriyanont, S.; Chandler, G. K.; Gunawardena, G. A.; Pletcher, D. *J. Electroanal. Chem.* **1984**, *177*, 229.

[191] Zhou, M.; Heinze, J. *Electrochim. Acta* **1999**, *44*, 1733.

[192] Sezer, E.; Van Hooren, M.; Sarac, A. S.; Hallensleben, M. L. *J. Polm. Sci., Polym. Chem. Ed.* **1999**, *37*, 379.

[193] Roncali, J. *Chem. Rev.* **1997**, *97*, 173.

[194] Pratt, J. R.; Pinkerton, F. H.; Thames, S. F. *J. Organomet. Chem.* **1972**, *38*, 29.

[195] Mazzara; Leonardi *Gazz. Chim. Ital.* **1892**, *22*, 572.

[196] Haga, K.; Iwaya, K.; Kaneko, R. *Bull. Chem. Soc. Jpn.* **1986**, *59*, 803.

BIOGRAPHICAL SKETCH

Dean Matthew Welsh was born on September 27, 1973 in Charleroi, Pennsylvania, and he spent his entire childhood in Monongahela, PA. He began his undergraduate studies in the fall of 1991 at St. Vincent College in Latrobe, PA, where he graduated in 1995 with highest honors with a Bachelor of Science degree in chemistry. During this time, he worked on polymer synthesis and characterization under the advisement of Dr. Daryle Fish. In 1995, after getting married to Annie, he came to the University of Florida to begin doctoral studies with Professor John R. Reynolds in the area of electroactive polymers.

Both Dean and Annie enjoyed their time in Florida very much, where Dean became a particularly avid Gator. His first job as a Ph.D. will be as a Senior Research Chemist at The Dow Chemical Company in Midland, Michigan working in the light-emitting polymer group. Dean is very thankful for the time spent in Florida, and he is ready to begin his new life in Michigan and move on to new and exciting things.

I certify that I have read this study and that in my opinion it conforms to acceptable standards of scholarly presentation and is fully adequate, in scope and quality, as a thesis for the degree of Doctor of Philosophy.

John R. Reynolds, Chairman
Professor of Chemistry

I certify that I have read this study and that in my opinion it conforms to acceptable standards of scholarly presentation and is fully adequate, in scope and quality, as a thesis for the degree of Doctor of Philosophy.

Kenneth B. Wagener
Professor of Chemistry

I certify that I have read this study and that in my opinion it conforms to acceptable standards of scholarly presentation and is fully adequate, in scope and quality, as a thesis for the degree of Doctor of Philosophy.

Kirk S. Schanze
Professor of Chemistry

I certify that I have read this study and that in my opinion it conforms to acceptable standards of scholarly presentation and is fully adequate, in scope and quality, as a thesis for the degree of Doctor of Philosophy.

Daniel R. Talham
Professor of Chemistry

I certify that I have read this study and that in my opinion it conforms to acceptable standards of scholarly presentation and is fully adequate, in scope and quality, as a thesis for the degree of Doctor of Philosophy.

Anthony B. Brennan
Associate Professor of Materials Science
and Engineering

This thesis was submitted to the Graduate Faculty of the Department of Chemistry in the College of Liberal Arts and Sciences and to the Graduate School and was accepted as partial fulfillment of the requirements for the degree of Doctor of Philosophy.

August 2001

_____

Dean of the Graduate School